



Skolkovo Institute of Science and Technology

OPTIMAL SITING, SIZING AND TECHNOLOGY SELECTION OF ENERGY STORAGE
SYSTEMS FOR POWER SYSTEM APPLICATIONS

Doctoral Thesis

by

TIMUR SAIFUTDINOV

DOCTORAL PROGRAM IN ENGINEERING SYSTEMS

Supervisor
Professor Janusz Bialek

Moscow - 2020

© Timur Saifutdinov 2020

Abstract

Energy storage systems can perform a number of power system applications, delivering multiple benefits to a utility, a network operator, and an end-customer. To estimate the viability of investment in energy storage and determine the most effective size, technology and location to install it, techno-economic analysis is required to account for various characteristics of storage such as investment cost, efficiency, self-discharge, degradation, as well as other assets' characteristics, i.e., power lines, transformers, demand, and generation cost. In the literature, such analysis is referred to as siting, sizing, and technology selection problem where an optimal solution is usually sought.

The present thesis addresses the problem of optimal siting, sizing, and technology selection of energy storage systems for power system applications by using formal optimization methods. A formal optimization allows finding a problem solution, where uniqueness and global optimality might be mathematically proven, as well as performing various sensitivity analyses to get more insights on a problem. Particularly, the proposed methodology implies using off-the-shelf solvers to approach the initially nonlinear and nonconvex problem. However, the numerical methods used to resolve a formal optimization problem impose certain limitations on its formulation to ensure tractability, uniqueness of a solution, and its accuracy. To perform an accurate techno-economic analysis with the formal optimization approach, a mixed-integer convex programming problem reformulation has been proposed, which allows accounting for a complex degradation mechanism of Li-ion energy storage. The main drawback of the proposed mixed-integer problem reformulation resides in its scalability, where the problem may become intractable with the increase of network size and number of storage technologies considered. The tractability issue of the combinatorial problem has been addressed with problem decomposition employing augmented Lagrangian relaxation and barrier function relaxation to decompose the original problem, which has been resolved with the alternating direction method of multipliers.

The present thesis is meant to be useful for a broad audience of engineers and economists, including investors in energy storage, network operators, energy storage developers, and policymakers. First, the proposed methodology performs an accurate techno-economic analysis

of energy storage deployment, which equips a potential investor with an effective tool to make an informed investment decision. Second, the results of a simulated network within the proposed framework are of sufficient interest for a system operator to define the most troublesome sites of a network and give the most cost-effective solution to resolve a problem. Third, an analysis performed within the study gives insights to energy storage developers on particular characteristics of storage technology to be improved and gives a performance value of storage technology to be competitive on the market. Finally, policymakers may use the proposed framework to estimate the effect of a particular policy on the attraction of energy storage and the global effects associated with it, i.e., change in fuel consumption, network operation cost, carbon dioxide emission.

Keywords: convex optimization, energy storage, power system, problem decomposition.

Publications

Journal publications:

1. V. Chirkin, A. Gorbunov, M. Goubko, V. Korepanov, N. Korgin, **T. Sayfutdinov**, A. Sharova, T. Vaskovskaya, “Gaming Experiments for Analysis of Pricing Mechanisms at Electricity Markets,” *IFAC-PapersOnLine*, vol. 49, no. 32, pp. 13–18, 2016.
2. **T. Sayfutdinov**, C. Patsios, J. W. Bialek, D. M. Greenwood, and P. C. Taylor, “Incorporating Variable Lifetime and Self-Discharge into Optimal Sizing and Technology Selection of Energy Storage Systems,” *IET Smart Grid*, vol. 1, no. 1, pp. 11–18, 2018.
3. **T. Sayfutdinov**, C. Patsios, P. Vorobev, E. Gryazina, D. M. Greenwood, J. W. Bialek, P. C. Taylor, “Degradation and Operation-Aware Framework for the Optimal Siting, Sizing and Technology Selection of Battery Storage,” *IEEE Trans. Sustain. Energy*, Early Access.
4. **T. Sayfutdinov**, M. Ali, O. Khamisov, “Alternating Direction Method of Multipliers for the Optimal Siting, Sizing, and Technology Selection of Li-ion Battery Storage,” *Electric Power Systems Research*, under review.

Conference proceedings:

1. **T. Sayfutdinov**, P. Lyons, and M. Feeney, “Laboratory Evaluation of a Deterministic Optimal Power Flow Algorithm using Power Hardware in the Loop,” in *IET Conference Publications (CIRED 2016)*, 2016, pp. 1–4.

2. Vanin A.S., **Sayfutdinov T.R.**, Tulskiy V.N. “Centralized Voltage Control System in Intelligent Distribution Networks,” (In Russ.) *Electroenergetica glazami molodezhi-2016 = Power System through Youth’s eyes-2016*, 2016, pp. 169-172.
3. **Sayfutdinov T.R.**, Chirkin V.G. “Research on Demand Elasticity at Electricity Markets based on Business Simulation Games,” (In Russ.) *Vserossiyskaya shkola-conferencia molodih uchenih «Upravlenie Bolshimi Sistemami» = Russia-wide school-conference of young scientists «Control in Large Systems»*, 2016, pp. 477-487
4. **T. Sayfutdinov**, “Optimal Siting, Sizing and Technology Selection of Energy Storage Systems,” in *Proceedings of the Skoltech Energy Ph.D. Seminar*, 2018, pp. 20–29.

Acknowledgments

I am very grateful to my wife Evgenia, who was looking all this time after two babies – me and our lovely daughter Leila.

Also, I would like to express my gratitude to my research supervisor professor Janusz Bialek and my co-supervisors, Dr. Charalampos Patsios from Newcastle University and Dr. Elena Gryazina from Skoltech.

Last but not least are my parents, who were always supportive and helpful.

Thank you all!

Table of Contents

Abstract.....	2
Publications	4
Acknowledgments	6
Table of Contents.....	7
Abbreviations.....	11
Nomenclature.....	13
List of Figures.....	17
List of Tables	20
Chapter 1. Introduction.....	21
1.1 Current Situation and Challenges in Power Systems	21
1.2 Research Focus and Objectives	26
1.3 Research Overview and Contributions	27
1.4 Thesis Outline.....	30
Chapter 2. Review of the Literature	32
2.1 Energy Storage Technologies	32
2.1.1 Electrical Storage.....	34
2.1.2 Mechanical Storage	35
2.1.3 Thermal Storage	39
2.1.4 Hydrogen Storage.....	41
2.1.5 Electrochemical Storage.....	42
2.2 Energy Storage Applications	48

2.2.1 Bulk Energy Applications	51
2.2.2 Ancillary Services.....	54
2.2.3 Transmission and Distribution Infrastructure Applications	59
2.2.4 Customer Energy Management Applications.....	63
2.2.5 Stacked Applications	65
2.3 Methods for Optimal Siting, Sizing and Technology Selection	66
2.3.1 Analytical.....	67
2.3.2 Exhaustive Search.....	67
2.3.3 Heuristic Search.....	68
2.3.4 Mathematical Programming	70
2.4 Models Overview	72
2.4.1 Energy Storage Modelling.....	73
2.4.2 Power Flow Modelling	81
2.4.3 Demand Modelling.....	85
2.4.4 Renewable Generation Modelling.....	87
2.5 Literature on Optimal Siting, Sizing and Technology Selection.....	88
2.6 Conclusions	94
Chapter 3. Optimization Problem Formulation and Resolution	97
3.1 Problem Formulation.....	97
3.1.1 Objective Function	97
3.1.2 Constraints	98
3.2 Problem Analysis and Resolution.....	103

3.3 Decomposed Optimization Subproblem.....	107
3.3.1 Objective Function	107
3.3.2 Constraints	109
3.3.3 Algorithm.....	111
3.4 Conclusions	113
Chapter 4. Results and Analysis	115
4.1 Case Study	115
4.1.1 Application	115
4.1.2 Network, Generation, and Power Lines Data	117
4.1.3 Demand Data	118
4.1.4 Energy Storage Characteristics.....	120
4.2 Results Analysis	120
4.2.1 Optimal Solution.....	120
4.2.2 Comparison with State-of-the-Art	122
4.2.3 Network and Energy Storage Operation.....	125
4.3 Performance Value Analysis	129
4.3.1 Performance Value of Energy Storage Technologies.....	129
4.3.2 Breakeven Cost of New Energy Storage	130
4.3.3 Breakeven Cost of Second-Life Energy Storage	131
4.4 Discussion.....	134
4.4.1 Siting, Sizing, and Technology Selection Decision Making	134
4.4.2 Method Applicability.....	136

4.4.3 Cycle Counting Method.....	136
4.4.4 Computational Time	137
4.4.5 Convergence of ADMM.....	139
4.5 Conclusions	140
Chapter 5. Conclusion	142
5.1 Summary.....	142
5.2 Fulfillment of Research Objectives	144
5.3 Conclusions	148
Bibliography	149
Appendix A: Technical Data of Energy Storage Technologies	166
Appendix B. Degradation Data of Li-ion Technologies.....	167
Appendix C. IEEE 10 Generators 39-Bus Network Data	169
Appendix D. Energy Storage Applications’ Requirements.....	171
Appendix E. Results of Optimal Siting, Sizing, and Technology Selection for IEEE Benchmark Systems	172

Abbreviations

AC – alternating current

ADMM – alternating direction method of multipliers

ALR – augmented Lagrangian relaxation

BD – Benders decomposition

C-Rate – charge-discharge rate

CAISO – California Independent System Operator

CP – convex programming

DER – distributed energy resource

DoD – depth of discharge

EoL – end of life

FACTS – flexible AC transmission system

JuMP – Julia for Mathematical Optimization

LFP – lithium ferrophosphate

Li-ion – lithium-ion

Li⁺ – positively charged lithium ions;

LMO – lithium manganese oxide

LMP – locational marginal price

LP – linear programming

LTO – lithium titanium oxide

MICP – mixed-integer convex programming

MILP – mixed-integer linear programming

NMC – nickel manganese cobalt

RE – renewable energy

RES – renewable energy source

RFC – Rainflow-counting

SoC – state of charge

SST – siting, sizing, and technology selection

T&D – transmission and distribution

Nomenclature

Sets and indices

T	Set of time intervals, indexed by t
G	Set of generators, indexed by g
B	Set of transmission grid nodes, indexed by b
Br	Set of branches, indexed by bb' (from/to)
J	Set of energy storage technologies, indexed by j
S	Set of representative scenarios, indexed by s
C	Set of charge-discharge cycles, indexed by c
k	Iteration index of ADMM

Given parameters

C^E	Investment cost per MWh
C^P	Investment cost per MW
$k^{E/P}$	Energy to power ratio
Δt	Time-step
R_{in}	Internal resistance of a battery
η_{Ch}	Charge efficiency
η_{Dis}	Discharge efficiency
$A_{SoC}^{Idl}, B_{SoC}^{Idl}, C_{SoC}^{Idl}$	Quadratic, linear and constant terms of idling degradation from SoC
$A_{\tau}^{Idl}, B_{\tau}^{Idl}, C_{\tau}^{Idl}$	Quadratic, linear and constant terms of idling degradation from temperature

$A_{DoD}^{Cyc}, B_{DoD}^{Cyc}$	Quadratic and linear terms of cycling degradation from DoD
$A_{\tau}^{Cyc}, B_{\tau}^{Cyc}, C_{\tau}^{Cyc}$	Quadratic, linear and constant terms of cycling degradation from temperature
τ^{Amb}	Ambient temperature
C^{Tm}	Thermal capacitance of energy storage per unit mass
m	Mass of energy storage
k_j^{Tm}	Mass of a storage per MWh of installed energy capacity
k^{HD}	Heat dissipation coefficient
$R_{bb'}, X_{bb'}$	Active and reactive resistance of a power line
$b_{bb'}^{Sh}$	Shunt admittance of a power line
$y_{bb'}$	Admittance of a power line
$\vartheta_{bb'}$	Shift angle of a line
π_s	Probability of occurrence of a particular scenario
k^{SD}	Self-discharge coefficient
EoL_j	End of life criterion of a particular storage technology
$\overline{PF}_{bb'}$	Thermal limit of a power line
γ	Positive constant value required by ALR
ε	Convergence tolerance
a_g, b_g	Quadratic and linear coefficients of the generation cost function
$C_{bb',t}^{APL}$	Energy price for active power losses

$\overline{P}_{g,s}^G$ Maximum power output of a thermal generation unit

k_j^{SL} Second-life storage degradation rate

Estimated parameters

C^{Inv} Investment cost on energy storage

L Power losses

V_{OC} Open circuit battery voltage

V_T Terminal battery voltage

V_{in} Voltage drop on internal resistance

P_T Terminal power output

σ Self-discharge function

δ^{CF} Capacity fade of energy storage

δ^{Idl} Capacity fade from idling

δ^{Cyc} Capacity fade from cycling

SoC^D Average daily state of charge

τ^D Average daily storage temperature

DoD^C Cycle DoD

τ^C Average storage temperature of a particular cycle

t^{Start}, t^{End} Start and end time moments of a particular cycle

μ Heat dissipation function

P_b^G, Q_b^G Active and reactive power generated within a bus b

P_b^L, Q_b^L Active and reactive power consumed within a bus b

$P_b^{\text{Net}}, Q_b^{\text{Net}}$	Active and reactive net injected power to/from a bus b
V_b	Voltage magnitude at bus b
R_s	Reward function for representative scenario s
$y_{b,j}$	Operational lifetime periods per each year of operation
i_c	Full or half-cycle indicator
T_c	Cycle duration
$\lambda_{b,s,t}$	Dual auxiliary variable

Optimization problem variables

$\bar{E}_{b,j}$	Installed energy capacity
$\bar{P}_{b,j}$	Installed power capacity
$E_{b,j,s,t}$	Charge of energy storage
$P_{b,j,s,t}^{\text{Ch}}$	Charge power of energy storage
$P_{b,j,s,t}^{\text{Dis}}$	Discharge power of energy storage
$\tau_{b,j,s,t}$	Storage temperature
$T_{b,j}^{\text{LT}}$	Operational lifetime of a particular energy storage system
$DoD_{b,j,c}^{\text{Cyc}}$	Maximum DoD
$\tau_{b,j,c}^{\text{Cyc}}$	Average storage temperature during a cycle
$SoC_{b,j}^{\text{Idl}}$	Average daily SoC
$\tau_{b,j}^{\text{Idl}}$	Average daily temperature of energy storage
$\theta_{b,s,t}$	Voltage angle at bus b

List of Figures

Figure 1.1: Conventional power system structure [1]	22
Figure 1.2: Up-to-date power system structure [1].....	23
Figure 2.1: Typical power and energy capacities, and discharge time of energy storage technologies [6].	33
Figure 2.2: Capital cost and annual operating and maintenance cost for energy storage technologies [7].	34
Figure 2.3: Schematic of superconducting magnetic energy storage [7]	35
Figure 2.4: Schematic of pumped hydroelectric storage [7]	36
Figure 2.5: Schematic of compressed air energy storage [7]	38
Figure 2.6: Schematic of flywheel energy storage [7].....	39
Figure 2.7: Schematic of pumped heat electrical storage [22]	40
Figure 2.8: Schematic of liquid air energy storage [24]	41
Figure 2.9: Schematic of hydrogen energy storage [7]	42
Figure 2.10: Schematic of lead-acid battery [32]	44
Figure 2.11: Schematic of electrochemical capacitor [7]	45
Figure 2.12: Schematic of vanadium redox flow battery [7].....	46
Figure 2.13: Schematic of Li-ion battery [31].....	47
Figure 2.14: Power and discharge duration requirements for energy storage applications [41].	50
Figure 2.15: Application-specific 10-year benefit and maximum market potential estimates for the U.S. [37].....	51

Figure 2.16: Electric energy time-shift application [12]	53
Figure 2.17: Frequency regulation principle [12].....	55
Figure 2.18: Load following illustration [37].....	58
Figure 2.19: Upgrade deferral principle [55].....	62
Figure 2.20: The value of energy storage for providing multiple services [59].....	66
Figure 2.21: Principle of genetic algorithm [69]	69
Figure 2.22: Self-discharge rate characteristic of Li-ion cell [94]	75
Figure 2.23: Li-ion battery model [39].....	76
Figure 2.24: Degradation process of Li-ion battery	78
Figure 2.25: Energy capacity fade rate characteristic of Li-ion NMC cell	79
Figure 2.26: Example of a power system graph	82
Figure 2.27: Generalized pi branch model	82
Figure 2.28: Net load curve example [111].....	86
Figure 2.29: Solar and wind production [115]	87
Figure 3.1: ADMM flowchart	112
Figure 4.1: IEEE ten generators 39-bus network [126].....	118
Figure 4.2: Demand profiles	119
Figure 4.3: Objective function stacked chart.....	124
Figure 4.4: Network operation during high demand period	126
Figure 4.5: LMPs at 39-bus network	127
Figure 4.6: Charge of energy storage	127
Figure 4.7: Storage temperature	128

Figure 4.8: Energy storage capacity fade	129
Figure 4.9: Performance value of energy storage technologies.....	130
Figure 4.10: Breakeven cost of new energy storage technologies	131
Figure 4.11: Performance value of second-life energy storage technologies	133
Figure 4.12: Computational time vs. number of buses and number of scenarios.....	138
Figure 4.13: Primal residual during the optimization.....	140
Figure B.1: Capacity fade rate characteristics of Li-ion energy storage	168

List of Tables

Table 2.1: Energy storage applications.....	49
Table 2.2: Advantages and disadvantages of the SST methods	72
Table 4.1: Li-ion technologies’ characteristics.....	120
Table 4.2: Optimal solution	121
Table 4.3: Comparative study.....	123
Table 4.4: Breakeven cost of second-life energy storage technologies.....	134
Table A.1: Technical Characteristics of Energy Storage Technologies	166
Table B.1: Idling degradation data	167
Table B.2: Cycling degradation data	167
Table C.1: Generators’ data	169
Table C.2: Branches’ data	169
Table D.1: Energy storage applications’ requirements.....	171
Table E.1: Results of optimal siting, sizing, and technology selection.....	172

Chapter 1. Introduction

1.1 Current Situation and Challenges in Power Systems

An electric power system is one of the biggest systems that humankind built. It contains a big number of interconnected elements, which share the single objective – to provide a consumer with electrical energy. Before being useful electrical energy has to be generated, transmitted, and distributed to an end-customer.

Conventionally, the process starts at the supplier's site, where the energy of any type is converted to the electrical energy by means of a fossil fuel power stations, hydropower stations, or nuclear power stations. Then electrical energy produced by a supplier, which is typically located in the distance from a customer, has to be transferred through a transmission network. To avoid serious energy losses associated with transferring energy over the long distance, it is converted to a high voltage level at a supplier's site and back to a medium voltage level at a distribution network site by means of the step up and step down transformers. Finally, a distribution network delivers electrical energy to an end-customer, where the transformers again lower the voltage level to a utilization rate. The described conventional electric power system is characterized by unidirectional power flow (from supplier to consumer), where demand is predictable, and power stations are controllable. Figure 1.1 illustrates a conventional power system structure.

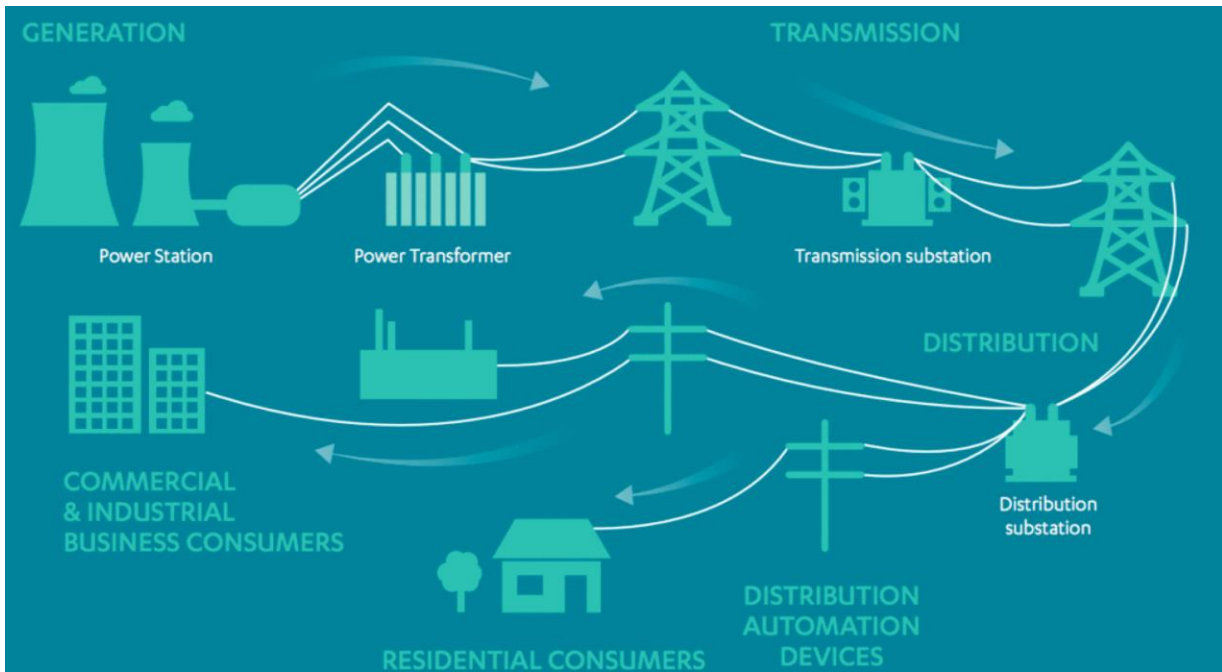


Figure 1.1: Conventional power system structure [1]

However, due to the developments in a distributed energy resources (DERs) sector, including industrial and domestic renewable energy sources (RESs), which are characterized by intermittent power generation, a conventional power system changed. Also, ubiquitous electrification of industry and households loads a power system to its maximum operating capability. Figure 1.2 illustrates up-to-date power system, which is characterized by bidirectional power flows and less controllable and less predictable generation and consumption of electrical energy. Due to the fact that a new power system is built on the basis of a conventional power system, which was not designed for new regimes, significant challenges are exerted in power system operation.

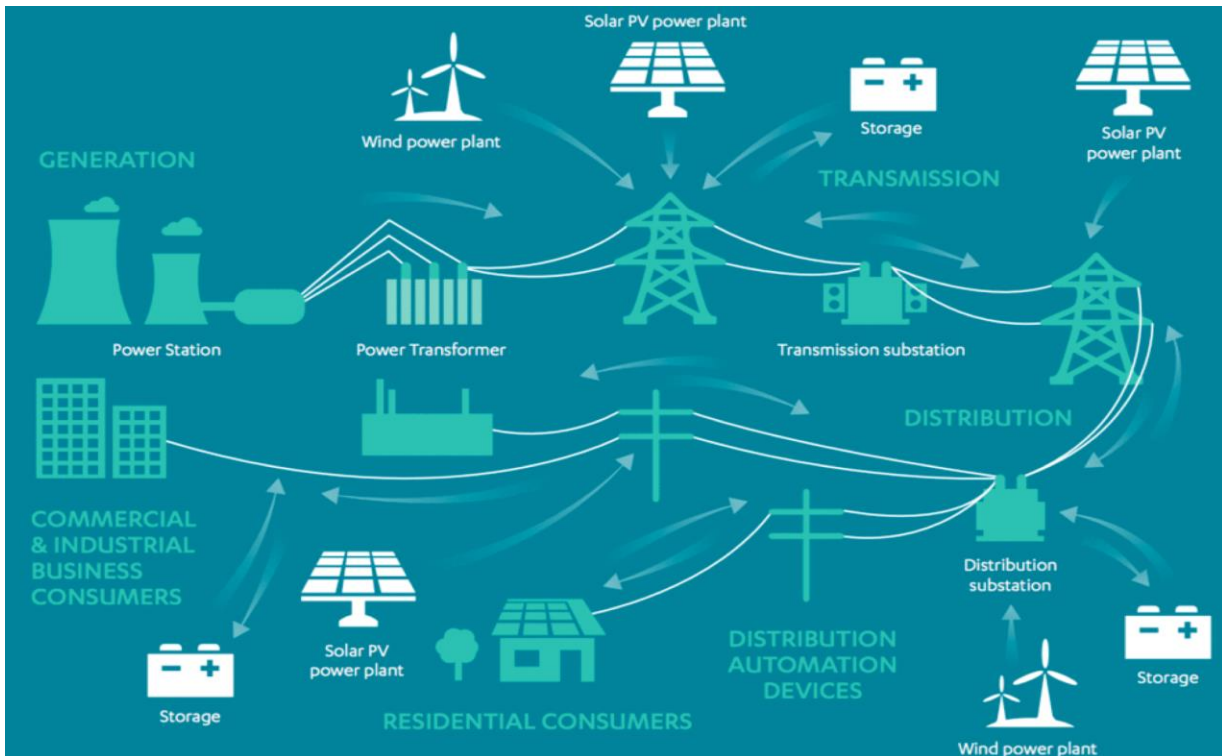


Figure 1.2: Up-to-date power system structure [1]

Electrical energy, like any other commodity, has to meet certain quality criteria to be valuable for a customer, which is typically referred to as electric power quality. For example, all domestic and industrial electric devices are developed to perform best at a certain voltage level (230 Volts for a single phase connection and 400 Volts for a multi-phase connection), frequency value (50 Hertz in the large part of the world), voltage and current waveform (has to follow the form of a sine function). However, due to overloaded power lines, intermittent generation, and unpredictable demand, as well as semiconducting elements being used in almost every device, the quality of electric power might be compromised. For instance, due to the Ohm's law saying that voltage drop is proportional to current and impedance, overloaded power line carrying a big current may result in a voltage sag at a customer's site, meaning that electrical devices would

not be operating or operating at a reduced performance rate. Non-significant frequency deviation from nominal value, which indicates the imbalance in electrical energy production and consumption, would not directly affect electrical devices, but if a frequency drops by 1 Hz indicating significant energy generation deficit, the system operator starts disconnecting consumers from power supply in an increasing importance order (first households, then industry, then municipal buildings, and so on). Not least important is a waveform of a voltage and current, which is affected by the non-uniform power consumption of modern electric devices made of semiconducting elements. Nonsinusoidal voltage waveform may result in non-flat power output of electric drives used in industry, which may cause spoilt production and lead to significant financial losses.

One of the greatest concern in an electrical power system is maintaining the power balance between generation and consumption of energy. In other words, generated energy has to be equal to consumed energy. To some extent, this constraint is relaxed due to the power system inertia, which is represented by a rotating mass of electro-mechanical synchronous generation machines that are mainly used in a conventional power production plants, including fossil fuel power stations, hydropower stations, and nuclear power stations. For example, if a power system experiences a power imbalance due to a sharp decrease in a generation (accidental generation unit shutdown), the kinetic energy of electric generators' rotors will even momentarily the imbalance resulting in a reduced system frequency, which can be then restored by generating more energy. However, in a modern electric power system, the total system inertia tends to decrease due to high penetration of RESs, which are connected to a power system through inertia-free power converters. As a consequence, an electric power system with a

substantial level of renewable generation possesses less ability to respond to power imbalance, which is further escalated by an intermittent nature of renewable generation.

The trends show that the situation is not going to be easier in the future. Societal demand for emission-free energy and a decreasing price for RESs result in severe deformation of a conventional electric power system and the ways that are used to operate it. For instance, according to the UK's 2009 Renewable Energy Directive, targeted energy consumption from renewable sources has to be at least 15% by 2020 [2]. According to the Digest of UK Energy Statistics [3], total energy consumption from RES in 2017 constituted to 10.2%, which required a share of renewables in the total generation mix to be equal to 27.9% of the total installed capacity. Following a linear dependency rule, to meet the target of 15%, the required share of renewable generation capacity has to be at least 41%. In [4] *Adrees et al.* state that the 30% of renewables penetration may lead to 15% decrease of system inertia, and almost 50% (48.4%) when renewables penetration comprises 45%. In the same article, authors show that a power system with a higher share of renewables is more vulnerable to major power disturbances.

To respond to the upcoming challenges power systems engineers and scientists have to develop new approaches and standards for electric power system design, planning, and operation. However, it cannot be made from scratch; it is not economically viable to abandon the existing infrastructure and build a new power system, which meets all requirements for the power system of today. It has to be done systematically step-by-step improving the existing system with clear objectives, like an evolution process of a living organism, which allows a smooth transition from a conventional power system to an electric power system of the future. Energy storage technology is one of the elements in assisting the transition to a new power

system paradigm. Energy storage provides means to decouple generation and consumption in time, relaxing the generation-consumption constraint and assisting the system in responding to major power disturbances, as well as provides an alternative to conventional equipment for network reinforcement and ancillary services.

1.2 Research Focus and Objectives

The present thesis is aimed to address the problem of optimal siting, sizing, and technology selection of energy storage, which consolidates the necessary knowledge into a formal optimization problem, i.e., convex programming and mixed-integer programming. The main advantage of a formal optimization resides in the fact that it allows finding the globally optimal solution, which uniqueness is mathematically proven. Particularly, the numerical methods (i.e., zero-order methods, first-order methods) applied to strictly convex problems guarantee that the obtained optimum is global and unique. While the brute force for mixed-integer convex programming (MICP) problems requires solving a convex problem for every combination of fixed integer variables – whole enumeration. In this case, the globality of the solution is also indisputable and it corresponds to a particular combination of integer variables for which the solution of the convex problem possesses the least objective function (in case of the minimization problem). Even though partial enumeration algorithms allow reducing the search space of a mixed-integer problem, their performance is not guaranteed. In addition to that, the numerical methods used to resolve a convex optimization problem impose certain limitations on a problem formulation to ensure its tractability, uniqueness of a solution, and its accuracy. These limitations include using only equalities and inequalities to model energy storage and its environment, which have to be either linear or convex, and accurately represent their physical

equivalence. For the particular problem, these requirements are found contradictory as accurate modeling of energy storage, particularly storage degradation processes, can be hardly done with convex equalities and inequalities.

Consequently, the main research objectives are:

- 1) Describe how an energy storage investment decision and benefits can be translated into a formal optimization problem and what challenges does it possess to find the optimal solution.
- 2) Propose a problem formulation for optimal siting, sizing, and technology selection of energy storage systems for power system applications that takes into account the most relevant characteristics.
- 3) Develop a methodology that can be effectively applied to resolve the design problem of energy storage for big-scale networks and the number of energy storage technologies considered.
- 4) Examine the main driving factors for energy storage siting, sizing, and technology selection.

1.3 Research Overview and Contributions

A comprehensive literature review has been done to study the main driving factors for energy storage integration for power system applications. This includes studying a variety of energy storage methods, power system applications, methodologies applied to determine the site, size, and technology, the models used within the methodologies, and finally, a detailed analysis of the literature on formal optimization methods for the problem of optimal siting, sizing, and technology selection has been made.

Based on the studied literature, the formal optimization problem formulation has been proposed, which extends the state-of-the-art. Particularly, the optimal site, size, and technology of energy storage are found concerning the optimal operation of a prospective asset, as well as its degradation, which is expressed as an incremental decrease of the available storage capacity. Since energy storage degradation affects energy capacity (size) and it is driven by the operation of energy storage, considering both as variables results in nonlinear and nonconvex problem formulation. In addition to that, a degradation mechanism of lithium-ion (Li-ion) technology, which is a focus of the present thesis, is found to be neither a linear nor convex function of many variables that makes it challenging to apply within a formal optimization approach.

To resolve the problem of nonconvexity, a mixed-integer problem reformulation is proposed, where continuous variables that cause nonconvexity are replaced with integer ones with respect to which the rest of the problem remains convex. Thus, the optimal solution can be found with a consecutive optimization of the convex problem for various combinations of fixed integer variables following a particular partial enumeration algorithm, e.g., Branch-and-Bound algorithm. And since the performance of partial enumeration algorithms depends on the numerical case study and it is not guaranteed for a general case, the main drawback of the proposed mixed-integer problem reformulation resides in a scalability issue, where the combinatorial problem may become intractable with the increase of integer variables (network size and a number of storage technologies considered).

The search space of a combinatorial problem, such as MICP, increases in a power-law dependence with the number of integer variables, which in the case of the proposed reformulated mixed-integer problem increases with network size and a number of storage technologies. To

overcome the problem of tractability and scalability, the proposed MICP problem has been decomposed per each network bus and energy storage technology with augmented Lagrangian relaxation (ALR), where power balance constraints of the original problem have been relaxed and added to the objective function according to ALR principle. As a result of the problem decomposition, the search space of each subproblem has been decreased to a tractable number, which does not depend on network size and a number of considered storage technologies. The distinctive characteristic of the proposed problem decomposition resides in the fact that the resulting optimization subproblems are independent of each other, hence, can be solved in parallel which further increases computational efficiency.

The proposed problem formulation and resolution methodology has been tested on the IEEE 39-bus network for transmission congestion management application. The optimal combination of site, size, and storage technology has been found concerning the optimal power flow, the optimal scheduling of all power generation and consumption units, as well as the accurate degradation modeling of the Li-ion battery storage. Finally, the proposed framework has been applied to determine a performance value of the considered energy storage technologies to compare by how much a particular technology is overpriced compared to the most efficient storage solution. In addition to that, second-life storage performance has been evaluated to define its equivalent value compared to an off-the-shelf solution, which cannot be done otherwise as a conventional price formation cannot be applied.

To conclude, the original contributions of the research are the following:

- 1) A complex degradation characteristic of energy storage is incorporated into the formal optimization problem by means of mixed-integer problem reformulation, which allows considering a degradation function of any form.
- 2) ALR problem decomposition has been applied to resolve the problem of scalability and tractability when a sufficient amount of possible combinations of site, size, and technology are considered.
- 3) The proposed methodology allows the computationally tractable formulation of a stochastic optimization problem to account for future network operation scenarios.
- 4) An analysis performed within the proposed framework allows determining a performance value of various energy storage technologies, which is especially valuable for second-life energy storage.

1.4 Thesis Outline

An introductory Chapter 1 is dedicated to describing the background for the research, research focus, objectives, overview, and contributions.

A literature review is provided in Chapter 2. First, energy storage technologies that are used for power system applications are covered in Section 1. Then, power system applications provided by energy storage are described in Section 2. Methods for siting, sizing, and technology selection of energy storage systems are reviewed in Section 3. Mathematical models for energy storage and its environment are studied in Section 4. State-of-the-art methodologies for the optimal siting, sizing, and technology selection problems are examined in detail in Section 5. Finally, Chapter 2 ends up with conclusions in Section 6.

Chapter 3 provides problem formulation and resolution methodology for the problem of optimal siting, sizing, and technology selection of energy storage systems. First, in Section 1, a problem formulation is provided, which accounts for self-discharge, charge-discharge efficiency, battery degradation, but cannot be applied in formal optimization. Then, in Section 2, a detailed analysis of the problem formulation is conducted, where the main difficulties are examined. Section 3 provides a new problem formulation, which can be effectively solved with an off-the-shelf convex optimizer. Finally, Chapter 3 ends up with conclusions in Section 4.

The proposed problem formulation is tested in Chapter 4. First, a case study is described in Section 1. Results analysis of the optimal siting, sizing, and technology selection is performed in Section 2. The performance value of energy storage technologies, including second-life storage solutions, is performed in Section 3. Section 4 provides a discussion on siting, sizing, and technology selection decision making, methodology applicability, cycle counting method, computational time and convergence of the proposed algorithm. Finally, Chapter 4 ends up with conclusions in Section 5.

The concluding Chapter 5 is dedicated to consolidated the results. First, a summary of the research findings is provided in Section 1. The fulfillment of the research objectives is discussed in Section 2. Finally, Chapter 5 ends up with conclusions in Section 3.

Chapter 2. Review of the Literature

2.1 Energy Storage Technologies

Energy exists in various forms, including radiation, chemical, gravitational potential, electrical potential, electricity, elevated temperature, latent heat, and kinetic [5]. Energy storage implies transforming energy from a form that is hard to store to an easier and economically viable form. In a general sense, energy storage is a mean to capture energy produced at one time for use at a later time.

Energy storage methods comprise a wide range of technological approaches to provide a controllable power output to create a more resilient power system infrastructure and bring benefits to utilities and consumers. Energy storage technologies are categorized based on the physical state of energy during the time when it is stored. Energy storage technologies that are used in power system applications resides in the five main groups:

- 1) Electrical storage – electrical energy is stored in an electric or magnetic field.
- 2) Mechanical storage – electrical energy is converted into a potential or kinetic energy of a mechanical matter.
- 3) Thermal storage – electrical energy is converted into heat.
- 4) Electrochemical storage – comprises solutions to store electrical energy in a chemical form.
- 5) Hydrogen storage – electrical energy is converted into a gaseous fuel like hydrogen.

A general overview of energy storage technologies has been done by *Schwunk* in [6], where technical data of various technologies is aggregated in Appendix A and a comparison of typical rated power, energy capacity, and discharge time is illustrated in Figure 2.1.

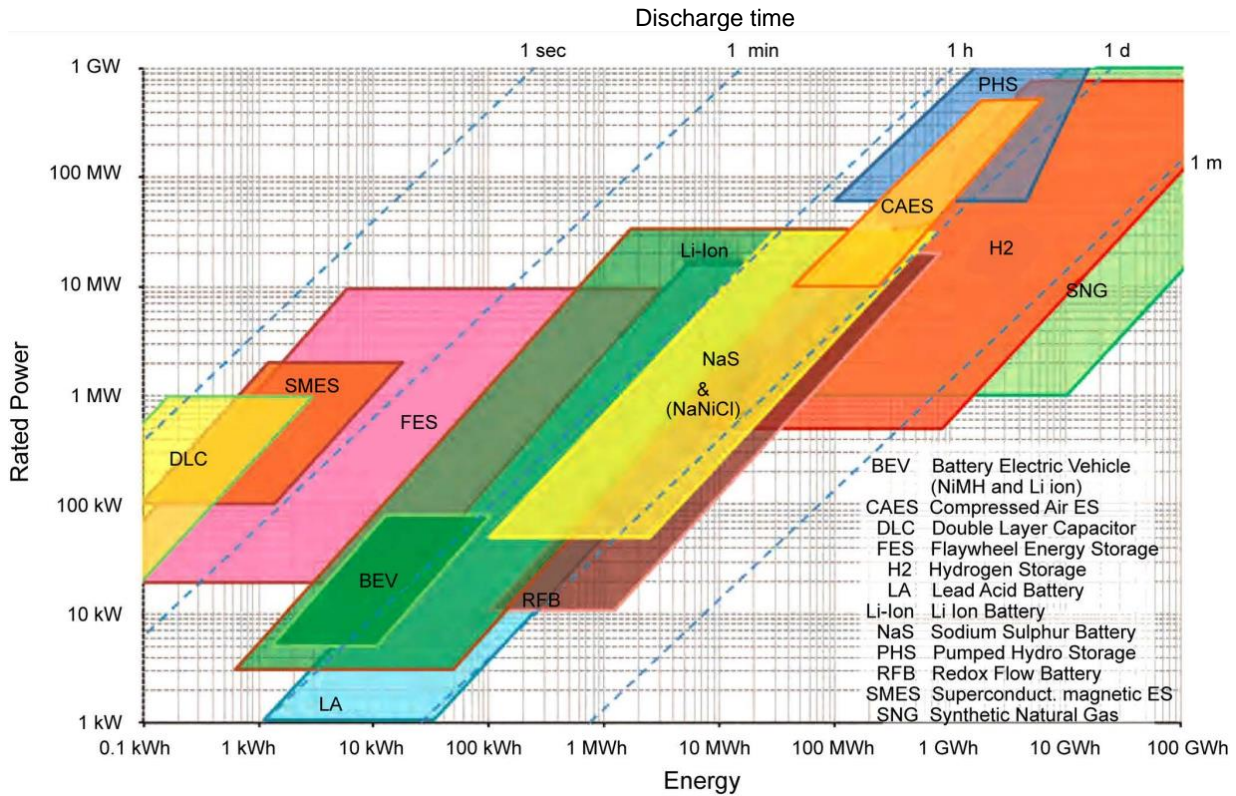


Figure 2.1: Typical power and energy capacities, and discharge time of energy storage technologies [6].

Comparison of capital, operating, and maintenance costs of different technologies have been performed by *Luo et al.* in [7], and it is depicted in Figure 2.2. The rest of the section is devoted to a description of each particular technology and methods used to store energy.

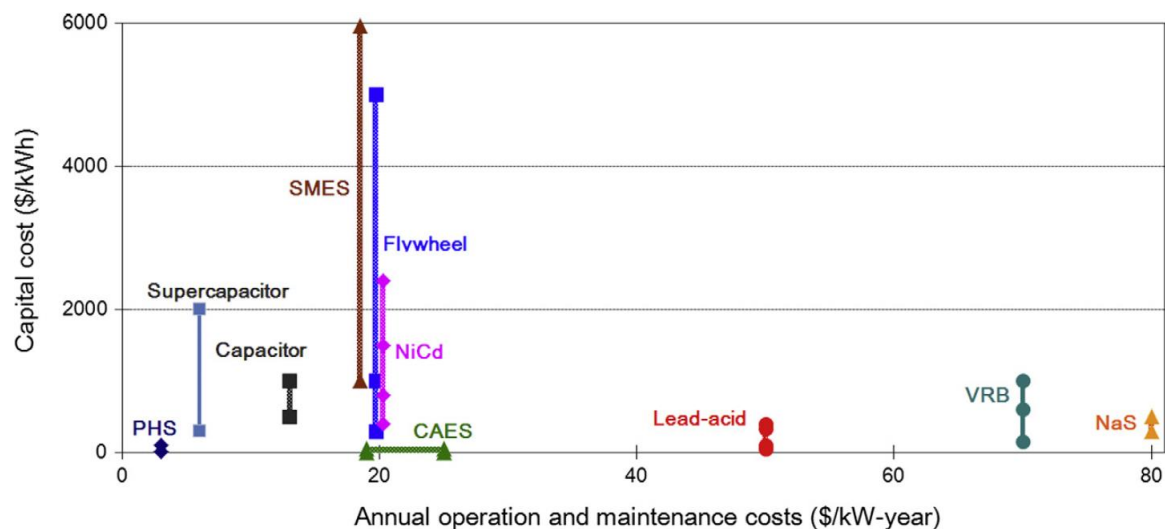


Figure 2.2: Capital cost and annual operating and maintenance cost for energy storage technologies [7].

2.1.1 Electrical Storage

Electrical storage methods are those where the electrical energy is stored in a magnetic field of a coil or an electric field of a capacitor. Conceptually, the latter is the best in terms of simplicity, reliability, and efficiency to obtain widespread use. However, due to the low gravimetric characteristics for energy density, capacitors did not find broad use in power system applications.

However, a superconducting magnetic energy storage system was one of the most promising technologies for power system applications in the 1980s resulting in big investments from the USA government, i.e., Department of Defense, which was looking at both defense system applications and the electric utility industry needs [8]. A typical superconducting magnetic energy storage system, depicted in Figure 2.3, includes three main parts: superconducting coil, power conditioning system, and refrigerator system. Energy is stored in

the magnetic field created by the flow of direct current in a coil which has been cooled to a temperature below its superconducting threshold [9]. When the superconducting coil is charged, the current in the coil will not decrease, and the stored magnetic energy can be kept until required. The stored energy is released by discharging the coil. Superconducting magnetic energy storage loses the least amount of electricity in the energy conversion process compared to other methods of storing energy [10]. However, because of the high energy needs for cooling and expensive superconducting wire, it is only used for short-term storage applications. Therefore, superconducting magnetic energy storage is most commonly devoted to improving power quality [11].

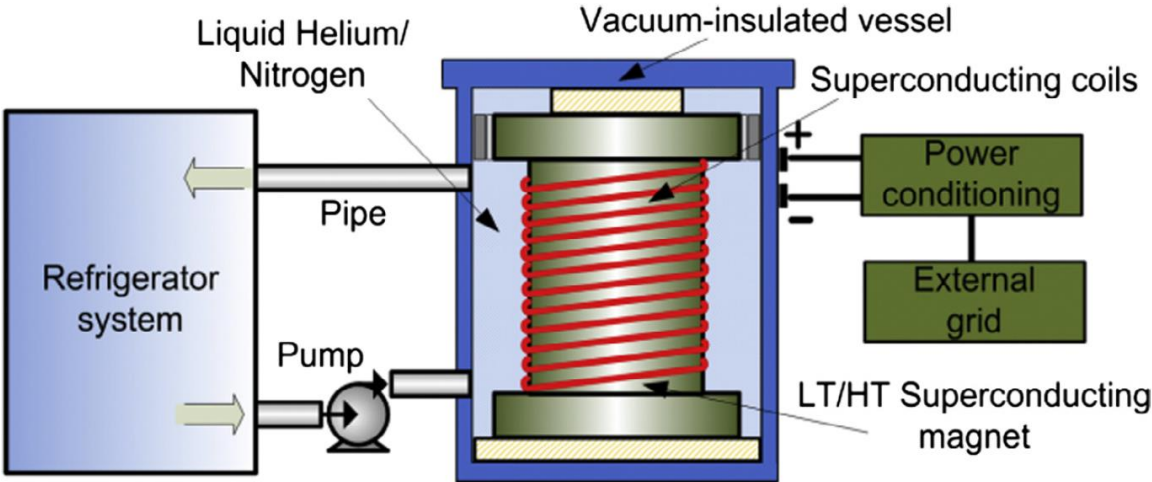


Figure 2.3: Schematic of superconducting magnetic energy storage [7]

2.1.2 Mechanical Storage

In mechanical storage, electrical energy is converted into a potential or kinetic energy of a mechanical matter. Energy can be stored into potential energy of water pumped to a higher level reservoir or by moving the solid matter to higher levels (gravity storage). Other commercially available mechanical methods include compressed air and flywheels. The grid

applications of a mechanical type of energy storage are manifold but yet specific for each type of technology.

Pumped hydro storage holds energy in the form of the potential energy of water pumped to a higher elevation from a lower level reservoir. Similar to hydropower station, the stored energy is released with the water flowing through turbines. Reversible turbine-motor assemblies can act as both pumps and turbines [12]. A reservoir of one kilometer in diameter, 25 meters deep, and an average head of 200 meters would hold enough water to store 10 GWh of energy [13]. A schematic diagram of a pumped storage facility is illustrated in Figure 2.4. Pumped storage, which is the largest form of energy storage used in power system accounting for more than 184 GW of installed capacity as of 2017 [14], is mainly used for bulk energy services and ancillary grid services, i.e., energy time-shift, supply capacity, frequency regulation, and reserve services [15].

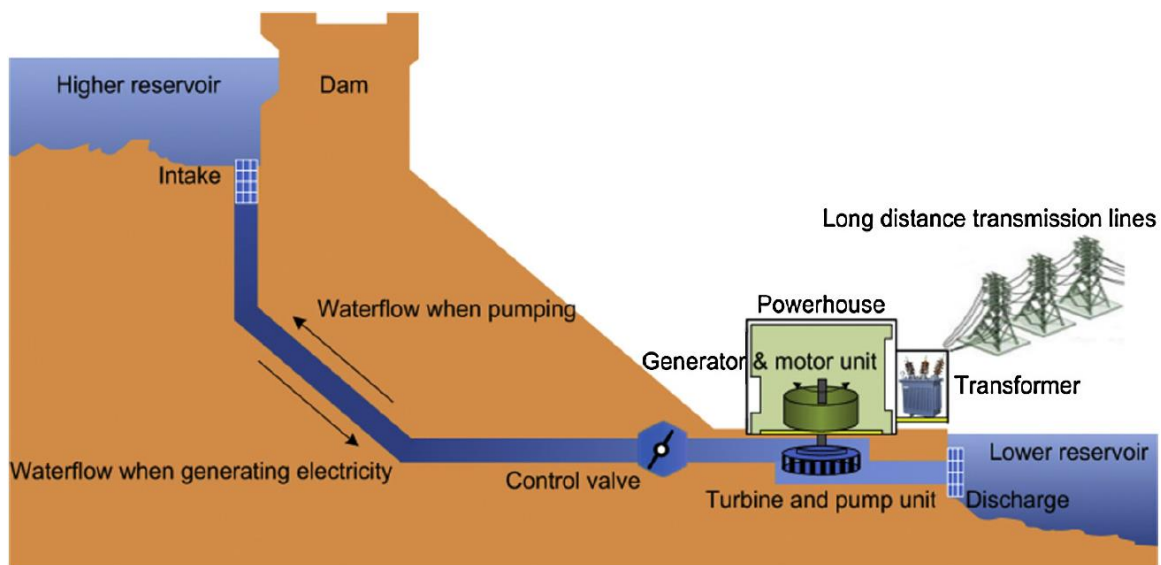


Figure 2.4: Schematic of pumped hydroelectric storage [7]

A similar principle of a gravitational potential might be applied to solid masses. In 2013 California Independent System Operator (CAISO) examined the potential use of earth-filled hopper wagons driven by an electric locomotive uphill and downhill [16]. Hopper wagon solution of gravitational potential energy storage possesses high-power and short discharge time characteristics, which are complementary with ancillary services, such as frequency response, spinning reserve, reactive power support, and ramping support for renewables [17].

An effect of gas compressibility is used in compressed air energy storage. A typical compressed air energy storage system, which schematic is depicted in Figure 2.5, includes six parts: a motor, a compressor, thermal storage, a cavern, an expander, and a turbine. Air from the atmosphere is pumped to a cavern using a compressor driven by a motor, which is powered by electric energy from the grid. Thermal storage is used to store heat from the air compression process when the storage system is being charged. When the storage system is discharging, the stored thermal energy is used to heat the released air, which would otherwise be much colder, resulting in a reduced efficiency [18]. The way to deal with the heat energy distinguishes the type of compressed air energy storage, which can be diabatic, adiabatic, or isothermal. Compressed air energy storage systems are used for bulk energy services and on-site renewable energy power plant-related applications for seasonal storage [19].

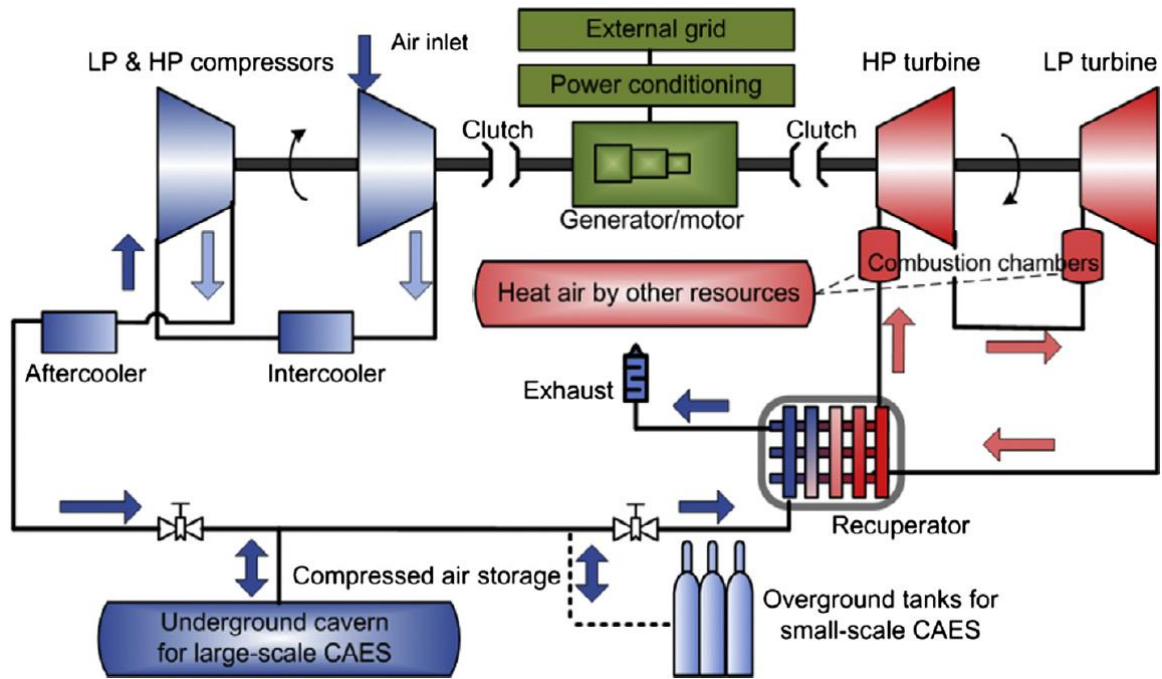


Figure 2.5: Schematic of compressed air energy storage [7]

Flywheel energy storage converts electrical energy to kinetic energy of a rotating mass by means of a motor, which acts as a generator when energy is released. State-of-the-art high-efficiency flywheel energy storage, which schematic is depicted in Figure 2.6, consists of vacuum enclosure, magnetic bearings, high inertia rotor, and brushless electric motor/generator. The rotating speed of a rotor may reach up to 50,000 rpm. Such flywheels can be fully charged or discharged within minutes, reaching a charge-discharge rate (C-Rate) of up to 20-30 C [20]. Due to the short discharge time, flywheel-based energy storage solutions are used for frequency response, short term spinning reserve, and ramping support for renewables [21].

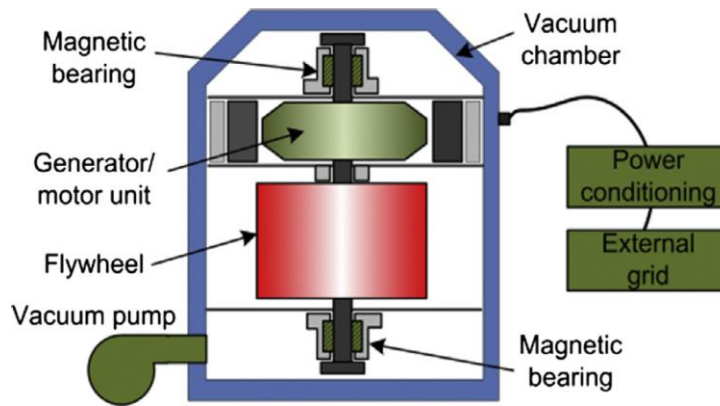


Figure 2.6: Schematic of flywheel energy storage [7]

2.1.3 Thermal Storage

Thermal energy storage technologies allow storing energy in the form of heat or cold to be used later at a required time. A well-insulated thermos is able to store energy effectively during a day or some times a week or a month. The main distinction between the methods used for thermal energy storage is the presence of a state change of coolant during the charge and discharge process.

Pumped heat electrical storage, which schematic is illustrated in Figure 2.7, is similar to the operation of a refrigerator. It contains two tanks filled with minerals (crushed rock or gravel), motor-driven compressor, expander driven generator, pipes that close circuit two tanks, and a coolant, usually, a monatomic gas such as argon. To store energy, the electrical energy from the grid drives the motor of a compressor to pump heat from the “cold tank” to the “hot tank.” To recover the energy, the expander uses heat energy from the “hot tank” to power a generator that produces electrical energy to the grid. The whole cycle occurs at the same pressure and aggregate state but with the temperature range of argon coolant from -160°C up to $+500^{\circ}\text{C}$ [12]. Pumped heat electrical storage is able to provide services that require response time in a matter of

minutes, which covers energy time-shift, frequency regulation, reserve services, and voltage support [12].

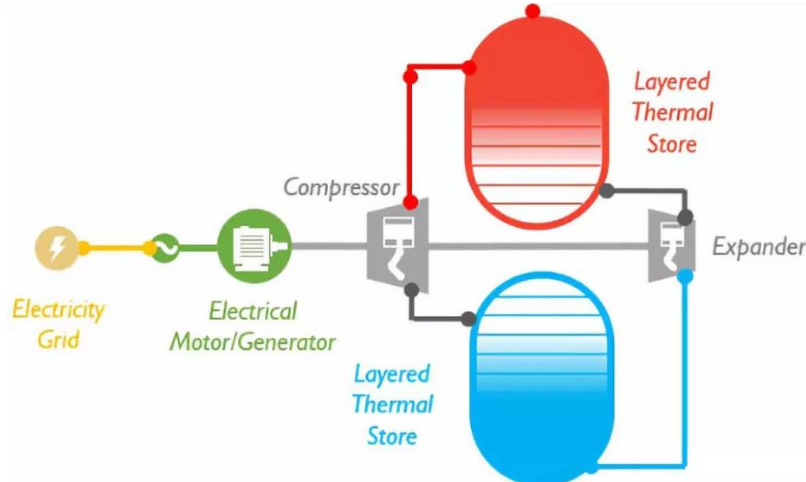


Figure 2.7: Schematic of pumped heat electrical storage [22]

Liquid air energy storage, sometimes called cryogenic energy storage uses liquefied air to create a powerful energy reserve. The schematic of liquid air energy storage is illustrated in Figure 2.8. The technology implies using electrical energy to cool air to a liquid state, storing it in a tank, and releasing the stored energy back by exposure of liquid air to ambient air or heat generated from the liquefaction stage. Liquid air energy storage contains the following equipment: compressor, refrigerator, liquid air storage, cold and heat thermal storages, expander, and generator. Liquid air energy storage systems use off-the-shelf components with a long lifetime of more than 30 years, resulting in low technology risk [12]. The system is well suited for long-duration applications, such as bulk energy services [23].

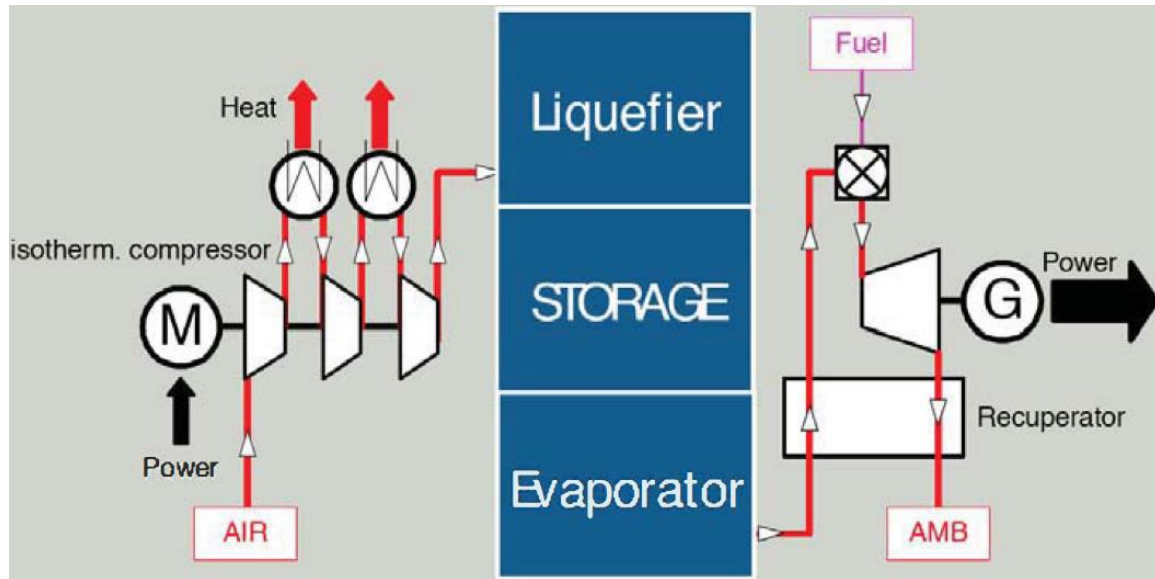


Figure 2.8: Schematic of liquid air energy storage [24]

2.1.4 Hydrogen Storage

In hydrogen energy storage, electrical energy is stored in the form of fuel – hydrogen – and the energy can be retracted at a required time through the oxidation process. Hydrogen energy storage includes three stages: hydrogen production, storage of hydrogen, and re-electrification.

Hydrogen is produced from water using electrolysis, where direct current is used to drive the chemical reaction. Currently, there are two techniques applied. Alkaline electrolysis is a well-developed technology suitable for large storage. A more mobile proton exchange membrane electrolyzers are applied for small systems. The conversion efficiency for both technologies is about 65%-70% [25]. The obtained hydrogen can be stored in several forms, including liquid, compressed gaseous, and compressed liquid. High-pressure storage has a good energy density per unit weight but very poor energy density per unit volume, while cryogenic storage implies

liquefaction of hydrogen, which improves energy density but requires additional energy to be applied to cool it down to 20 K (boiling point). Re-electrification of hydrogen may be done in fuel cells with an efficiency of up to 50%, or it can be burnt in a gas power plant with an efficiency of up to 60% [26]. A schematic diagram of hydrogen energy storage is depicted in Figure 2.9. Despite the low efficiency, hydrogen energy storage is of serious interest for power system applications. In many scientific papers, hydrogen energy storage is considered for power output smoothing of intermittent energy sources, i.e., solar and wind [27]. The application of hydrogen energy storage is not limited to grid applications. Particularly, the power-to-gas application implies converting electrical energy to a gaseous fuel. Blending with natural gas, the energy can be transmitted to a consumer through a gas pipe [28].

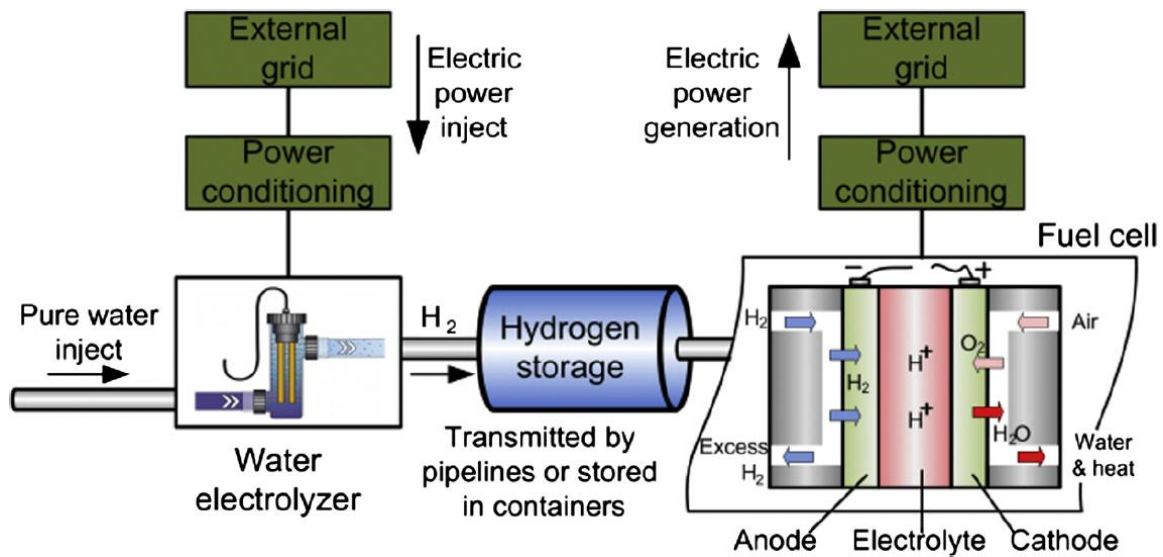


Figure 2.9: Schematic of hydrogen energy storage [7]

2.1.5 Electrochemical Storage

Electrochemical storage solutions comprise methods to store electrical energy in the form of chemical energy contained in the active materials, which is converted to electrical energy by

means of the reversible oxidation-reduction process [29]. This involves a substantial number of technologies, including lead-acid batteries, electrochemical capacitors, flow batteries, and Li-ion batteries.

A lead-acid battery contains two electrodes, positive (made of lead dioxide) and negative (made of lead), which are immersed in a water solution of sulphuric acid. A schematic of a lead-acid battery is illustrated in Figure 2.10. In the discharged state, both electrodes become lead sulphate, and the electrolyte loses much of its dissolved sulphuric acid and becomes water primarily [30]. When completely charged, the negative electrode consists of lead, and the positive electrode consists of lead dioxide, while the electrolyte becomes concentrated sulphuric acid, which stores most of the chemical energy. There are two typical types of lead-acid batteries: flooded and sealed valve-regulated solutions. A flooded solution is less expensive but requires regular maintenance to check for the electrolyte level and require good ventilation at the place where it is installed as it may produce flammable hydrogen during the operation [31]. Valve regulated lead-acid battery type is specially designed to be low-maintenance and fireproof. The main advantages of lead-acid batteries are high energy efficiency, low self-discharge rate, and low up-front cost [31]. In a power system, lead-acid batteries are used for various applications, which include renewable power output smoothing, power reliability, reserve, time-shifting, and power quality [13].

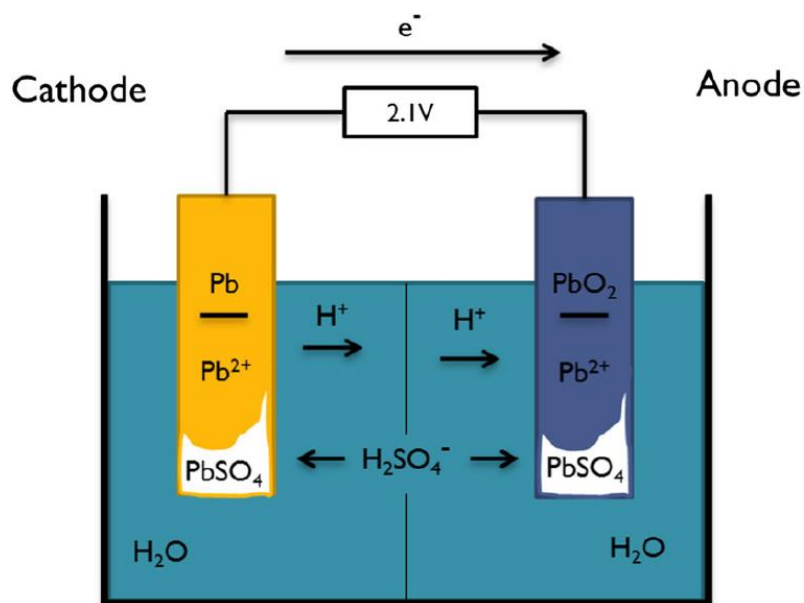


Figure 2.10: Schematic of lead-acid battery [32]

Electrochemical capacitors or electric double-layer capacitors contain two electrodes, an ion-permeable membrane, and an electrolyte that ionically connects the electrodes. A schematic of the electrochemical capacitor is depicted in Figure 2.11. When the electrodes are exposed to an applied voltage, ions in the electrolyte form an electric double layer charge of opposite polarity on the electrode. The capacity kept in a double-layer capacitor is mostly a function of the electrode surface area. High power-dense electrochemical capacitors are applied mostly for ancillary services, i.e., frequency response, voltage control, load following, and ramping support for renewables [33]. Some asymmetric (with different materials for the two electrodes) electrochemical capacitors are specifically designed for long charge and discharge applications, such as bulk energy services [12].

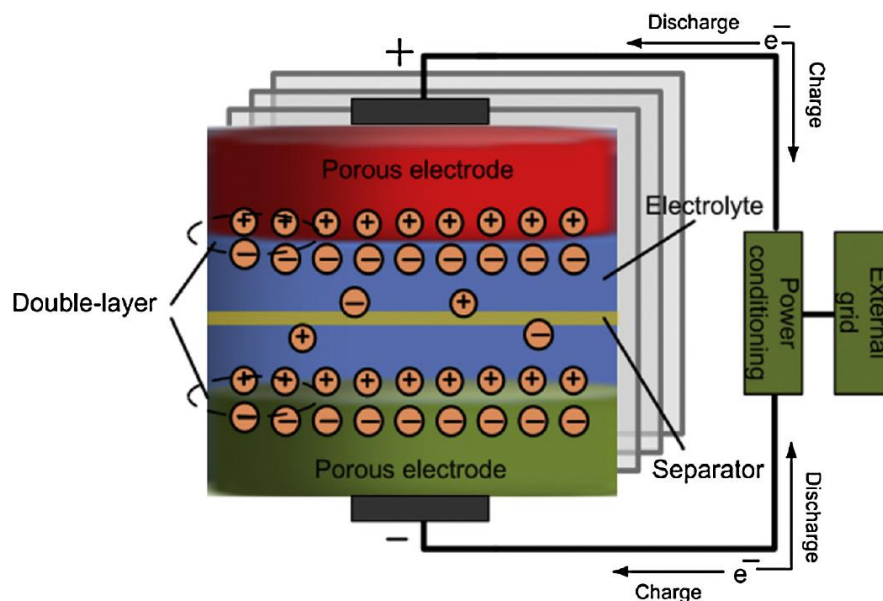


Figure 2.11: Schematic of electrochemical capacitor [7]

A flow battery or redox flow battery is a type of electrochemical cell where energy is stored in two liquid solutions separated by a membrane, which circulates in each own system. A schematic of a flow battery is depicted in Figure 2.12. The energy capacity is determined by the volume of both electrolytes, and the power capacity is determined by the size of the membrane. The most widely used flow batteries in power system applications are vanadium redox flow and zinc-bromine flow batteries. Flow batteries are specifically designed for long charge and discharge applications, such as bulk energy services and renewable energy related applications.

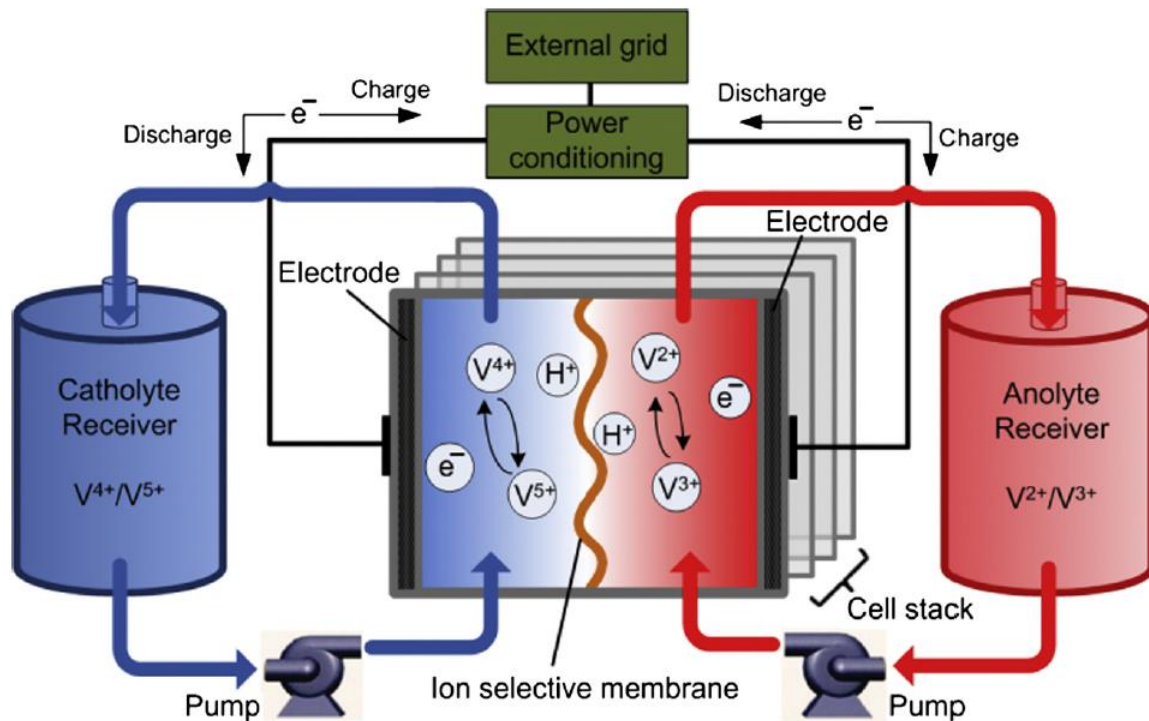


Figure 2.12: Schematic of vanadium redox flow battery [7]

The most advantageous electrochemical energy storage is considered to be Li-ion technology. The main advantages of Li-ion batteries compared to other batteries resides in the high energy density, high efficiency, long cycle lifetime, and environmental friendliness [29], [31], [34]. The term “lithium-ion” refers not to a single electrochemical couple but to a wide array of different chemistries, all of which are characterized by the transfer of lithium ions between anode and cathode during the charge and discharge reactions [35]. A schematic of a Li-ion battery is illustrated in Figure 2.13. During the charge, ions of lithium (Li^+), which carry a positive charge, are deintercalated from the cathode oxide compound and stored into the lattice space of the anode. When the battery is charged, the cathode is short on Li^+ , whereas the anode is rich on Li^+ which results in the voltage difference. During discharge, the voltage difference between anode and cathode induces a current into a circuit and Li^+ travel back to cathode

reducing the voltage difference, hence, the charge of a battery. Li-ion batteries have been deployed in a variety of power system applications, which include all ancillary services, transmission and distribution infrastructure applications, customer energy management applications, and sometimes bulk applications [36].

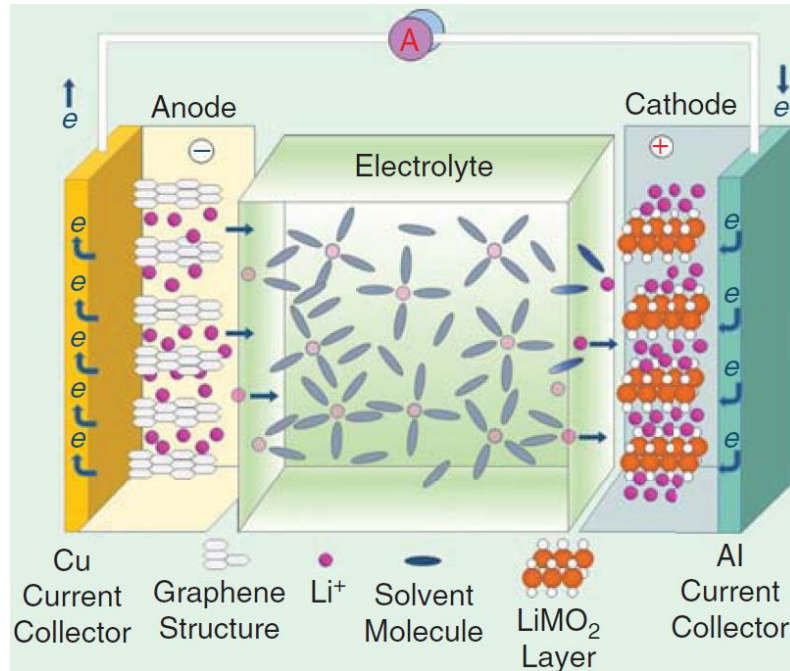


Figure 2.13: Schematic of Li-ion battery [31]

According to IEC White Paper: Electrical Energy Storage [34] and Sandia National Laboratory Report [37], Li-ion technology has the greatest potential for many power system applications and the recent increase in production and deployment supports this point [14]. Even though Li-ion batteries possess a long cycle lifetime, the available capacity loss due to degradation, which is mostly influenced by storage operation [38], requires performing operation and degradation aware techno-economic analysis, which results in a nonlinear and nonconvex optimization problem formulation. In addition to that, degradation characteristics of Li-ion technology is found to be a complex function of many variables that make it challenging to apply

within formal optimization [38]–[40]. All of the above make Li-ion based storage to be the perfect choice to resolve a relevant and timely problem and to show how a complex degradation function can be incorporated into a formal optimization problem. More details on Li-ion based energy storage operation and degradation are provided in Section 2.4 of the present chapter, where models of Li-ion storage are studied.

2.2 Energy Storage Applications

Energy storage technologies have been used for more than 100 years. Before the middle of the 1980s, energy storage was used only to shift the energy in time from coal power station off-peak to replace natural gas stations on-peak so that coal station remained at the optimal power generation state as system demand varied [13]. The physical realization of the conventional energy storage system was done in the form of the pumped hydro storage facility. Environmental opposition for building more pumped hydro energy storage, developments in other technologies (i.e., electrochemical, thermal, mechanical), and power system deregulation resulted in a growth of energy storage applications that can be provided to a grid.

In [12], The Energy Storage Association identifies 18 grid energy storage applications, which are consolidated into four groups: bulk energy applications, ancillary services, transmission and distribution infrastructure applications, and customer energy management applications. Table 2.1 provides the list of energy storage applications and their attributes to a particular group, which are studied in more detail within the present section.

Table 2.1: Energy storage applications

#	Application	Group
1	Electric Energy Time-Shift (Arbitrage)	Bulk Energy Applications
2	Electric Supply Capacity	
3	Regulation	Ancillary Services
4	Spinning, Non-Spinning and Supplemental Reserves	
5	Voltage Support	
6	Black Start	
7	Load Following	
8	Frequency Response	
9	Ramping Support for Renewables	
10	Transmission Support	Transmission and Distribution (T&D) Infrastructure Applications
11	Transmission Congestion Management	
12	T&D Upgrade Deferral	
13	T&D Equipment Life Extension	
14	Substation On-site Power	Customer Energy Management Applications
15	Power Quality	
16	Power Reliability	
17	Retail Electric Energy Time-Shift	
18	Demand Charge Management	

Energy and power requirements for power system applications are reported by The International Energy Agency in Energy Storage Technology Roadmap [41]. Particularly, power and discharge duration requirements for some applications are illustrated in Figure 2.14. Table D.1 in Appendix D summarizes the applications' requirements for typical discharge time, power, and energy capacities of energy storage.

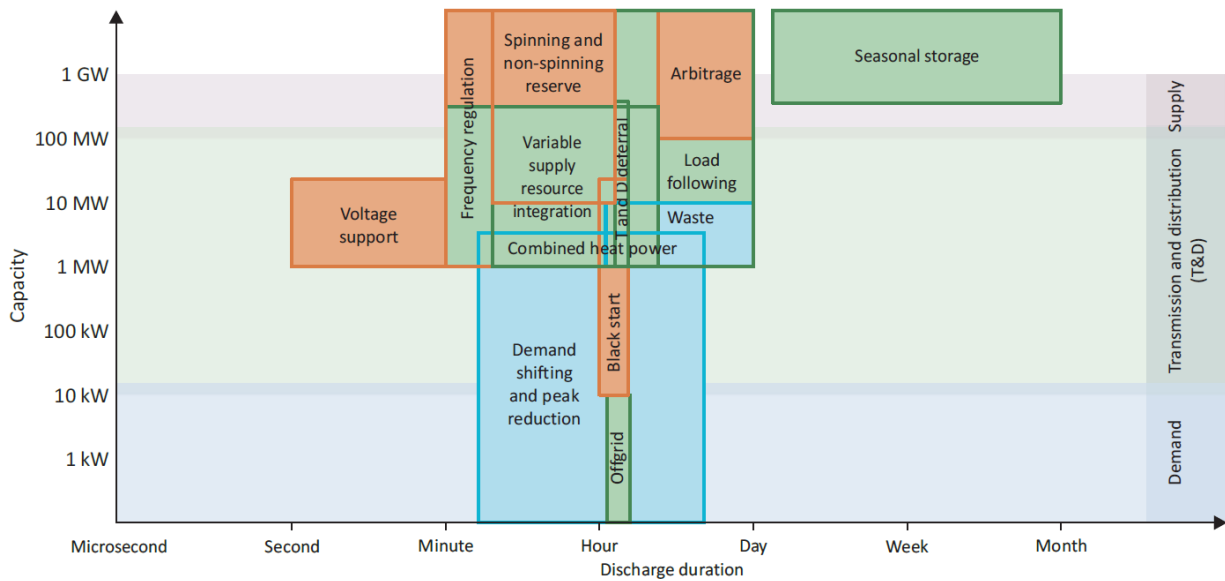


Figure 2.14: Power and discharge duration requirements for energy storage applications [41].

The financial benefit and maximum market potential of energy storage providing the applications are studied for the USA power system by Sandia National Laboratories in [37]. Figure 2.15 summarizes the obtained results, according to which most of the benefit from energy storage comes from on-site substation needs and frequency regulation (Area Regulation) service. However, the market potential for the applications is near zero. Most of the potential is expected for electric energy time-shift applications, including retail electric energy time-shift (Time-of-use Energy), renewable energy time-shift (RE Time-shift), as well as ramping support for renewables (RE Firming), and transmission congestion management (Transmission Congestion).

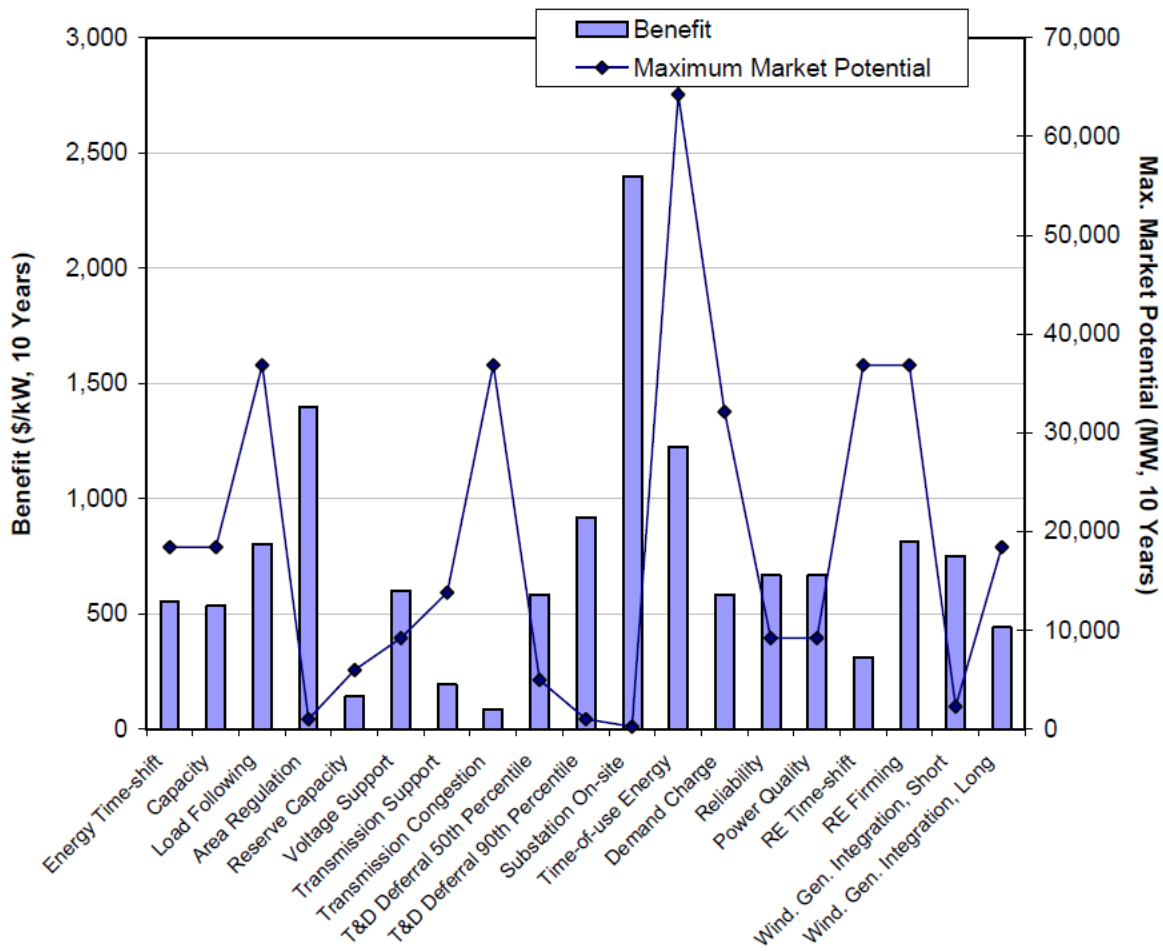


Figure 2.15: Application-specific 10-year benefit and maximum market potential estimates for the U.S. [37]

2.2.1 Bulk Energy Applications

In bulk energy type of applications, energy storage is used to provide energy and supply capacity during peak demand periods. The benefits of bulk energy applications include reduced expenses for energy production and a lesser need for generation assets. Energy production expense reduction comes from the reduced fuel consumption and reduced wear and tear of generation units. The capacity benefit is associated with the reduced need for generation assets,

i.e. power capacity [42]. In other words, the benefit from energy storage arises from the reduced or avoided cost related to building and owning new generation equipment.

The main principle of the electric energy time-shift application is shown graphically in Figure 2.16. In the operational timescale, it implies price arbitrage, which is well studied in economics. Energy time-shift application implies to use cheap energy during the time of high demand when the price to buy it is high (e.g., peak demand periods). The high price for energy during peak demand periods is a result of high demand, and the high production cost for electricity during, mainly because the least cost-effective generator is used. Time-shifting may be done by electric utilities to reduce energy-related cost or by merchant storage owners seeking to profit by time-shifting of wholesale electric energy – buying low and selling high [42]. A typical energy storage solution for time-shifting operation may vary from 1 MW to 500 MW with a discharge duration from minutes up to eight or more hours. Energy storage used for energy time-shift from a photovoltaic or a wind farm would be in the lower end of the typical size and discharge duration ranges, while energy storage used for utility-wide arbitrage can be found in the upper end of the size and discharge duration ranges [13]. The problem of optimal siting, sizing, and technology selection of energy storage systems for efficient network operation was studied by the author during the Ph.D. program and reported in [43].

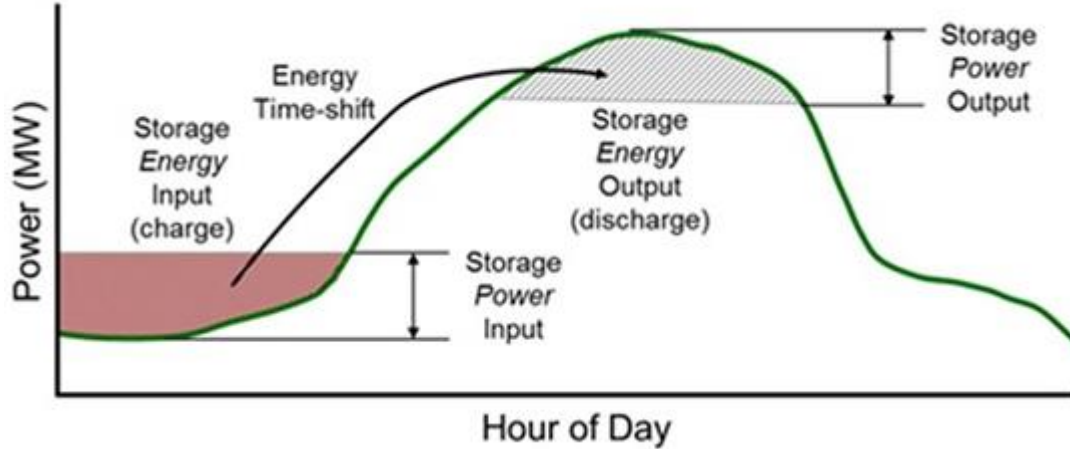


Figure 2.16: Electric energy time-shift application [12]

Electric supply capacity or peaking capacity is the other side of time-shifting, where energy storage deployment compensates the need for peaking generation assets resulting in an electric supply capacity benefit. By how much energy storage integration reduces the need for generation equipment is indicated by the storage power output in Figure 2.16. The reduced need for power capacity corresponds to the amount of installed storage capacity. Storage may be used for electric supply capacity by a utility to reduce capacity-related costs or by merchant storage owners seeking profit in a regional capacity market [42]. The typical size of storage for electric supply capacity application ranges from megawatts to hundreds of megawatts. Discharge duration is determined by the pricing principle, for example, if capacity is priced for a specified period of time (e.g., six hours), then energy storage must be able to provide energy during an entire time period. If capacity is priced per hour, then energy storage discharge duration is flexible [13].

2.2.2 Ancillary Services

According to the Federal Energy Regulatory Commission of USA [44], ancillary services are “those services necessary to support the transmission of electric power from seller to purchaser given the obligations of control areas and transmitting utilities within those control areas to maintain reliable operations of the interconnected transmission system.” In other words, the functions delivered by generation, transmission, distribution, system control, and other equipment to support the operation of a power system are called ancillary services.

The flexibility of energy storage technologies is well-matched for the provision of ancillary services required for efficient, stable, and reliable operation of the power system. Energy storage use for ancillary services compensates the need for conventional assets, i.e., generation units, capacitor banks, FACTS devices, and the costs associated with their operation.

Frequency regulation – is one of the ancillary services that implies instant coordination of energy production and consumption mismatch. The primary purpose of frequency regulation is to maintain the stability and accuracy of the system-wide alternating current (AC) frequency [45]. The principle of frequency regulation is shown in Figure 2.17. During the excessive supply, when energy production exceeds consumption, frequency regulation down is required to reduce the difference. In a reverse situation, during a supply deficit, when energy production is short, frequency regulation up is required to reduce the difference. With the increased share of RESs in the generation mix, i.e., wind turbines and photovoltaics, the electric supply curve (green line) will vary similar to demand, which actually is a result of intermittent power generation. In the context of energy storage, frequency regulation up corresponds to storage discharging, while regulation down corresponds to charging. Energy storage with a fast ramp rate characteristic that

is designed for at least 15 minutes of charge/discharge is especially suited for the service. Energy storage with a high ramp rate is almost twice as effective as conventional resources, which ramp rate is slow [46]. The typical capacity for frequency regulation service is from 10 to 40 MW with a discharge duration from 15 minutes to one hour. The annualized number of cycles may reach 10,000.

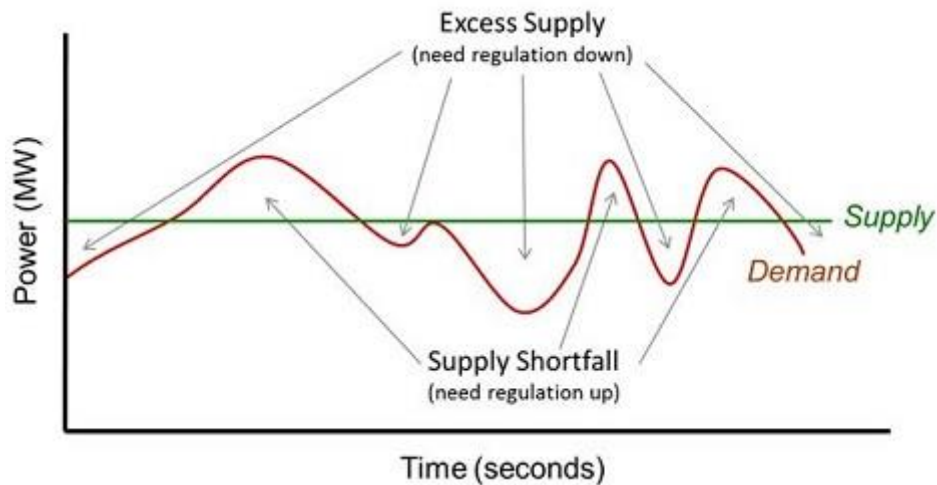


Figure 2.17: Frequency regulation principle [12]

Spinning, non-spinning, and supplemental reserves are three types of backup generation to be called if a large power source becomes accidentally unavailable. Bringing energy storage as an electric supply reserve is considered as an offset of generation-based reserve resulting in benefits associated with avoided or reduced cost of buying and owning generation resources. Energy storage can provide reserve mostly by being ready to discharge as in reality, these types of reserve are needed not frequently, while generation-based spinning reserves must be spinning and ready to pick up a load on short notice [45]. The amount of reserve capacity required is defined by electric supply reliability-related standards (typically, from 15 to 20% of the nominal capacity) [37]. Since it is uncertain where exactly a possible disturbance will occur, energy

storage systems have to be strategically placed within a network to be able to respond to any unexpected shutdown of a generation unit. Since a non-frequent operation is expected, a small cycle lifetime energy storage can be used for the reserves.

Voltage support or reactive power support is provided by reactive power sources to keep the voltage within statutory limits. Historically, reactive power support is delivered by generation assets that can produce reactive power to offset reactance of the lines and cover reactive power demand of loads [47]. Energy storage, along with power electronics technologies, created an alternative for voltage support provision. Distributed energy storage, which can be located close to an end-consumer, where voltage level is required to be maintained, is especially attractive because reactive power cannot be transmitted extensively over long distances [48]. A big share of power outages is at least partially related to problems of transmitting reactive power to load centers [49]. Apart from costly outages, electrical energy is a commodity, which has to meet certain power quality standards. The voltage level is the main power quality characteristic, which has to be satisfied to be bought by a customer. Energy storage systems have to be strategically placed in a network to ensure voltage stability at an end-customer site. The power capacity is derived from the amount of reactive power required to compensate for voltage drop. Cycling requirements are not applicable for this type of service as reactive power injection, and absorption does not lead to the actual charge/discharge cycling. A study of the centralized and distributed voltage control techniques in future network conditions has been performed by the author during the Ph.D. program and reported in [50].

Black start resources are used to restore service of the grid after a blackout. Conventionally, the black start service is provided by specially equipped generators that are able

to start up without power from the grid [51]. Energy storage is well-suited to perform as a black start resource due to the fact that unlike thermal generators, it does not require comprehensive machinery, and it does not have to run in idle mode while waiting for the call. Energy storage based resources may be used by electric utilities to offset or replace the need for black start generation units to be built and spinning. Energy storage for black start purposes is typically sized from 5 MW to 50 MW with a discharge duration from 15 minutes to one hour [13]. Cycling requirements are minimal, as the service is very rare.

Load following service is needed during the “shoulder hours” in the daily demand profile. The shoulder hours happen twice a day when power demand grows rapidly in the morning when a community wakes up and gets ready for work, and when power demand decreases in the evening as activities reduce and people go to sleep. As shown in Figure 2.18, load following up is provided when electric demand increases, and load following down is provided when demand decreases. The main benefit of load following is the offset of ramping generation resources. Other benefits are related to reduced generation output variability and reduced part load operation of a generation, which, in turn, may lead to reduced fuel use and air emissions and may reduce generation equipment wear and extend its life [45]. The typical size of energy storage for load following application ranges from 1 MW to 100 MW with a discharge duration from 15 minutes to one hour [13]. As the demand profile repeats everyday, load following up and down is provided on a daily basis.

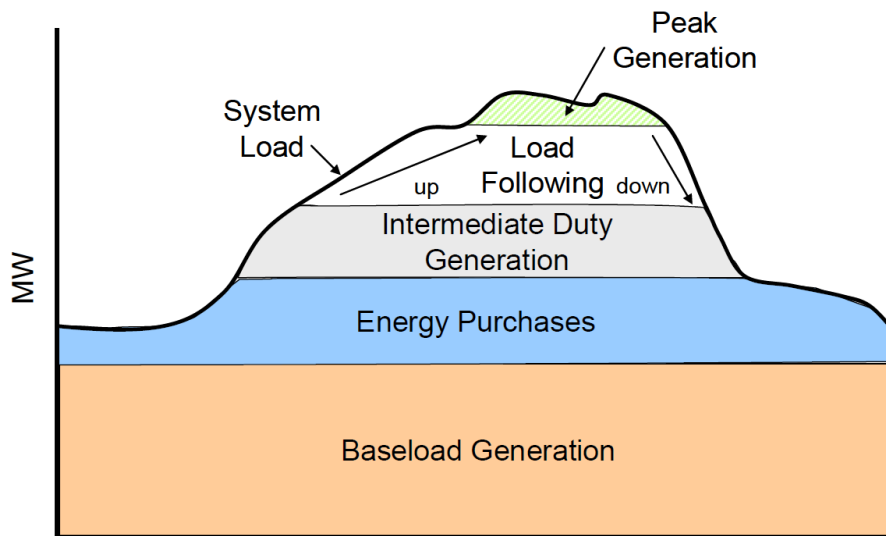


Figure 2.18: Load following illustration [37]

Fast frequency response generation equipment tracks the grid frequency and responds to a frequency deviation. At present, there are not many conventional generation resources, which ramp rate is high enough to respond to second or sub-second signals [12]. Flexible and responsive energy storage is especially well-matched for frequency response. Energy storage used for the service is able to respond to frequency anomalies in millisecond timeframes to keep the AC frequency close to 50 Hz. Storage used for frequency response service reduces the need for conventional generation resources, reduces the number of on-off switches, power output fluctuations, and underload operation what leads to a reduction of fuel consumption and air emission. Conventionally, the capacity for frequency response service provided by fossil-fueled generators is around 2% of normal operating capacity [46]. The studies showed that fast frequency response performed by energy storage is able to reduce power capacity reserved for this service twice [46]. Siting of energy storage is a nontrivial issue, and it plays a significant role in the effectiveness of frequency response and system stability.

The ramping ancillary service is aimed to compensate output ramping of renewable generation and provide a smooth power output of the integrated system. Photovoltaic and wind farms are the most vivid examples of intermittent generation sources due to the intermittent nature of a primary energy source – wind speed and solar radiation. Energy storage used for ramping service provides ramping up by discharging. Conversely, storage provides ramping down by charging. Ideally, the overall power output of a renewable generation unit, in conjunction with ramping support resources, should provide stable power output irrelevant to the intermittence of a primary energy source. The benefits for the use of energy storage for ramping service are the reduced need for generation capacity, reduced generation start-ups, reduced generation output variability and part load operation, reduced wind and solar energy spillage, and thus, reduced fuel use and air emission [45]. For ramping support service, usually energy storage is installed next to a RES or a point of common coupling [52]. Sizing requirement is dictated by the capacity of a renewable source and a primary energy source intermittency to analyze which historical data is usually used. Frequent operation of prospective energy storage allows using only those technologies that are characterized by a significant cycle lifetime [13].

2.2.3 Transmission and Distribution Infrastructure Applications

Transmission and distribution (T&D) infrastructure applications are those which involve energy storage to improve the performance of the existing assets, increase their service lifetime, avoid or defer the need for additional T&D equipment, and manage congestions. Relatively small-sized energy storage is capable of providing significant benefits associated with T&D infrastructure development [13].

Energy storage is capable of improving the utilization rate of the transmission system by increasing the overall load carrying capacity. A benefit occurs when an extra load carrying capacity defers the need to install conventional equipment. Transmission support is provided by well-located storage that improves T&D system performance by compensating for electrical anomalies and disturbances, such as voltage sags [53]. A typical power capacity ranges from 10 MW to 100 MW with a discharge duration from two to eight hours. Cycling requirements reach 50 cycles per year on average [13].

Transmission congestion management is required if available least cost energy cannot be transferred to some loads when transmission facilities cannot support that. This leads to congestion costs associated with non-uniform locational marginal prices on a wholesale electricity market. To resolve that energy might be stored at the receiving end of a transmission line during the off-peak periods as nights or weekends. Then the stored energy is released during the high demand time to decrease the amount of power that has to be transmitted by the transmission system during peak demand time. The transmission congestion management benefit accrues if storage use reduces congestion-related charges [53]. Also, energy storage utilization increases total energy transmission during a day, increasing asset utilization rate. This implies that a significant amount of energy is transmitted during the low demand periods to storage located near load aggregation [54]. To reduce transmission congestion, storage is installed at one or more locations that are electrically downstream from the congested portion of the transmission system [53]. Typical capacity ranges from 1 MW to 100 MW with a discharge duration from one to four hours. Usually, congestion management is required on a seasonal basis, which requires the annual number of cycles to be no more than 100 [13].

T&D upgrade deferral implies using small amounts of storage to postpone or avoid investments in transmission or distribution system development. Consider a transmission line as in Figure 2.19, which load-carrying capacity approaches its thermal limits. The conventional solution is to increase its capacity by installing a new power line, which in practice is done lumpy by 33% or 50% increase [55]. In some cases, installing a small amount of energy storage downstream from the nearly overloaded transmission line could defer the need for the upgrade for a few years until the lumpy capacity increase becomes more viable [13]. For transmission and distribution upgrade deferral application, the benefit arises when the upgrade of equipment can be postponed or avoided. The benefit can be as high as a few hundred dollars per kW of storage for one year of deferral [53]. Similarly to the previous application, energy storage has to be installed electrically downstream from the overloaded transmission line. Typical capacity for distribution upgrade deferral ranges from 0.5 MW to 10 MW with a discharge duration from one to four hours. In case of a transmission system, the size ranges from 10 MW to 100 MW with a discharge duration from two to eight hours. In both cases, the service is required no more than 100 times per year [13]. The problem of optimal sizing and technology selection for infrastructure upgrade deferral has been studied by the author during the Ph.D. program and reported in [56].

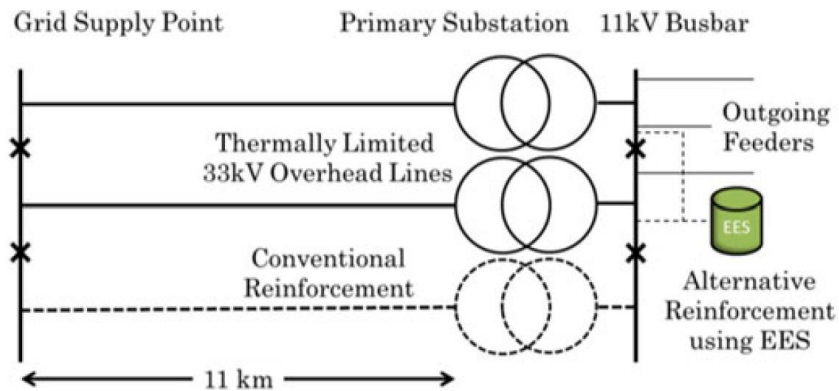


Figure 2.19: Upgrade deferral principle [55]

As for the previous application, small amounts of energy storage are able to prolong the useful lifetime of T&D assets when storage deployment compensate loading of the existing equipment that is near the end of its lifetime. One of the examples of such an application is the use of small amounts of storage to compensate peak loading of an old transformer that is near the end of its lifetime [57]. Lifetime extension is particularly attractive where underground lines and transformers are located in highly developed and densely populated city areas, where replacement and maintenance costs are high, the disruption would be significant during construction, and work permits can be expensive and challenging to acquire [53]. Energy storage has to be installed in a way that reduces the loading of T&D equipment that requires lifetime extension. Typical capacity for distribution upgrade deferral ranges from 50 kW to 1 MW with a discharge duration from one to four hours. In the case of a transmission system, the size ranges from 1 MW to 10 MW with a discharge duration from two to eight hours. An average annual number of charge and discharge cycles reaches 100 [13].

Substation on-site back-up application is the most widely used application of energy storage [37]. In this case, storage is needed at substations to provide back-up power to communication and control equipment when power from the grid is not available.

2.2.4 Customer Energy Management Applications

Energy storage can provide at least four benefits for electricity end-customer. Two of them are bill management related applications, which include reduced energy costs and demand charges. Power reliability and power quality improvements are two other applications of energy storage for an end-customer.

End-users can use storage to reduce energy costs by storing energy when the retail price for it is low, so the energy can be used later during times when the high energy price is applied. Retail energy time-shift application is similar to bulk energy time-shift with the distinction being that the price for energy is based on the retail tariff, which is fixed and specified in the contract. The typical size of energy storage for retail energy time-shift application ranges from 1 kW to 1 MW. Discharge duration ranges from one to six hours, and it is determined based on a particular tariff to cover the peak price period. The charge and discharge cycle happens on a daily basis, which yields 250 cycles per year (one cycle per labor day).

An attractive energy storage use for electricity end-customer is related to the reduction of demand in a way that the charges for peak demand are reduced or avoided. The opportunity for demand charge management comes from utility tariffs for commercial electricity customers with high power requirements, where different charges for power and energy are applied [58]. Power related charges depend on the customer maximum power consumption during high demand time periods. To reduce power charges, energy storage is charged when demand charges

are low, and the stored energy is used during the high demand charge periods. The typical size of energy storage for demand charge management ranges from 50 kW to 10 MW with a discharge time from one to four hours and 250 cycles per annum [13].

The storage can be used to protect on-site electric equipment from various effects associated with low power quality. With the increase of demand and renewables penetration, power quality problems tend to be more frequent. The main power quality problems include voltage sag or surge, high-frequency disturbances, flicker, blackout. The benefit from energy storage for power quality applications is based on an avoided cost related to the non-optimal operation of electric equipment, equipment downtime, and its damage. Commercially available energy storage for power quality application ranges from 100 kW to 10 MW with a discharge time from 10 seconds to 15 minutes. Annual cycles requirement is a case-specific and may reach 200 cycles per year [13].

Power reliability application of energy storage is aimed at the uninterruptable power supply, an example of which is applied as the uninterruptible power supply used in business and homes. Energy storage can back-up customer loads in case of the power supply failure. This requires islanding of customer sites, including energy storage and loads, when the grid failure occurs. When power is restored to operational conditions, the islanded microgrid is resynchronized with the grid. The storage can be owned by an end-customer or by a utility. In the latter case, the storage might be considered as a controllable demand-side resource that serves the customer needs as well as being available to the utility as a demand reduction resource [13]. The power capacity of storage depends on the power consumption of the protected load, and the energy capacity depends on the time duration that the storage can fulfill.

2.2.5 Stacked Applications

The flexibility of energy storage can also be exploited to deliver a combination of applications or a stack of applications to increase the overall benefit from energy storage deployment by adding more revenue streams for a single storage solution. This opportunity is especially attractive for the investors in energy storage, who expect a fast and secure return on the investment. Due to operating and regulatory constraints, a combination of applications might be limited, and it requires to be considered on a case-by-case basis [13].

In [59], *Strbac et al.* assess the value of energy storage for providing multiple applications. Figure 2.20 depicts the value for a single energy time-shift application (Arbitrage in Figure 2.20), which provides the least benefit, as well as added value for the provision of balancing, photovoltaic support, network support, frequency response, and supply capacity applications. According to the results, the provision of multiple applications can increase the value of energy storage up to ten times.

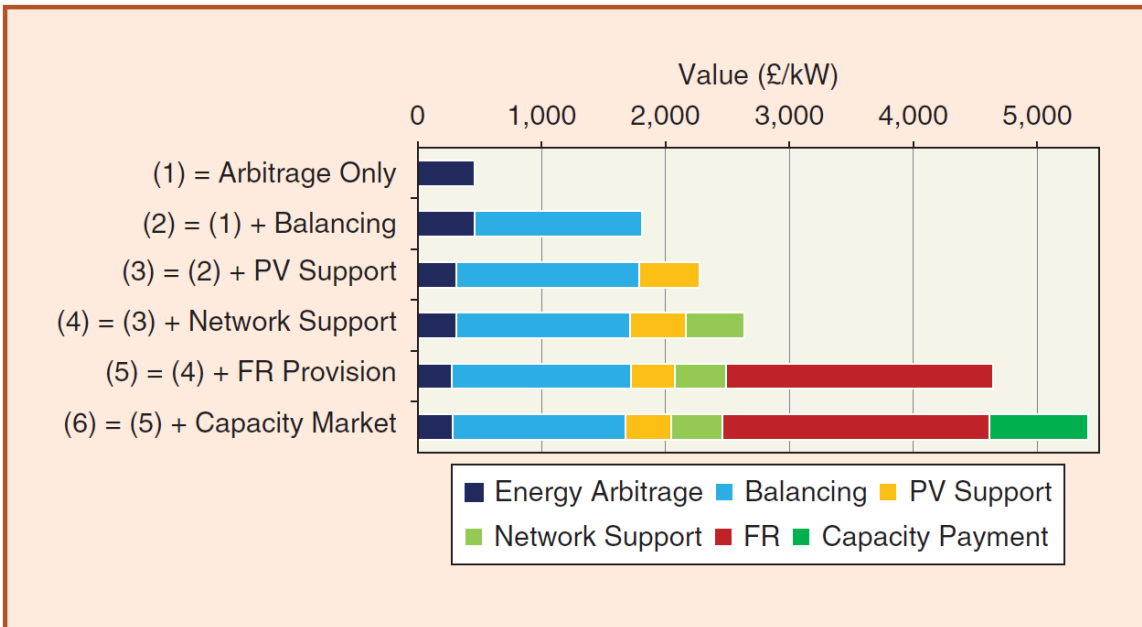


Figure 2.20: The value of energy storage for providing multiple services [59]

2.3 Methods for Optimal Siting, Sizing and Technology Selection

Discussions in the previous chapter on siting, sizing, and technology selection have been mostly qualitative based on the requirements for a particular application and the main characteristics of energy storage, i.e., cycle lifetime, scalability, discharge duration. However, the quantitative analysis requires a more detailed study of all related phenomena associated with energy storage itself and the environment (e.g., power network). The methods studied in the literature can be divided into four groups, which include analytical approaches (including statistical analysis), exhaustive search, heuristic search, and mathematical programming. These methods are explained in the present section.

2.3.1 Analytical

Approaches that do not use a particular optimization technique are referred to as analytical. The most commonly studied energy storage applications within an analytical framework are related to RE and those where the site for storage is predefined or intuitively obvious, such as RES power output smoothing, investment deferral, and others. Most of the analytical approaches rely on historical demand curves or statistical data analysis [60].

Network constraints or different market operation signals are not considered in these approaches. In [61], network investment deferral applications (peak-shaving) is addressed by means of energy storage. The methodology is based on a statistical analysis of demand data. In [62], a problem of the intermittent power output of a wind power plant is addressed by studying historical measurements of wind data. In [63], backup power supply application is considered, where energy storage size is determined based on statistical data of outage duration and targeted level of reliability. In [64], energy storage is sized for flexible reserve application, where a scaled historical data of wind power production is used.

The main drawbacks of analytical approaches comprise a limited application range, ignorance of market signals, and non-optimal solution.

2.3.2 Exhaustive Search

Exhaustive search approaches are based on a whole enumeration of a limited search space with a discrete step. In most cases, every possible state space is evaluated using various software to simulate the performance of energy storage. The combination of a particular site, size, and technology that gives the best result in simulation is considered to be the optimal solution, which is meaningful if the search space is comprehensively defined.

In [65], a MATLAB Simulink energy controller simulation is performed for every possible combination of power and energy ratings of a storage system, where site and technology are predefined. In [56], the size and technology of energy storage are first defined for every possible combination of demand and energy price profiles using optimization problem formulation. Then the performance value is statistically evaluated for all possible combinations of demand and energy price profiles concerning the probability of their occurrence. In [66], the cost-effectiveness of energy storage is evaluated with a dynamic programming approach for all possible combinations of energy and power ratings.

The main disadvantage of the exhaustive search approaches resides in computational burden, which requires to evaluate the performance of energy storage for all possible combinations of site, size, and technology, which can easily yield an intractable number of combinations for relatively small problems.

2.3.3 Heuristic Search

Heuristic approaches, in general, are those where experience and knowledge about a specific problem are incorporated in the algorithm [60]. Recent trends in heuristic methods reside in search of a solution space in an ingenious way, which is inspired by a natural process or animal behavior.

To get an idea of a heuristic search, it is better to study one particular approach, for example, a genetic algorithm, which is a search procedure that is originated based on the theory of natural evolution by Charles Darwin. The algorithm reflects the process of natural selection where the fittest individuals are selected for reproduction in order to produce offspring of the next generation [67]. The principle of a genetic algorithm is illustrated in Figure 2.21. The

algorithm starts with defining a set of initial starting points, or in genetic algorithm terms – initial population. Usually, starting points are uniformly spread across the state space or randomly generated. Next, a fitness function is evaluated for each starting point. After that, a crossover happens between a pair of individuals, which have the highest fitness function values. Each of the individuals possesses certain genes, which in practice are values of variables. Crossover results in a breed, which shares genes of their parents. Also, a newborn breed is prone to mutation, which changes some genes (variables) in a random way. After that, the fitness function is determined for a new generation, and the process of selection, crossover, and mutation is repeated again until a termination criterion is met. This might be a maximum number of generations, allocated budget (time/money) for computation, no improvements of fitness function from generation to generation, solution satisfy minimum criteria and any combination of these [68].

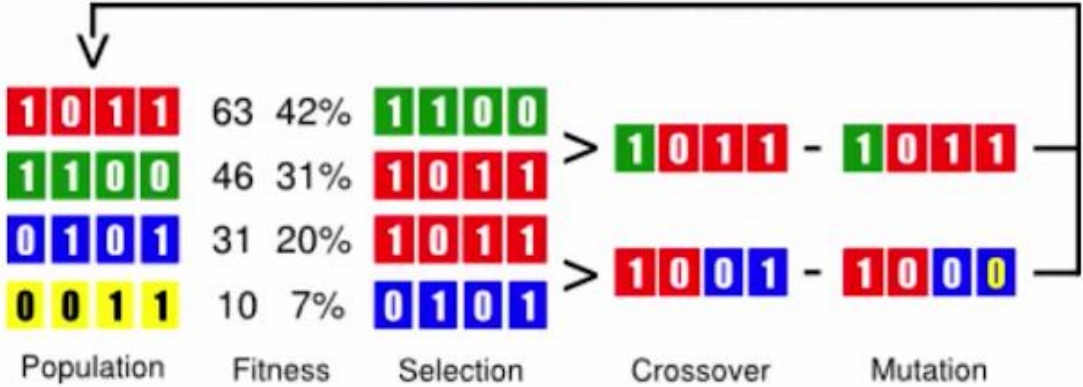


Figure 2.21: Principle of genetic algorithm [69]

For siting, sizing, and technology selection of energy storage systems, heuristic methods comprise a genetic algorithm [70]–[74], particle swarm optimization [75]–[77], artificial bee colony [78], bat algorithm [79].

In [72], optimal size and location of distributed generation and energy storage is sought with a combination of genetic algorithm and sequential quadratic programming, where the size and location of units are found by genetic algorithm, and the optimal dispatch, as well as power flows, are found with the formal optimization method – sequential quadratic programming. In [77], energy storage size for smart households is determined with particle swarm optimization. In [78], artificial bee colony heuristic is applied to find the optimal site and size for battery-based charging stations for electric vehicles. In [79], the optimal size of energy storage for microgrid applications is found with bat algorithm heuristic.

The main drawback of the heuristic search methods resides in the fact that the quality of the obtained “optimal” solution cannot be mathematically proven, meaning that it is not certain that the obtained solution is globally optimal. In addition to that, these methods allow finding a solution for a particular problem, but they do not allow performing any sensitivity analyses of the result, which significantly decreases their field of applications. And finally, the methods require high computational time, which is, however, not crucial for design and planning problems.

2.3.4 Mathematical Programming

In the mathematical programming approaches, numerical methods are applied to find the optimal solution using approximated models. Optimization theory, which is the theoretical background of such approaches, places restrictions on a problem formulation. Firstly, the problem has to be formulated using only equalities and inequalities, which does not allow using sequentially structured (or algorithmic) models as those for energy storage degradation from cycling [38]. Secondly, the models used in a problem formulation have to be accurate enough to

represent the subject of interest (energy storage) and the environment (network and other equipment) with a reasonable error. Finally, to guarantee the globally optimal solution, the functions that are used in a problem formulation have to be either linear or convex.

In the literature of the optimal siting, sizing, and technology selection problems, mathematical programming approaches comprises linear programming (LP) methods [80]–[82], convex programming (CP) methods [83]–[85], mixed-integer linear programming (MILP) methods [86]–[90] and mixed-integer convex programming (MICP) problem formulation has been proposed by the author in [43]. The considered approaches are efficient in terms of computational time and provide a single solution, which is guaranteed to be globally optimal. However, to achieve such a convergence, usually the models are oversimplified to meet the requirement for formal problem formulation mentioned above.

The mathematical programming approaches are found to be the most favorable in the applied field, as it allows finding the most efficient combination of site, size, and technology with the minimum investment or the maximum benefit objective, as well as performing various sensitivity analyses for the optimal solution. The advantages and disadvantages of the studied approaches are summarized in Table 2.2.

Table 2.2: Advantages and disadvantages of the methods for optimal siting, sizing and technology selection

#	Method	Advantages	Disadvantages
1	Analytical	<ul style="list-style-type: none"> • Simple 	<ul style="list-style-type: none"> • No insights • No market signals • Non-optimal solution
2	Exhaustive Search	<ul style="list-style-type: none"> • No restrictions on formulation • Globally optimal solution 	<ul style="list-style-type: none"> • Computationally demanding • No insights
3	Heuristic Search	<ul style="list-style-type: none"> • No restrictions on formulation • Plenty commercial and academic solvers 	<ul style="list-style-type: none"> • Computationally demanding • Non-global solution • No insights
4	Mathematical Programming	<ul style="list-style-type: none"> • Computationally efficient • Globally optimal solution • Allow insights • Plenty commercial and academic solvers 	<ul style="list-style-type: none"> • Formulation restriction (approximated models)

The present thesis is focused on the development of a methodology to formulate the optimal siting, sizing, and technology selection problem that complies with the requirements for formal optimization mentioned above, specifically, using only equalities and inequalities, that accurately represent energy storage and the environment with only linear or convex formulas. Hence, the literature on energy storage models and problem formulations has been studied in more detail in the next two sections.

2.4 Models Overview

This section provides an overview of the models used in the problems of siting, sizing, and technology selection. Particularly, the overview covers energy storage modeling as a subject of study and modeling of power flows, demand, and renewable generation as an environment.

2.4.1 Energy Storage Modelling

Energy storage technologies can be distinguished by a number of physical characteristics, such as power and energy ratings, charge and discharge efficiencies, self-discharge rate, ramp rate, location, response granularity, and response frequency [91]. The number of these characteristics can go further and depends on a particular task. Particularly, for an energy storage design or network planning problems, where the most effective site, size, and technology are sought, it is very important to consider degradation of an energy storage as the available energy capacity during its operational lifetime, and a designer must be aware that after a while energy storage would not be able to perform the same as it was just after commissioning. This is especially relevant for electrochemical storage technologies. Li-ion battery family is an illustrative example of how degradation effect might be multifactor, depending on several characteristics at the same time, i.e., temperature, state of charge, depth of discharge of each cycle, number of cycles, and the power at which it was charged or discharged.

2.4.1.1 Investment Costs

Originally the investment cost for energy storage is discrete as it is usually built-in blocks, which can be bonded with each other creating a big energy storage system [92]. Each of these blocks has a fixed energy and power ratings, which could be different for various form factors and technologies. This makes the original optimization problem to be mixed-integer what increases its complexity significantly. To avoid that energy and power capacity ratings might be considered as continuous variables while respecting the energy to power ratio of an original block. This way the investment cost is calculated based on the installed energy rating \bar{E} in MWh and/or power rating \bar{P} in MW as follows

$$C^{Inv} = \bar{E}C^E + \bar{P}C^P, \quad (2.1)$$

where C^E and C^P are upfront costs of the installed energy per MWh and power capacity per MW.

Energy to power ratio is respected with the following equality

$$\frac{\bar{E}}{\bar{P}} = k^{E/P}. \quad (2.2)$$

In case of a decoupled energy and power ratings of an energy storage solution (e.g., flow batteries), the equality above might be relaxed with inequality or even omitted.

2.4.1.2 General Energy Storage Characteristics

In general, the basic lossless energy storage can be represented as follows

$$E(T) = E(0) + \int_0^T P(t)dt, \quad (2.3)$$

where a positive value of power output $P(t)$ corresponds to the charging state of energy storage, and a negative value corresponds to the discharge.

In the optimal problem formulations, to make the number of power output variables feasible, a discrete representation is used

$$E(T) = E(0) + \sum_{t=0}^T P(t)\Delta t \quad (2.4)$$

or effectively this looks as follows

$$E(t + 1) = E(t) + P(t)\Delta t, \forall t \in T. \quad (2.5)$$

In the literature, it is called the energy storage continuity equation.

To incorporate self-discharge and inefficiency effects, the basic energy storage model is transformed into the following form

$$E(t + 1) = \sigma E(t) + P(t)\Delta t - L(t)\Delta t, \forall t \in T, \quad (2.6)$$

where σ represents the self-discharge effect, and power losses associated with energy storage inefficiency are in $L(t)$.

Self-discharge is a phenomenon of energy storage, where internal reactions reduce the stored charge of the battery while in the idle state. For Li-ion batteries, self-discharge is considered to be a function of the state of charge, charging current, cell temperature, and other factors [93]. A typical characteristic of the self-discharge rate as a function of the cell temperature is depicted in Figure 2.22. However, in the literature on the optimal siting, sizing, and technology selection, the self-discharge characteristic is considered constant to avoid nonlinear problem formulation.

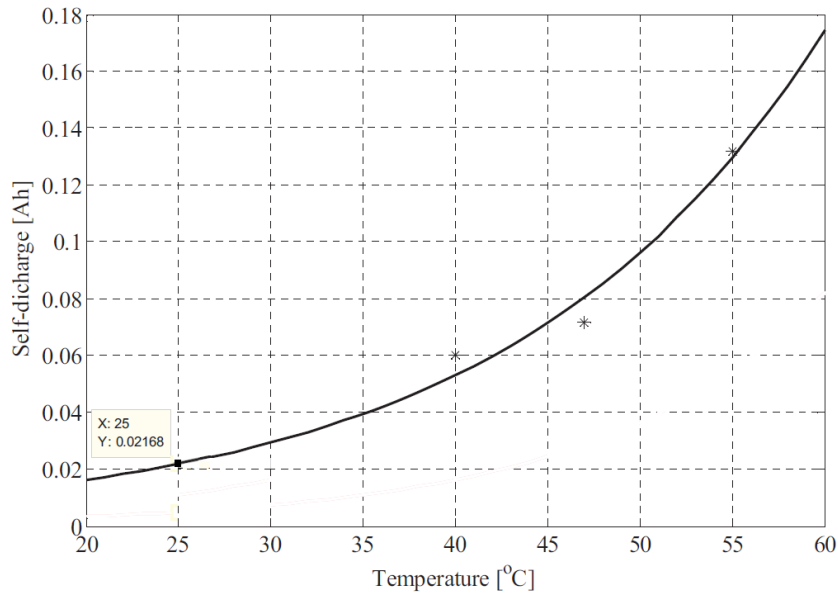


Figure 2.22: Self-discharge rate characteristic of Li-ion cell [94]

Active power losses during charge and discharge depend on the value of power output, state of charge, and internal resistance. For that consideration, energy storage can be represented with Rint model [95] depicted in Figure 2.23 (a), which represents the total internal resistance

R_{in} of energy storage and a voltage source associated with its state of charge (SoC). Open circuit voltage V_{oc} is considered to be a function of SoC [96], which is illustrated in Figure 2.23 (b).

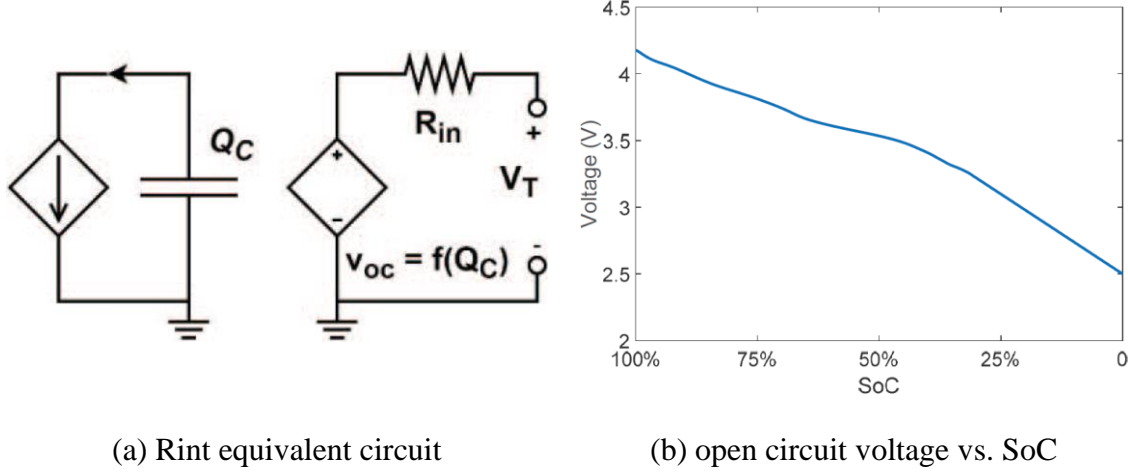


Figure 2.23: Li-ion battery model [39]

Applying Kirchhoff's voltage law, instant active power losses associated with charge and discharge can be formulated as follows

$$L(P_T, V_{OC}) = \frac{V_{in}^2}{R_{in}} = \frac{\left(V_{OC} - \sqrt{V_{OC}^2 - 4P_T R_{in}} \right)^2}{4R_{in}}, \quad (2.7)$$

where R_{in} is an internal battery resistance, V_{in} is a voltage drop on internal resistance, V_{OC} is open-circuit voltage, P_T is terminal power output.

This formulation is highly nonlinear and cannot be used in the formal optimization problem. Generally accepted form for the active power losses associated with charge and discharge inefficiency is considered with the following linear formulation

$$L(t) = (1 - \eta_{Ch}) P^{Ch}(t) - (1 - \eta_{Dis}) P^{Dis}(t), \quad (2.8)$$

where the power output of energy storage is divided into two parts – positive (charge) $P^{Ch}(t)$ and negative (discharge) $P^{Dis}(t)$. This formulation increases the number of variables and

constraints within an optimization problem, but keeps the formulation linear; otherwise, the nonlinear absolute function would be required.

To make sure that the linear formulation above is valid, it is important to satisfy the following equalities

$$P(t) = P^{\text{Ch}}(t) + P^{\text{Dis}}(t), \quad (2.9)$$

$$P^{\text{Ch}}(t) P^{\text{Dis}}(t) = 0. \quad (2.10)$$

The latter equality implies that the simultaneous charge and discharge is not possible.

2.4.1.3 Charge/Discharge Constraints

Charge of energy storage at every moment of time is limited to its energy rating \bar{E} subject to a capacity fade due to degradation

$$0 \leq E(t) \leq \bar{E}(1 - \delta^{\text{CF}}), \quad (2.11)$$

where the capacity fade function δ^{CF} represents the degradation of energy storage.

Power output is limited with the power rating \bar{P} of energy storage as follows

$$-\bar{P} \leq P(t) \leq \bar{P}. \quad (2.12)$$

2.4.1.4 Degradation Model

In the context of energy storage, degradation is an integral decrease of energy capacity during the lifetime of energy storage. It is specific for each particular technology and chemistry. Li-ion battery technologies are a good example of how degradation might be multifactor, depending on several characteristics at the same time. In [97], *Bole et al.* explain the relevant physical aging mechanisms in Li-ion batteries, which include solid electrolyte interface layer growth, lithium corrosion, lithium plating, contact loss, and diffusion stress. In [98], *Spotnitz* reports on battery aging tests and illustrates the degradation rate of a Li-ion cell as a nonlinear

lifetime process, which is generalized in Figure 2.24. Such that, the degradation rate is divided into three parts: early lifetime period drop, linear degradation period, and rapid decrease after reaching end of life (EoL) point.

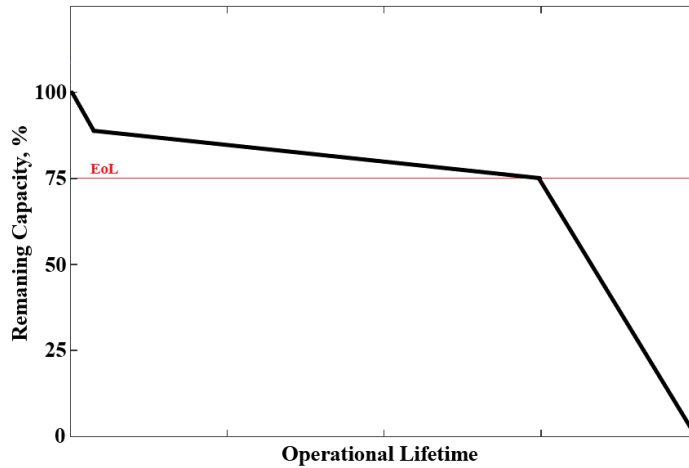
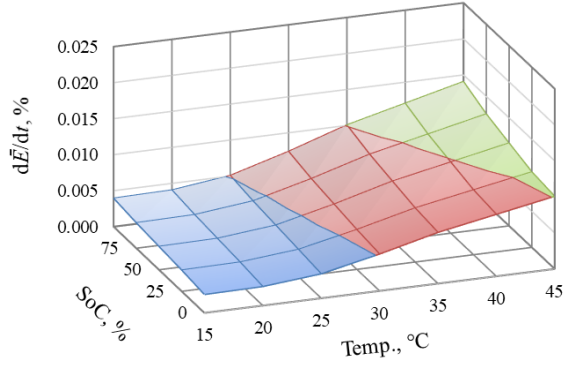
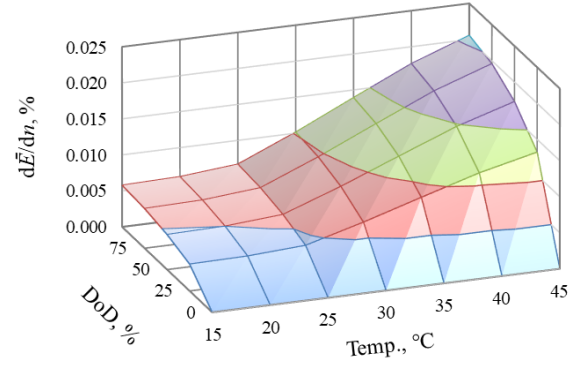


Figure 2.24: Degradation process of Li-ion battery

In the literature, the degradation of Li-ion batteries is divided into two types: idling and cycling [38]–[40]. Degradation from idling is influenced by the time, state of charge, and cell temperature during the lifetime of a battery. Degradation from cycling is found for each individual cycle, and it is influenced by the cycle depth (depth of discharge), power at which it was charged and discharged (C-rate), average state of charge, and cell temperature. Figure 2.25 illustrates the capacity fade rate characteristic of nickel manganese cobalt oxide (NMC) Li-ion battery cell during the linear degradation period as a function of state of charge and the cell temperature for the degradation from idling (a), and the depth of discharge and the cell temperature for the degradation from cycling (b) at the C-rate less or equal to one. Similar behavior is observed for other types of Li-ion technology (see Appendix B).



(a) idling



(b) cycling at C-rate ≤ 1

Figure 2.25: Energy capacity fade rate characteristic of Li-ion NMC cell

Due to the fact that these degradation characteristics are derived from battery cycle laboratory tests, they do not have a formal definition. However, it is possible to reproduce them with standard functions (e.g., quadratic functions) as in (2.13) and (2.14) using any available fitting technique (e.g., the least-squares fitting method described in [99]). The resulting parameters are presented in Tables B.1 and B.2 of Appendix B, which are used in the proposed methodology for the degradation concerns.

$$\delta^{\text{Idl}} = \left(A_{\text{SoC}}^{\text{Idl}} \text{SoC}^{\text{D}^2} + B_{\text{SoC}}^{\text{Idl}} \text{SoC}^{\text{D}} + C_{\text{SoC}}^{\text{Idl}} \right) \left(A_{\tau}^{\text{Idl}} \tau^{\text{D}^2} + B_{\tau}^{\text{Idl}} \tau^{\text{D}} + C_{\tau}^{\text{Idl}} \right), \quad (2.13)$$

$$\delta^{\text{Cyc}} = \left(A_{\text{DoD}}^{\text{Cyc}} \text{DoD}^{\text{C}^2} + B_{\text{DoD}}^{\text{Cyc}} \text{DoD}^{\text{C}} \right) \left(A_{\tau}^{\text{Cyc}} \tau^{\text{C}^2} + B_{\tau}^{\text{Cyc}} \tau^{\text{C}} + C_{\tau}^{\text{Cyc}} \right), \quad (2.14)$$

To apply with the degradation functions (2.13) and (2.14), average daily state of charge SoC^{D} , average daily temperature τ^{D} , cycle depth of discharge DoD^{C} , and the average cycle temperature τ^{C} are found as follows

$$\text{SoC}^{\text{D}} = \frac{1}{T\bar{E}} \sum_{t=1}^T E(t) \Delta t \quad (2.15)$$

$$\tau^D = \frac{1}{T} \sum_{t=1}^T \tau(t) \Delta t \quad (2.16)$$

$$DoD^C = \frac{1}{2\bar{E}} \sum_{t=t_c^{\text{Start}}}^{t_c^{\text{End}}} (P^{\text{Ch}}(t) - P^{\text{Dis}}(t)) \Delta t \quad (2.17)$$

$$\tau^C = \frac{1}{T} \sum_{t=t_c^{\text{Start}}}^{t_c^{\text{End}}} \tau(t) \Delta t \quad (2.18)$$

The equalities (2.17) and (2.18) requires knowledge of moments of time when a particular cycle occurs. As it is shown further in Chapter 4, the plausible suggestions for the start and the end time moments for each cycle can be made based on the demand profile.

The equalities (2.15) and (2.17), as well as the degradation characteristics (2.13) and (2.14), fail to meet requirements for convex problem formulation. In Chapter 4, it will be shown how these nonconvex equalities can be used in the formal optimization problem formulation and how the global optimum can be found for an arbitrarily complex function of degradation.

2.4.1.5 Thermal Model

As both self-discharge and degradation depend on the cell temperature, it is important to include into consideration a thermal model of energy storage. Thermal model formulation mostly depends on a particular design of an energy storage solution (e.g., form-factor and cooling system). However, it is possible to generalize the model by considering electrical energy storage as thermal storage. Following the concept of energy balance, which implies that energy loss during charge or discharge due to inefficiency result in heating of storage elements [39]. Inspired by energy storage continuity constraint and assuming that the energy lost during charge or discharge stays inside storage as a heat, thermal model of energy storage may look as follows

$$\tau(t + 1) = \tau(t) - \mu \left(\tau(t) - \tau^{\text{Amb}}(t) \right) \Delta t + \frac{L(t) \Delta t}{C^{\text{Tm}} m}, \quad (2.19)$$

where μ is a heat dissipation function, which depends on the difference between the storage temperature and ambient (coolant) temperature, C^{Tm} is a heat capacitance per unit mass, and m is a mass of storage, which is proportional to energy rating \bar{E} .

Generally, a heat dissipation function is exponential [100]. However, it is effectively linearized as in [101]. Thus, the resulting linear formulation looks as follows

$$\tau(t + 1) = \tau(t) - k^{\text{HD}} \left(\tau(t) - \tau^{\text{Amb}}(t) \right) \Delta t + \frac{L(t) \Delta t}{C^{\text{Tm}} m}, \quad (2.20)$$

where k^{HD} is a heat dissipation coefficient, which defines a cooling rate.

2.4.2 Power Flow Modelling

Power-flow studies are of great importance in planning and designing the future expansion of power systems as well as in determining the best operation of the existing systems [102]. In the problem of optimal siting, sizing, and technology selection, energy storage operates within a particular network, i.e., transmission, distribution, microgrid. Accurate modeling of a network is essential for finding the best location, size, and technology of energy storage to perform more effectively.

A power system is modeled as a network of electric nodes (buses) connected with edges (power lines and transformers), and similar power conducting equipment [103]. Thus, a power network can be represented as a graph, as in Figure 2.26.

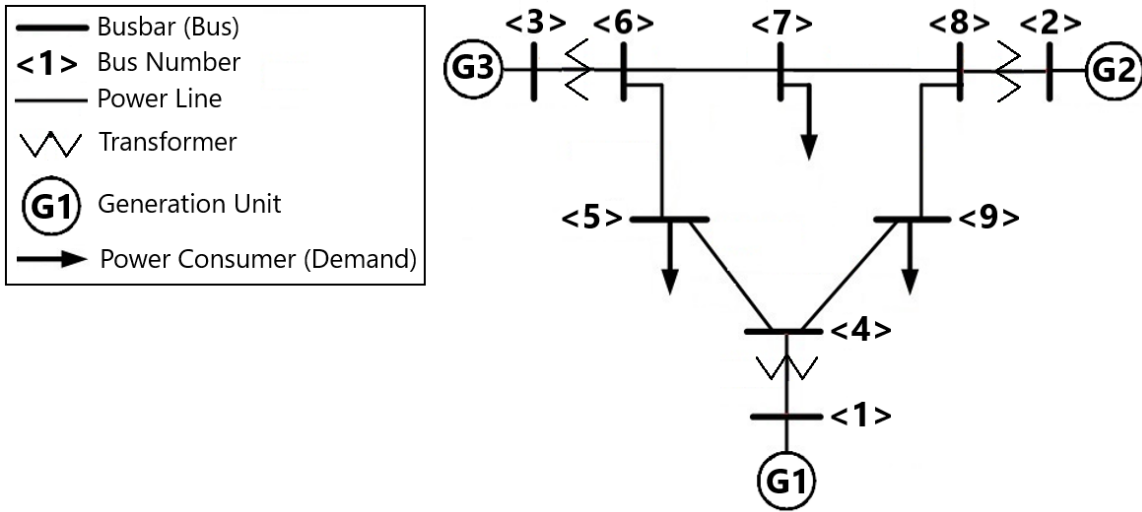


Figure 2.26: Example of a power system graph

Classic power flow formulation is instantaneous [104], [105], hence, solved for each time period separately. However, when incorporating energy storage, the standard formulation becomes a multi-period problem, where all time instances are linked with each other with energy storage continuity equality (2.6) and thermal continuity equality (2.20).

2.4.2.1 Branch Model

The generalized Pi branch model presented in Figure 2.27 is sufficient for modeling the majority of power system branch elements, such as transmission lines, cables, and transformers [103].

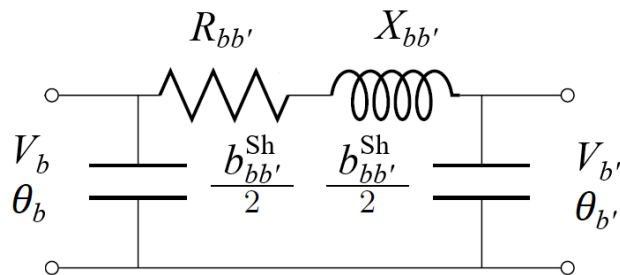


Figure 2.27: Generalized Pi branch model

The line characteristics for transmission lines and cables are most often represented as a series impedance $R_{bb'} + jX_{bb'}$ and a branch shunt admittance $jb_{bb'}^{\text{Sh}}$, which is sometimes given as “line charging” reactive power [103]. Subscript bb' specify a particular branch that connects two nodes b and b' .

The Pi branch series admittance for a cable or a line is found as follows

$$y_{bb'}^{\text{Cab/Line}} = \frac{1}{R_{bb'} + jX_{bb'}} = \frac{R_{bb'}}{R_{bb'}^2 + X_{bb'}^2} - j \frac{X_{bb'}}{R_{bb'}^2 + X_{bb'}^2}. \quad (2.21)$$

However, the transformer series resistance is often neglected in power flow analysis, which makes a transformer series admittance looks as follows

$$y_{bb'}^{\text{Tran}} = -j \frac{1}{X_{bb'}}. \quad (2.22)$$

Shift angle of a line is found as follows

$$\vartheta_{bb'} = \text{atan} \left(\frac{\text{Im}(y_{bb'})}{\text{Re}(y_{bb'})} \right) \quad (2.23)$$

2.4.2.2 AC power-flow formulation

Power-flow is found by solving a set of a power balance equations defined per each bus.

The power balance equations for real and reactive power are formulated as follows

$$\begin{cases} P_b^{\text{G}}(t) + P_b^{\text{L}}(t) + P_b^{\text{Net}}(t) = 0 \\ Q_b^{\text{G}}(t) + Q_b^{\text{L}}(t) + Q_b^{\text{Net}}(t) = 0 \end{cases} \quad \forall b \in B, t \in T, \quad (2.24)$$

where $P_b^{\text{G}}(t)$ and $Q_b^{\text{G}}(t)$ are active and reactive power generated within a bus, $P_b^{\text{L}}(t)$ and $Q_b^{\text{L}}(t)$ are active and reactive power consumed within a bus, $P_b^{\text{Net}}(t)$ and $Q_b^{\text{Net}}(t)$ are active and reactive net injected power to/from a bus, which are found as follows

$$P_b^{\text{Net}} = |V_b| \sum_{bb' \in Br} |V_{b'}| |y_{bb'}| \cos(\theta_b - \theta_{b'} - \vartheta_{bb'}), \quad (2.25)$$

$$Q_b^{\text{Net}} = |V_b| \sum_{bb' \in Br} |V_{b'}| |y_{bb'}| \sin(\theta_b - \theta_{b'} - \vartheta_{bb'}), \quad (2.26)$$

where $|V_b|$ and θ_b are voltage magnitude and voltage angle at bus b , and Br is a set of branches within a power system.

It is worth noting that for each network bus a system of two equations contain four variables P_b^{Net} , Q_b^{Net} , V_b and θ_b . Hence, a deterministic solution to the conventional power flow problem requires fixing the values of two out of four variables at each bus [103]. To resolve that each bus of a system is assigned to one of the three types:

- Slack bus: voltage magnitude and angle are fixed, while the active and reactive power injections are variables.
- Load bus: active and reactive power injections are fixed, and the voltage magnitude and angle are variables.
- Voltage bus: real power injection and voltage magnitude are fixed, and reactive power and the voltage angle are variables.

Assigning buses to each of these types results in an equal number of equalities and unknowns. However, when applied to the optimization problem formulation, this nonlinear interpretation requires linearization. The linearization techniques applied to the formulation above include various methods, i.e., Newton-Raphson method, Gauss-Seidel method, semidefinite relaxation [106], Branch-and-Bound algorithm-based [107], relaxation and convexification [108].

2.4.2.3 DC power-flow formulation

For most of the active power-related applications and networks (e.g., transmission network), considering reactive power is not required, and only active power is of interest. To make the problem linear and decrease the computational burden, it is possible to approximate AC power flow formulation with the three basic assumptions:

- The resistance $R_{bb'}$ for each branch bb' is negligible compared to the reactance $X_{bb'}$ and can, therefore, be set to 0.
- The voltage magnitude at each node is equal to the base voltage V_0 .
- The voltage angle difference $\theta_b - \theta_{b'}$ for every branch bb' is sufficiently small in magnitude so that $\cos(\theta_b - \theta_{b'}) \approx 1$ and $\sin(\theta_b - \theta_{b'}) \approx \theta_b - \theta_{b'}$.

These assumptions reduce (2.25) and (2.26) as in (2.27) and (2.28)

$$P_b^{\text{Net}} = \frac{V_0^2}{X_{bb'}} (\theta_b - \theta_{b'}), \quad (2.27)$$

$$Q_b^{\text{Net}} = 0. \quad (2.28)$$

In such a manner, each bus of a network is represented by one linear equality (2.27) with only one variable θ_b . Thus, the analysis of power flows using DC approximation requires solving a set of linear equations, the number of which corresponds to a number of buses.

2.4.3 Demand Modelling

Demand or power consumption is considered as input data for the problem of siting, sizing, and technology selection of energy storage. Demand data is required to be measured for each particular case. There is a number of repositories where demand data is measured for a particular location. Customer-Led Network Revolution project [109] is one of the examples.

Demand is usually modeled by a load profile expected in the future network operation, and it is very important to forecast the profiles for at least a lifetime horizon of energy storage for which techno-economic analysis is to be done. There is no general rule of how to predict the future profile, and it depends on a number of factors, i.e., commercial and population growth, environmental restrictions, penetration of domestic and commercial distributed energy resources, their types, and many more [110]. An illustrative example of how the net load profile changes with the increased penetration of renewable energy sources and demand growth is depicted in Figure 2.28.

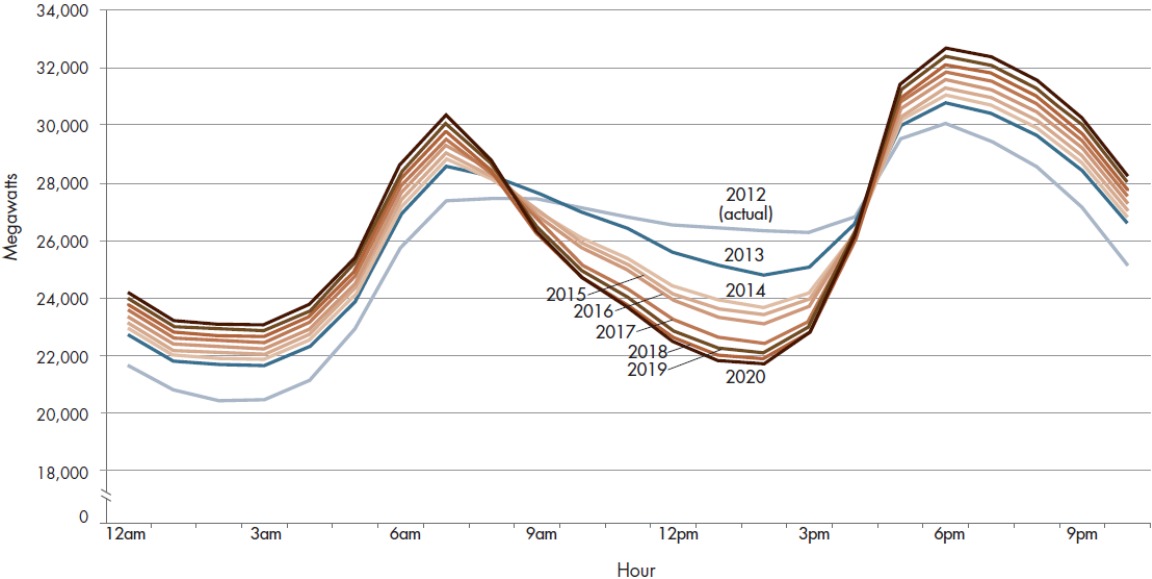


Figure 2.28: Net load curve example [111]

In the literature on optimal siting, sizing, and technology selection of energy storage, where the goal is to develop a methodology but not forecast a demand, demand data is usually taken from historical observations, for which a set of representative profiles is derived, usually, one per season or year. One of the methodologies of how to derive representative demand

profiles from the big data is explained in [112]. Further, a simple rule is applied to project the obtained profile for the future, e.g., expected annual load growth in percentage as in [113].

2.4.4 Renewable Generation Modelling

In opposite to conventional thermal generation resources, renewable energy sources are able to produce the power that is available in the primary energy source, e.g., wind speed, solar radiation. Similarly to demand data, it is required to be measured on-site. However, as wind speed or solar radiation are mostly seasonal, there is no requirement to forecast it for the future. Moreover, it is possible to exploit meteorological models, which exist in plenty, to obtain wind speed or solar radiation data. An informative repository of wind data can be found in [114]. An example of renewable energy production of wind turbines and a photovoltaic system, as well as their combination, is depicted in Figure 2.29.

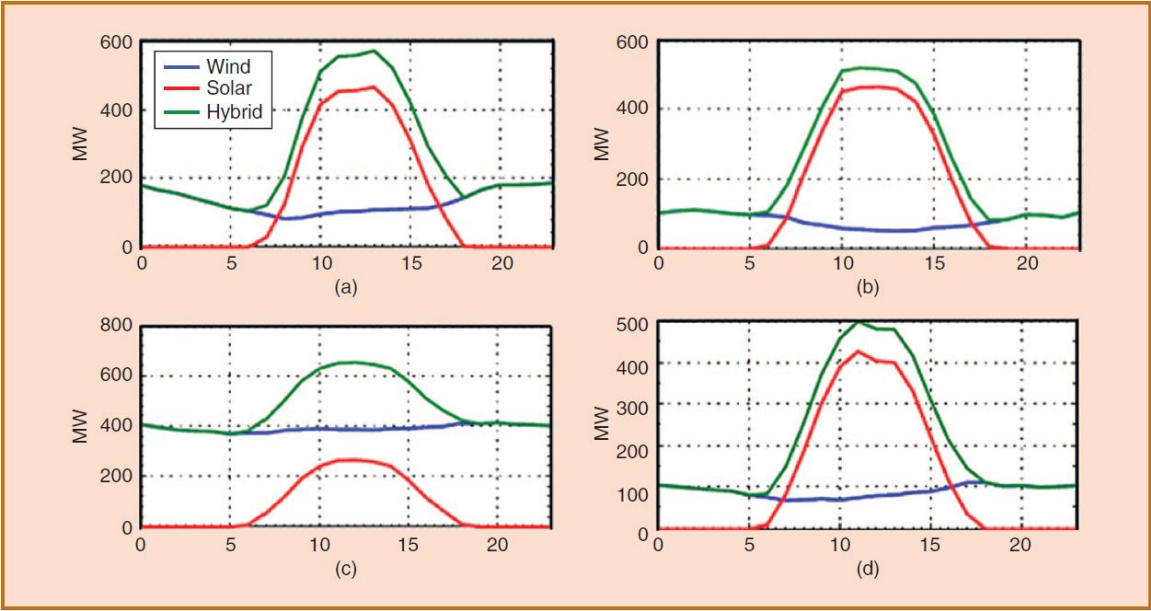


Figure 2.29: Solar and wind production [115]

2.5 Literature on Optimal Siting, Sizing and Technology Selection

The problem of optimal siting, sizing, and technology selection of energy storage systems for power system applications has been considered in many papers. In these papers, authors solve either design or planning problems. In a design problem, which is the focus of the present thesis, authors search for the optimal site, size, and technology of energy storage considering various demand and renewable generation scenarios for a given case study network. In a planning problem, authors find not only the optimal site, size, and technology but also a year of installation concerning various demand and renewable generation scenarios along with scenarios for network development. The time horizon of the design problems is 10-15 years, which corresponds to the lifetime of energy storage, and 20+ for the planning problems.

The methods used for resolving design or planning problems are various, and the choice of a particular method depends on the effects required to be considered within the problem, uncertainties, and assurance of unity of a solution. The general overview of the most vivid example of this particular problem formulation and resolution is presented below with the focus on problem formulation and complexity.

In [65], *Brekken et al.* proposed a methodology for optimal sizing of energy storage for wind power output smoothing application. Authors apply various control techniques, i.e., simple rule-based, fuzzy controller, and artificial neural network controller, to model operation of energy storage. The methodology is limited to only Zinc-Bromine flow battery and the particular application. To find the optimal storage capacity and controller, its operation has been simulated for 282 scenarios of historical wind data for various combinations of energy and power ratings, as well as the controller. The most cost-effective result is considered to be optimal. Even though

the number of all possible combinations of power rating, energy rating, and the controller is great, linear models used within the proposed simulation approach are performed in a fraction of a second, resulting in a very high computational efficiency.

In [83], *Wogrin and Gayme* proposed a DC OPF based framework for optimal energy storage siting, sizing, and technology selection within a transmission network. In this paper, energy storage is used to minimize the operational cost of a particular network by shifting the energy in time from low price to high price periods. The authors extend OPF with storage design problem to incorporate multiple storage technologies, which increases the size of a problem significantly. To deal with the increased complexity, authors apply DC OPF linear approximation as well as linear energy storage models to keep the problem tractable with the provable optimal solution. The proposed methodology is generic for various networks and energy storage technologies. The case study has been solved for modified by the authors' IEEE 14-bus transmission test network for four particular technologies, i.e., pumped-storage hydro, compressed air energy storage, lithium-ion batteries, and flywheel energy storage. As was declared by the author, the resulting convex optimization problem for one 24-hour scenario contains a quadratic objective, ~65,000 variables, and ~160,000 linear constraints and it is solved in GAMS [116] in 7-13 seconds. Even though the authors state that the proposed methodology can be used for stochastic problem formulation, the study on the dependency of computational time on the number of scenarios has not been done.

In [87], *Pandzic et al.* proposed a near-optimal method for siting and sizing of energy storage in a transmission network that deals with stochasticity of demand and renewable generation. In this paper, energy storage is used for congestion management. The authors

proposed a methodology which contains solving unit commitment optimization problem for a big number of scenarios and perform statistical analysis of the results to determine the site, where storage is required most of the times, and the maximum power and energy required to perform congestion management. The proposed methodology is generic for various networks, and energy storage technologies, however, it does not allow considering a hybrid energy storage solution. The methodology has been tested on the IEEE RTS 96-bus system for a general energy storage model, which accounts only for investment cost, charge, and discharge efficiencies. The computational time required to solve the proposed MILP unit commitment and storage sizing problem for 365 days of wind and demand data reaches 38 hours in GAMS.

While omitting important processes that occur in energy storage, i.e., self-discharge, and degradation, two previous papers provide good frameworks of DC OPF reformulation for the optimal siting, sizing, and technology selection of energy storage. In [56], the author of the present thesis incorporates self-discharge and variable lifetime into the problem of optimal sizing and technology selection of energy storage for energy arbitrage and peak-shaving applications. The proposed optimization problem is solved for each representative scenario of wind and demand individually, and then it is statistically determined which of the obtained result is more beneficial. The methodology requires the solution of a nonlinear optimization problem 100 times, when the time required to solve one 24-hour scenario for the one-bus network, and six energy storage technologies in MATLAB is around 10 minutes. The resulting nonlinear optimization problem is addressed using a global search algorithm [117], which perform multiple optimization procedures starting from different starting point randomly spread on a problem domain.

In [118], *Qiu et al.* solve the optimal planning problem for a transmission network, where energy storage is applied for investment deferral. The planning problem is formulated as a MILP unit commitment problem for 25 years of a planning period, each of which is represented with five representative scenarios of demand and wind generation. The objective criterion is a minimum operating cost over the whole time horizon. As for other papers, the energy storage model is technology agnostic. However, in contrast to the papers above, the authors take into account linear energy capacity fade of energy storage, particularly, 6% of capacity is considered to be lost each year. The methodology has been tested on the IEEE RTS 24-bus system for a single energy storage technology. The proposed stochastic MILP problem has been resolved in GAMS using the Hyak supercomputer system [119], while the computational time is not reported.

In [89], *Miranda et al.* developed an optimization tool for the planning and operation of battery energy storage in an island power system with high wind penetration. In the paper, energy storage is applied to minimize the operational cost of an island electric grid and maximize wind power utilization. The planning problem is formulated as a unit commitment MILP problem for the 15-year horizon with a one-year epoch, where the power flows are omitted. Similar to the previous paper, the energy capacity of a battery is considered to be fading each year but with the variable rate, which is proportional to the relationship between the total energy throughput of the energy storage and its technology-dependent cycle lifetime. Considering energy capacity to be proportional to the energy throughput makes the optimization problem bilinear. Hence, the optimal site, size, and technology are found by a simulation of an energy storage operation for every combination of the fixed decision variables – whole enumeration approach. The proposed

methodology has been tested on a real 30kV electric grid of the Azore island in Portugal. Even though the authors do not declare the time required to resolve the problem, the proposed deterministic approach is not computationally efficient due to the high number of possible combinations of decision variables and the brute force methodology.

A more detailed degradation model has been proposed for the problem of optimal sizing and technology selection by *Alsaidan et al.* in [90]. In this paper, energy storage is used for energy time-shift application to reduce microgrid operational cost and improve supply reliability. A nonlinear relationship between the energy storage depth of discharge and lifecycle has been linearized with piecewise linear characteristics to model storage degradation. DC OPF is applied for the linear representation of power flow within a microgrid. However, the linearization of the degradation model required including integer variables to the problem, which resulted in MILP problem formulation, which increased the computational burden. The methodology has been tested on a five-bus microgrid to find the optimal size and technology of four considered storage technologies, i.e., Lead-Acid, NiCd, Li-ion, and NaS. The proposed stochastic MILP problem has been resolved in GAMS on a personal computer, and it took 18 hours of computation time for five representative scenarios.

In [86], *Dvorkin et al.* presented computationally tractable bilevel problem formulation for the optimal siting and sizing of energy storage. The proposed optimization framework links short-term scheduling optimization problem, which minimizes the expected system-wide operating cost, and a long-term investment problem, which minimizes the investment decision, where all of the decision variables are exchanged between the problems. Such a formulation allows decomposing a short-term stochastic problem into a set of subproblem for every

representative wind and demand scenario what decreases computational burden significantly. Even though the authors apply a very simple energy storage model, which does not account for self-discharge or charge and discharge efficiencies, it gives a very illustrative example of how a stochastic energy storage design problem might be decomposed and solved in parallel for every considered scenario. The resulting optimal siting, sizing, technology selection, and unit commitment MILP problem for the IEEE 39-bus test system for 5 representative days contains 3,633,153 constraints, 947,057 continuous variables, and 29,760 binary variables. The problem was solved in GAMS on the Hyak supercomputer system [119] in 72 hours.

The general problem decomposition technique – alternating direction method of multipliers (ADMM) – has been applied for optimal siting and sizing problem by *Nick et al.* in [84]. In contrast to the papers above, energy storage siting and sizing are done for the distribution network, where energy storage is used for multiple applications, i.e., voltage support, network losses reduction, and energy arbitrage. The authors applied a convex approximation of AC OPF [120] to account for voltage deviation and power losses. To decompose the stochastic optimization problem per scenario, the power and energy capacity constraints are relaxed and incorporated into the objective function. Such that, the operational cost for every scenario is optimized in each subproblem in parallel concerning the fixed investment decision (power and energy capacity), while the investment decision is updated based on the obtained results according to the ADMM procedure [121]. The problem has been tested on a real distribution network, which contains 287 nodes, for 15 demand and PV generation scenarios. The computational time to resolve the decomposed optimization problem is declared to be 400 seconds, in case of an informative choice for ADMM auxiliary variables. The computational

time required to resolve the original problem without decomposition is 14 hours, and this number increases exponentially with the number of considered scenarios.

In [85], *Fortenbacher et al.* apply the Benders decomposition (BD) technique for the optimal siting and sizing of an energy storage problem. Similar to the previous paper, energy storage is used for distribution network application but for a different objective – maximize photovoltaic utilization in a local residential area. The authors applied linearized OPF power flow representation that approximates voltage level values, branch flows, and network power losses, as explained in detail by the authors in [122]. The proposed problem formulation is enhanced with a capacity loss aware degradation model of energy storage, which is represented with a piecewise-affine degradation map (or convex hull) as a function from the state of charge and power output. The BD technique is applied to decompose the original optimization problem into a master problem, where a storage investment problem is solved, and a set of subproblems, where the optimal scheduling is done concerning the capacity constraints defined in the master problem. The proposed methodology has been tested on the 18-bus CIGRE test grid [123] for 30 representative scenarios of demand and photovoltaic generation. Even though the authors do not report the exact time required to resolve the problem, they state that the convergence of an algorithm is achieved in 80 iterations of the BD algorithm, which contain one master problem and 30 subproblems, which are solved in parallel. Therefore, it can be concluded that significant computational efficiency is achieved by means of the BD technique.

2.6 Conclusions

Energy storage is one of the key elements to address the upcoming challenges in power systems, that come from the ubiquitous electrification and increased share of renewables in the

generation mix. In addition to that, energy storage provides an alternative means to conventional network reinforcement. Particularly, 18 applications have been considered within the chapter, where energy storage can bring benefits to various parties, which include utility companies, transmission and distribution network operators, and end-customers. However, the high upfront investment cost for energy storage technologies requires performing a detailed techno-economic analysis to find the best combination of site, size, and technology of energy storage to be installed to bring the most benefit and justify the investment. Such an analysis is known as optimal siting, sizing, and technology selection.

Even though energy storage technologies comprise a significant number of methods to store energy, Li-ion based technology is found as the most promising technology used in power system applications due to its cost, volumetric and other characteristics. Moreover, from the research point of view, Li-ion technology possesses a complex degradation function which makes it the perfect case study to show how a complex degradation function can be considered within a formal optimization problem. Particularly, as was shown in the previous section, the degradation from idling might be represented as a piecewise-affine map, while degradation from cycling is more complex. Thus, such degradation characteristics cannot be used both at the same time in the convex problem formulation. Filling this gap is one of the contributions of the present thesis, where it has been shown how a complex degradation mechanism can be used in the problem of optimal siting, sizing, and technology selection.

In the literature on optimal siting, sizing, and technology selection, the researchers are applying more and more complicated models of energy storage and the environment, as well as trying to consider a greater number of expected future scenarios to perform an informative

techno-economic analysis. Even though the authors that choose a formal optimization approach are keeping an eye on tractability, the resulting optimization problems become more complex as the authors include more complicated models, and scalability becomes an issue. To respond to that, a problem decomposition techniques are applied to decompose a problem per representative scenario. This is particularly important for stochastic optimization problem formulations, where a big number of scenarios are considered. However, scalability in terms of a network size has not been addressed for the particular problem. Filling this gap is another contribution of the present thesis.

Chapter 3. Optimization Problem Formulation and Resolution

3.1 Problem Formulation

The present section provides the formal optimization problem formulation, which takes into account all necessary knowledge, including energy storage models that account for self-discharge, charge-discharge efficiency, operational and calendar lifetime, investment cost, and degradation, as well as environment models.

For illustration purposes, all of the primary and auxiliary variables of the optimization problem, such as energy rating $\bar{E}_{b,j}$, power rating $\bar{P}_{b,j}$, scheduled charge $P_{b,j,s,t}^{\text{Ch}}$, and discharge $P_{b,j,s,t}^{\text{Dis}}$, and other variables are indicated in *italic, bold font*, while the functions that depend on the primary and auxiliary variables are indicated in *italic font*, and the constant parameters operate in the normal (upright) font. For the sake of generality, the optimization problem is formulated as a minimization problem, where the formulation has to be convex.

3.1.1 Objective Function

The objective function (3.1) of the optimal design problem consists of two terms. The first is a short-term revenue, which yields benefit from energy storage day to day operation, which is usually formulated for a number of representative scenarios S with the expected probability of occurrence π_s . Ideally, these scenarios have to cover the whole lifetime of energy storage. Thus, the first term represents the average daily benefit from energy storage operation. The second term represents a per diem investment cost for energy storage, which is a long-term investment cost that is independent of daily operation. Such a formulation resolves a trade-off

between long-term investment cost, which is a function of the installed capacity, and daily benefits as a result of the storage operation. Thus, it is important to consider these terms in one timescale, either per diem or lifetime.

$$F = - \sum_{s \in S} \pi_s R_s + \sum_{b \in B} \sum_{j \in J} \frac{\bar{E}_{b,j} \left(C_j^E + \frac{C_j^P}{k_j^{E/P}} \right)}{365 T_{b,j}^{LT}}, \quad (3.1)$$

where R_s is a reward function applied for representative scenario s , C_j^E and C_j^P are the investment costs per MWh and MW of the installed capacity, $k_j^{E/P}$ is an energy to power ratio specific for each technology, $\bar{E}_{b,j}$ is energy capacity (rating) of energy storage technology j installed at bus b , and $T_{b,j}^{LT}$ is an operational lifetime of a particular energy storage system.

In most of the cases, the reward term in (3.1) is determined by the reward policy for a particular application (i.e., a case study). To make the formulation general for most applications, it is assumed that the reward term R_s is known, and it satisfies convexity requirements, which in general is true as the reward policies are designed to be compatible with a standard optimizer.

3.1.2 Constraints

The objective function (3.1) is to be minimized subject to a set of constraints that are used to model energy storage and a corresponding environment.

Energy to power ratio of the final installation is satisfied with the equality constraint, which is the case of those technologies, where power and energy ratings are coupled, as is a case of Li-ion energy storage

$$\frac{\bar{E}_{bj}}{\bar{P}_{bj}} = k_j^{E/P} \quad \forall b \in B, j \in J. \quad (3.2)$$

Energy storage charge is modeled with energy storage continuity constraint, which is the main equality constraint that is considered within the energy storage-related optimization problems. The following equality constraint accounts for constant self-discharge rate, charge, and discharge efficiencies

$$\begin{aligned} E_{bj,s,t+1} &= (1 - k_j^{SD})E_{bj,s,t} + (P_{bj,s,t}^{Ch} + P_{bj,s,t}^{Dis})\Delta t - \\ &\quad - \left((1 - \eta_j^{Ch})P_{bj,s,t}^{Ch} - (1 - \eta_j^{Dis})P_{bj,s,t}^{Dis} \right) \Delta t \\ &\quad \forall b \in B, j \in J, s \in S, t \in T, \end{aligned} \quad (3.3)$$

where energy storage power output is represented by the positive charge variable $P_{bj,s,t}^{Ch}$ and negative discharge variable $P_{bj,s,t}^{Dis}$ to form a linear representation of energy storage efficiency and avoid using the nonlinear absolute function.

Temperature evolution is modeled with the temperature continuity constraint as follows

$$\begin{aligned} \tau_{bj,s,t+1} &= \tau_{bj,s,t} - k_j^{HD}(\tau_{bj,s,t} - \tau_{s,t}^{Amb}) + \\ &\quad + \frac{\left((1 - \eta_j^{Ch})P_{bj,s,t}^{Ch} - (1 - \eta_j^{Dis})P_{bj,s,t}^{Dis} \right) \Delta t}{C_j^{Tm} k_j^{Tm} \bar{E}_{bj}} \\ &\quad \forall b \in B, j \in J, s \in S, t \in T, \end{aligned} \quad (3.4)$$

where k_j^{HD} is a heat dissipation coefficient, $\tau_{s,t}^{Amb}$ is ambient temperature profile, which might be constant if energy storage is equipped with climate control, C_j^{Tm} is a thermal capacitance of an energy storage per unit mass, and k_j^{Tm} defines a mass of storage per MWh of installed energy capacity.

A net daily charge of energy storage is set to zero, which is essential when considering daily scenarios independently

$$\mathbf{E}_{b,j,s,1} = \mathbf{E}_{b,j,s,T+1} \quad \forall b \in B, j \in J, s \in S. \quad (3.5)$$

The maximum power output of energy storage is limited with the power rating in the following constraints

$$-\bar{\mathbf{P}}_{b,j} \leq \mathbf{P}_{b,j,s,t}^{\text{Dis}} \leq 0 \quad \forall b \in B, j \in J, s \in S, t \in T. \quad (3.6)$$

$$0 \leq \mathbf{P}_{b,j,s,t}^{\text{Ch}} \leq \bar{\mathbf{P}}_{b,j} \quad \forall b \in B, j \in J, s \in S, t \in T. \quad (3.7)$$

The charge of energy storage at every moment of time is limited to its energy rating, which is subject to a capacity fade due to degradation. Since stochastic optimization deals with a limited number of representative scenarios, which represent certain periods of time in future, charge constraint is satisfied for each period of a lifetime separately

$$\begin{aligned} 0 \leq \mathbf{E}_{b,j,s,t} &\leq \bar{\mathbf{E}}_{b,j} (1 - 365 y_{b,j} \delta_{b,j}^{\text{CF}}) \\ \forall y_{b,j} &\in [1, 2, \dots, \mathbf{T}_{b,j}^{\text{LT}}], b \in B, j \in J, s \in S_{T_{b,j}^{\text{LT}}}, t \in T, \end{aligned} \quad (3.8)$$

where $y_{b,j}$ is operational lifetime periods per each year of operation of a particular energy storage system.

Energy storage operational lifetime is a function of an energy storage degradation, and it is calculated as a ratio of the maximum capacity fade ($1 - \text{EoL}_j$) of a specific technology to the average daily energy capacity fade value

$$\mathbf{T}_{b,j}^{\text{LT}} = \frac{1 - \text{EoL}_j}{365 \delta_{b,j}^{\text{CF}}} \quad \forall b \in B, j \in J, \quad (3.9)$$

where capacity fade for each scenario is found as a sum of capacity fade functions from idling and cycling as follows

$$\delta_{b,j}^{\text{CF}} = \delta^{\text{Idl}} + \sum_{c \in C} (i_c \delta_c^{\text{Cyc}}) \forall b \in B, j \in J, \quad (3.10)$$

where δ^{Idl} and δ_c^{Cyc} are degradation functions defined in (2.13) and (2.14), and i_c takes either 1 or 0.5, indicating full and half-cycles, respectively.

In (2.13) and (2.14) degradation from idling and cycling are found for the average daily SoC, the average daily temperature, the depth of discharge (DoD) of a cycle, and the average storage temperature during a cycle, which have to be defined in the constraints of the optimization problem. In the proposed problem formulation, SoC and DoD values are treated as operational strategy, which limits the operation of energy storage. Hence, inequality constraints are applied.

The DoD of each individual cycle is limited by inequality constraint as follows

$$\text{DoD}_{b,j,c}^{\text{Cyc}} \geq \frac{1}{2 \bar{E}_{b,j}} \sum_{t=t_{s,c}^{\text{Start}}}^{t_{s,c}^{\text{End}}} (P_{b,j,s,t}^{\text{Ch}} - P_{b,j,s,t}^{\text{Dis}}) \Delta t \quad \forall b \in B, j \in J, s \in S, c \in C \quad (3.11)$$

The average temperature during a cycle is found with equality constraint as follows

$$\tau_{b,j,c}^{\text{Cyc}} = \frac{1}{T_c} \sum_{t=t_{s,c}^{\text{Start}}}^{t_{s,c}^{\text{End}}} (\tau_{b,j,s,t}) \Delta t \quad \forall b \in B, j \in J, s \in S, c \in C \quad (3.12)$$

where T_c is a duration of a cycle.

The plausible suggestions for the start $t_{s,c}^{\text{Start}}$ and the end $t_{s,c}^{\text{End}}$ time moments for each of the cycles are made based on the demand profile, as shown in Chapter 4.

The average daily SoC of energy storage is limited by inequality constraint as follows

$$SoC_{b,j}^{Idl} \geq \frac{1}{T \bar{E}_{bj}} \sum_{t \in T} (E_{b,j,s,t}) \Delta t \quad \forall b \in B, j \in J, s \in S \quad (3.13)$$

And the average daily temperature of energy storage is found with equality constraint as follows

$$\tau_{b,j}^{Idl} = \frac{1}{T} \sum_{t \in T} (\tau_{b,j,s,t}) \Delta t, \quad \forall b \in B, j \in J, s \in S. \quad (3.14)$$

To model an environment (i.e., network, loads, and generators), a power balance equality is applied

$$\sum_{j \in J} (P_{b,j,s,t}^{Ch} + P_{b,j,s,t}^{Dis}) + P_{b,s,t}^G + P_{b,s,t}^L + P_{b,s,t}^{Net} = 0 \quad \forall b \in B, s \in S, t \in T, \quad (3.15)$$

where $P_{b,s,t}^G$ is a nodal power generation by a generation unit, $P_{b,s,t}^L$ is a nodal power consumption by a load, and $P_{b,s,t}^{Net}$ is net real power injection at node b , which is found as follows

$$P_{b,s,t}^{Net} = \sum_{bb' \text{ or } b'b \in Br} \frac{(\theta_{b,s,t} - \theta_{b',s,t})}{X_{bb'}} \quad (3.16)$$

To satisfy the thermal limits of power lines and transformers, the power flow constraint is applied

$$-\overline{PF}_{bb'} \leq \frac{(\theta_{b,s,t} - \theta_{b',s,t})}{X_{bb'}} \leq \overline{PF}_{bb'} \quad \forall bb' \in Br, s \in S, t \in T. \quad (3.17)$$

3.2 Problem Analysis and Resolution

The problem formulation proposed in the previous section extends the state-of-the-art by incorporating a thermal model of energy storage and operation-aware degradation from idling and cycling. However, the proposed formulation cannot be directly solved using off-the-shelf solvers as it contains a number of challenges to be addressed first.

First, the objective function (3.1) and constraints (3.3), (3.4), (3.8), (3.11), (3.13) contain a product of variables, which make the problem bilinear. Moreover, degradation functions from idling δ^{idl} and cycling δ_c^{Cyc} in (3.10) are not convex due to (2.13) and (2.14), meaning that they cannot be used in convex problem formulation that guarantees a global optimum of a solution. Finally, constraints (3.8) contain indices $y_{b,j}$ and sets $S_{T_{b,j}^{\text{LT}}}$ that depend on variable $T_{b,j}^{\text{LT}}$, which does not allow generalizing the problem.

To overcome the problems of nonconvexity in (3.1), (3.3), (3.4), (3.8), (3.10), (3.11), (3.13) it has been proposed to substitute continuous variables $\bar{E}_{b,j}$, $T_{b,j}^{\text{LT}}$, $\text{SoC}_{b,j}^{\text{Idl}}$, $\text{DoD}_{b,j,c}^{\text{Cyc}}$, which are the cause of nonconvexity, with discrete integer variables. Therefore, the nonconvex continuous objective function and the constraints become mixed-integer convex, which possess the property of convexity for the fixed integer variables.

To overcome the problem related to a variable dependent indices $y_{b,j}$ and sets $S_{T_{b,j}^{\text{LT}}}$, and taking into the fact that the variable $T_{b,j}^{\text{LT}}$ is no longer continuous, a dynamic programming approach is proposed to be used to dynamically reformulate constraints (3.8) of the optimization problem while varying integer variable $T_{b,j}^{\text{LT}}$. In addition to that, an additional constraint is required that puts operational limits on an energy storage power output after its lifetime

$$P_{b,j,s,t}^{\text{Ch}} + P_{b,j,s,t}^{\text{Dis}} = 0 \quad \forall b \in B, j \in J, s \in S_{T_{b,j}}^{\text{LT}}, t \in T, \quad (3.18)$$

where the set of scenario $S_{T_{b,j}}^{\text{LT}}$ contains those scenarios that are not in $S_{T_{b,j}}^{\text{LT}}$.

The main drawback of the proposed mixed-integer problem reformulation resides in its scalability. Particularly, the whole enumeration approach to finding the optimal solution of the MICP problem requires solving the convex part of the optimization problem for every combination of integer variables, which number is in a power law dependence with the number of network buses, energy storage technologies, and performed cycles. For example, if each integer variable has 10 discrete values, and the problem is solved for B-bus network, J energy storage technologies, and C charge-discharge cycles, the number of all possible combinations for which the convex optimization problem has to be solved would reach $10^{\text{BJ}(3+\text{C})}$ (equivalent to $\text{BJ}(3 + \text{C}) \log_2 10$ binary variables), which yields an intractable number even for a relatively small problem. Even though the existing partial enumeration techniques, e.g., Branch-and-Bound algorithm, reduce the number of the considered combinations, none of them guarantee a specific ratio of partitioning. Hence, the evaluation of problem complexity is done for the whole enumeration case, while the Branch-and-Bound algorithm is still used for efficient problem-solving.

To make the original problem tractable and reduce the number of discrete combinations, it is possible to exploit a superposition principle of an optimization problem formulation and decompose the problem into a set of independent subproblems per each bus b and energy storage technology j by relaxing power balance constraints (3.15) and power flow limit constraints (3.17). Particularly, constraints (3.15) have been relaxed and put into the objective function (3.1)

according to the ALR procedure, and the logarithm barrier function is used to consider constraints (3.17) within the objective function (3.1).

The relaxation of complicating constraints implies considering them within the objective function. First, for relaxing the power balance constraints (3.15), the original objective function (3.1) is enhanced with the auxiliary fixed dual variables $\lambda_{b,s,t}$ multiplied by the constraint itself plus an additional (augmented) 2-norm function of the constraint aimed to penalize its violation with the positive constant value $\frac{\gamma}{2}$. The latter augmented term is included to make the problem reformulation generic for various objective functions, including linear, which cannot always be resolved by means of the conventional Lagrange relaxation approach [124]. Second, for relaxing the power flow limit constraints (3.17), the resulting objective function is enhanced with the logarithm functions, which approach infinity when the constraint is binding. The resulting objective function now looks as follows

$$\begin{aligned}
F = & - \sum_{s \in S} \pi_s R_s + \sum_{b \in B} \sum_{j \in J} \frac{\bar{E}_{b,j} \left(C_j^E + \frac{C_j^P}{k_j^{E/P}} \right)}{365 T_{b,j}^{LT}} + \\
& + \sum_{b \in B} \sum_{s \in S} \sum_{t \in T} \left[\lambda_{b,s,t} \left(\sum_{j \in J} (P_{b,j,s,t}^{\text{Ch}} + P_{b,j,s,t}^{\text{Dis}}) + P_{b,s,t}^G + P_{b,s,t}^L + \sum_{bb' \in Br} \frac{(\theta_{b,s,t} - \theta_{b',s,t})}{X_{bb'}} \right) \right. \\
& + \frac{\gamma}{2} \left\| \sum_{j \in J} (P_{b,j,s,t}^{\text{Ch}} + P_{b,j,s,t}^{\text{Dis}}) + P_{b,s,t}^G + P_{b,s,t}^L + \sum_{bb' \in Br} \frac{(\theta_{b,s,t} - \theta_{b',s,t})}{X_{bb'}} \right\|^2 \left. \right] + \tag{3.19} \\
& + \sum_{bb' \in Br} \sum_{s \in S} \sum_{t \in T} \rho \left[\left(-\log \left(\overline{\text{PF}}_{bb'} + \frac{(\theta_{b,s,t} - \theta_{b',s,t})}{X_{bb'}} \right) \right) + \right. \\
& \left. + \left(-\log \left(\overline{\text{PF}}_{bb'} - \frac{(\theta_{b,s,t} - \theta_{b',s,t})}{X_{bb'}} \right) \right) \right].
\end{aligned}$$

As a result of constraints relaxation and following the superposition principle, the original optimization problem might be decomposed into a set of independent subproblems per each bus b and technology j

$$\begin{aligned}
\min \sum_{b,j} F_{b,j} & \quad \Leftrightarrow \quad \sum_{b,j} \min F_{b,j} \\
s.t. G_{b,j,s,t} \leq 0 \quad \forall b \in B, j \in J, s \in S, t \in T & \quad s.t. G_{b,j,s,t} \leq 0 \quad \forall s \in S, t \in T \\
H_{b,j,s,t} = 0 \quad \forall b \in B, j \in J, s \in S, t \in T & \quad H_{b,j,s,t} = 0 \quad \forall s \in S, t \in T
\end{aligned} \tag{3.20}$$

This way the number of all possible combinations of discrete variables within one subproblem equals to 10^{3+C} , which can be further reduced by applying various partial enumeration procedures, e.g., Branch-and-Bound algorithm, which is used in most of the existing mixed-integer solvers [125].

3.3 Decomposed Optimization Subproblem

ADMM is proposed to resolve the decomposed subproblems in a systematic manner. Following the principles of ADMM, the formulation below provides subproblem formulation for a particular bus b and energy storage technology j .

3.3.1 Objective Function

The use of the ALR for the power balance complicating constraints (3.15) is explained by the fact that the Lagrangian multiplier of the constraint (fixed dual variables $\lambda_{b,s,t}$) represents the locational marginal price (LMP) of a node by controlling which it is possible to redistribute the power flows that correspond to economic dispatch. The logarithm barrier function is used to respect the power flow limit complicating constraints (3.17), while the leverage of power flows is at the former one. To perform a systematic search for the fixed dual variables $\lambda_{b,s,t}$, which correspond to the optimal solution, ADMM performs an iterative procedure with a systematic way to update the value of the fixed dual variables $\lambda_{b,s,t}$ in each iteration. Particularly, ADMM directly fixes each variable of the whole optimization problem to the values obtained in the previous iteration and solves it only with respect to the variables that correspond to a particular subproblem (indexed by b and j). Thus, the resulting objective function (3.21) consists of the terms that can be influenced by the variables that are related to bus b and technology j , while the rest of the terms are considered to be redundant.

$$\begin{aligned}
F = & - \sum_{s \in S} \pi_s R_s^{(k)} + \frac{\bar{\mathbf{E}}_{b,j}^{(k)} \left(C_j^E + \frac{C_j^P}{k_j^{E/P}} \right)}{365 \mathbf{T}_{b,j}^{LT(k)}} + \\
& + \sum_{s \in S} \sum_{t \in T} \lambda_{b,s,t}^{(k-1)} \left[\mathbf{P}_{b,j,s,t}^{\text{Ch}(k)} + \mathbf{P}_{b,j,s,t}^{\text{Dis}(k)} + P_{b,s,t}^{\text{G}(k)} + \sum_{bb' \in Br} \left(\frac{\boldsymbol{\theta}_{b,s,t}^{(k)}}{X_{bb'}} \right) \right] - \\
& - \sum_{b' \in Br} \sum_{s \in S} \sum_{t \in T} \lambda_{b',s,t}^{(k-1)} \left[\frac{\boldsymbol{\theta}_{b',s,t}^{(k)}}{X_{bb'}} \right] + \\
& + \frac{\gamma}{2} \left\| \mathbf{P}_{b,j,s,t}^{\text{Ch}(k)} + \mathbf{P}_{b,j,s,t}^{\text{Dis}(k)} + \sum_{j' \in J^*} \left(P_{b',j',s,t}^{\text{Ch}(k-1)} + P_{b',j',s,t}^{\text{Dis}(k-1)} \right) + \right. \\
& \left. + P_{b,s,t}^{\text{G}(k)} + P_{b,s,t}^{\text{L}} + \sum_{bb' \in Br} \frac{\left(\boldsymbol{\theta}_{b,s,t}^{(k)} - \boldsymbol{\theta}_{b',s,t}^{(k-1)} \right)}{X_{bb'}} \right\|^2 + \tag{3.21} \\
& + \sum_{b' \in Br} \frac{\gamma}{2} \left\| \sum_{j \in J} \left(P_{b',j,s,t}^{\text{Ch}(k-1)} + P_{b',j,s,t}^{\text{Dis}(k-1)} \right) + P_{b',s,t}^{\text{G}(k-1)} + P_{b',s,t}^{\text{L}} + \right. \\
& \left. + \sum_{b' \in Br} \frac{\left(\boldsymbol{\theta}_{b',s,t}^{(k-1)} - \boldsymbol{\theta}_{b,s,t}^{(k)} \right)}{X_{b'b}} \right\|^2 + \\
& + \sum_{bb' \in Br} \sum_{s \in S} \sum_{t \in T} \rho \left[\left(-\log \left(\overline{\text{PF}}_{bb'} + \frac{\left(\boldsymbol{\theta}_{b,s,t}^{(k)} - \boldsymbol{\theta}_{b',s,t}^{(k-1)} \right)}{X_{bb'}} \right) \right) + \right. \\
& \left. + \left(-\log \left(\overline{\text{PF}}_{bb'} - \frac{\left(\boldsymbol{\theta}_{b,s,t}^{(k)} - \boldsymbol{\theta}_{b',s,t}^{(k-1)} \right)}{X_{bb'}} \right) \right) \right],
\end{aligned}$$

where set J^* contains all energy storage technologies except j -th, k is the current iteration of ADMM, and $k-1$ is the previous one. Here, index (k) in superscript indicates the variables with respect to which a particular subproblem is to be solved, while index $(k-1)$ indicates the fixed variables

obtained in the previous iteration that does not correspond to bus b and technology j (i.e., not variables of a subproblem).

3.3.2 Constraints

The objective function (3.21) is to be minimized subject to the energy storage constraints described in Section 3.1.2 but only for the particular bus b and technology j . Particularly, energy to power ratio constraint

$$\frac{\bar{E}_{b,j}^{(k)}}{\bar{P}_{b,j}^{(k)}} = k_j^{E/P}. \quad (3.22)$$

Energy storage continuity constraints

$$\begin{aligned} \mathbf{E}_{b,j,s,t+1}^{(k)} &= \left(1 - k_j^{\text{SD}}(\tau_t)\right) \mathbf{E}_{b,j,s,t}^{(k)} + \left(\mathbf{P}_{b,j,s,t}^{\text{Ch}(k)} + \mathbf{P}_{b,j,s,t}^{\text{Dis}(k)}\right) \Delta t - \\ &- \left(\left(1 - \eta_j^{\text{Ch}}\right) \mathbf{P}_{b,j,s,t}^{\text{Ch}(k)} - \left(1 - \eta_j^{\text{Dis}}\right) \mathbf{P}_{b,j,s,t}^{\text{Dis}(k)}\right) \Delta t \quad \forall s \in S, t \in T. \end{aligned} \quad (3.23)$$

Temperature continuity constraints

$$\begin{aligned} \tau_{b,j,s,t+1}^{(k)} &= \tau_{b,j,s,t}^{(k)} - k_j^{\text{HD}} \left(\tau_{b,j,s,t}^{(k)} - \tau_{s,t}^{\text{Amb}} \right) + \\ &+ \frac{\left(\left(1 - \eta_j^{\text{Ch}}\right) \mathbf{P}_{b,j,s,t}^{\text{Ch}(k)} - \left(1 - \eta_j^{\text{Dis}}\right) \mathbf{P}_{b,j,s,t}^{\text{Dis}(k)} \right) \Delta t}{C_j^{\text{Tm}} k_j^{\text{Tm}} \bar{E}_{b,j}^{(k)}} \quad \forall s \in S, t \in T. \end{aligned} \quad (3.24)$$

Net zero charge constraints

$$\mathbf{E}_{b,j,s,1}^{(k)} = \mathbf{E}_{b,j,s,T+1}^{(k)} \quad \forall s \in S. \quad (3.25)$$

Power rating constraints

$$-\bar{P}_{b,j}^{(k)} \leq \mathbf{P}_{b,j,s,t}^{\text{Dis}(k)} \leq 0 \quad \forall s \in S, t \in T. \quad (3.26)$$

$$0 \leq \mathbf{P}_{b,j,s,t}^{\text{Ch}(k)} \leq \bar{\mathbf{P}}_{b,j}^{(k)} \quad \forall s \in S, t \in T. \quad (3.27)$$

Energy rating constraints

$$0 \leq \mathbf{E}_{b,j,s,t}^{(k)} \leq \bar{\mathbf{E}}_{b,j}^{(k)} \left(1 - 365 y_{b,j} \delta_{b,j}^{\text{CF}(k)}\right) \quad (3.28)$$

$$\forall y_{b,j} \in [1, 2, \dots, \mathbf{T}_{b,j}^{\text{LT}(k)}], s \in S_{T_{b,j}^{\text{LT}}}, t \in T.$$

Operational lifetime constraint

$$\mathbf{T}_{b,j}^{\text{LT}(k)} \geq \frac{1 - \text{EoL}_j}{365 \delta_{b,j}^{\text{CF}(k)}}, \quad (3.29)$$

where capacity fade $\delta_{b,j}^{\text{CF}(k)}$ is found as follows

$$\delta_{b,j}^{\text{CF}(k)} = \delta^{\text{Idl}(k)} + \sum_{c \in C} (i_c \delta_c^{\text{Cyc}(k)}). \quad (3.30)$$

DoD limit constraints

$$\mathbf{DoD}_{b,j,c}^{\text{Cyc}(k)} \geq \frac{1}{2 \bar{\mathbf{E}}_{b,j}^{(k)}} \sum_{t=t_{s,c}^{\text{Start}}}^{t_{s,c}^{\text{End}}} (\mathbf{P}_{b,j,s,t}^{\text{Ch}(k)} - \mathbf{P}_{b,j,s,t}^{\text{Dis}(k)}) \Delta t \quad \forall s \in S, c \in C. \quad (3.31)$$

Cycle temperature constraints

$$\boldsymbol{\tau}_{b,j,c}^{\text{Cyc}(k)} = \frac{1}{T_c} \sum_{t=t_{s,c}^{\text{Start}}}^{t_{s,c}^{\text{End}}} (\boldsymbol{\tau}_{b,j,s,t}^{(k)}) \Delta t \quad \forall s \in S, c \in C. \quad (3.32)$$

Average daily SoC constraints

$$\mathbf{SoC}_{b,j}^{\text{Idl}(k)} \geq \frac{1}{T \bar{\mathbf{E}}_{b,j}^{(k)}} \sum_{t \in T} (\mathbf{E}_{b,j,s,t}^{(k)}) \Delta t \quad \forall s \in S. \quad (3.33)$$

Average daily temperature constraints

$$\tau_{b,j}^{\text{idl}(k)} = \frac{1}{T} \sum_{t \in T} (\tau_{b,j,s,t}^{(k)}) \Delta t \quad \forall s \in S. \quad (3.34)$$

Finally, after lifetime constraints

$$P_{b,j,s,t}^{\text{Ch}(k)} + P_{b,j,s,t}^{\text{Dis}(k)} = 0 \quad \forall s \in S_{T_{b,j}}^*, t \in T. \quad (3.35)$$

3.3.3 Algorithm

ADMM is an iterative procedure with a systematic way to update the value of the fixed dual variable in each iteration. The decomposed subproblems are solved for each bus b and technology j in parallel processes, after which dual fixed variables $\lambda_{b,s,t}^{(k)}$ are updated according to (3.36), where the value of increment (decrement) is determined by the value of violation of the relaxed power balance constraint (3.15) and constant parameter γ .

$$\lambda_{b,s,t}^{(k)} = \lambda_{b,s,t}^{(k-1)} + \gamma \left(\sum_{j \in J} (P_{b,j,s,t}^{\text{Ch}(k)} + P_{b,j,s,t}^{\text{Dis}(k)}) + P_{b,s,t}^{\text{G}(k)} + P_{b,s,t}^{\text{L}(k)} + \sum_{bb' \in Br} \frac{(\theta_{b,s,t}^{(k)} - \theta_{b',s,t}^{(k)})}{X_{bb'}} \right) \quad (3.36)$$

The procedure of solving subproblems for all $b \in B$ and $j \in J$ and updating the fixed dual variables $\lambda_{b,s,t}^{(k)}$ is repeated until the convergence criterion (3.37) is satisfied, which indicates that the value of the penalty (primal residual) is negligible, meaning that the value of the fixed dual variable does not change significantly anymore.

$$\left| \lambda_{b,s,t}^{(k)} - \lambda_{b,s,t}^{(k-1)} \right| \leq \varepsilon \quad \forall b \in B, s \in S, t \in T. \quad (3.37)$$

A flowchart of the proposed algorithm is depicted in Figure 3.1.

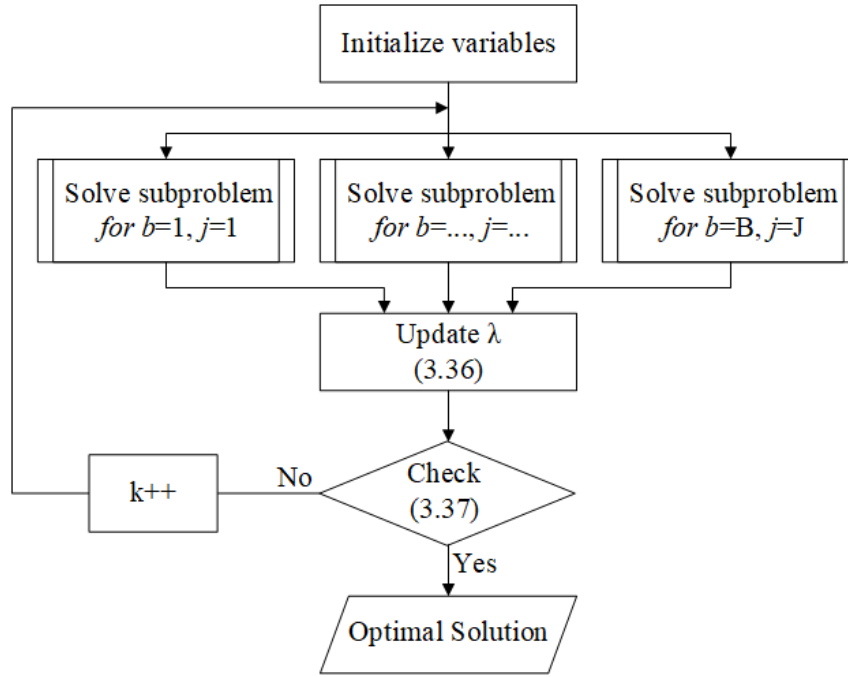


Figure 3.1: ADMM flowchart

At first, variables initialization is required. Each continuous variable of the optimization problem proposed in the previous section requires initialization, as well as the fixed dual variable $\lambda_{b,s,t}^{(0)}$ for all $b \in B, s \in S, t \in T$. The simplest way is to initialize them with zeros. However, for faster convergence, it is reasonable to initialize the variables with more meaningful values. In practice, the dual variable λ , associated with the power balance constraint (3.15), which is relaxed in our case, defines LMP for energy. Hence, for faster convergence, it is possible to initialize $\lambda_{b,s,t}^{(0)}$ with energy price or LMP values obtained beforehand by running DC OPF without storage. The variables associated with DC OPF, such as $\theta_{b,s,t}^{(0)}$, are also initialized with the obtained results. The variables associated with energy storage can be initialized with zeros.

After the initialization process, the proposed in the previous section subproblem is solved for all $b \in B, j \in J$. Since each subproblem does not depend on others during the same iteration,

they can be solved in parallel that can significantly decrease computational time. When all subproblems are solved, dual fixed variables $\lambda_{b,s,t}^{(k)}$ are updated according to (3.36). Then a convergence check is performed with (3.37). If the dual fixed variable did not change much after an iteration, the optimization is over, and the results obtained from the subproblems in the last iteration corresponds to the optimal solution. Otherwise, another iteration of subproblems solving is performed.

3.4 Conclusions

The proposed problem formulation of optimal siting, sizing, and technology selection of energy storage contained a number of challenges that do not allow solving the problem as is using off-the-shelf optimization packages. Particularly, when an operation and degradation-aware sizing is performed. In addition to that, a Li-ion based energy storage technology possesses a complex degradation mechanism that depends on many variables, which is neither linear nor convex. All of these comprise challenges to the optimization problem resolution.

To overcome the problem of nonconvexity, the mixed-integer convex problem reformulation has been proposed, where the continuous variables that cause nonconvexity have been replaced with integer ones. As a result, the reformulated problem meets the convexity requirements for the fixed integer variables. This implies that the optimal solution can be found by the consecutive optimization of the convex optimization problem for each combination of integer variables. The main drawback of the proposed problem reformulation resides in the fact that the number of all possible combinations of integer variables may easily reach an intractable

number even for a small problem, and partial enumeration techniques cannot resolve the intractability.

To resolve the problem of intractability, the proposed mixed-integer convex programming problem has been decomposed per each bus and energy storage technology, which can be solved in parallel. The search space of each subproblem has been decreased significantly, and more importantly, it does not depend on the network size and the number of considered storage technologies.

Chapter 4. Results and Analysis

4.1 Case Study

4.1.1 Application

As a demonstrator of the optimal siting, sizing, and technology selection, transmission congestion management is proposed to be considered for the application of energy storage. In the operational timescale, transmission congestion management is performed either by redirecting the power flows using so called FACTS devices or by energy time-shift provided by energy storage systems. The latter implies price arbitrage, which is well known and studied in the literature. Hence, the application provides tangible results, which can be evaluated with the existing metrics.

Transmission congestion management application requires knowledge about the price for energy at each bus or generation cost function of each generator as well as the thermal power flow limits of each power line within a considered network. The first option is much easier to implement. However, it does not provide a market response to the integration of energy storage [60]. In contrast to that, the second option provides the market response to the integration of energy storage; particularly, energy price responds to the net demand change resulting in a decrease of price volatility during a day until it becomes unprofitable for energy storage to install more capacity. Moreover, thermal power flow limits are creating a non-uniform price for energy within a network, when the power line limits are reached, which inform the optimizer with the most relevant location(s) to install energy storage.

To get the most insight from the problem solution, it has been proposed to follow the second option, which requires enhancing the optimization problem proposed in the previous chapter. This includes formulating the reward function and adding a few more constraints that model generation units.

The reward function is formulated as a negative generation cost plus active power losses on lines, meaning that the minimum operating cost of a network is sought within the objective function (3.21)

$$R_{b,j,s} = - \left(\sum_{g \in G} (a_g \mathbf{P}_{g,s,t}^{\mathbf{G}(k)} - b_g \mathbf{P}_{g,s,t}^{\mathbf{G}(k)}) + \sum_{bb' \in Br} \left(\frac{\theta_{b,s,t}^{(k)} - \theta_{b',s,t}^{(k-1)}}{X_{bb'} V_{bb',t}} \right)^2 R_{bb'} C_{bb',t}^{\text{APL}} \right), \quad (4.1)$$

where a_g and b_g are quadratic and linear coefficients of the generation cost function, $V_{bb'}$ is a line nominal voltage level, $R_{bb'}$ is a line active resistance, and $C_{bb',t}^{\text{APL}}$ is the energy price for active power losses per MWh. A constant part of the quadratic function is omitted as it cannot be influenced by any variable within the objective function, hence, redundant.

The proposed reward function extends the traditional DC OPF formulation by considering active power losses within the objective function, which are not considered in the power balance constraints as the quadratic dependence of power losses does not meet the affinity requirement for equality constraint in a convex problem formulation. For the same reason, to approximate the value of active power losses while keeping the objective function convex, the energy price for active power losses is considered constant but different for each bus and time moment. In the case study, the price of active power losses corresponds to the LMPs obtained beforehand by running DC OPF without storage, which was done during the initialization of

variables for ADMM in Section 3.3.3. However, since active power losses correspond to a power line between two nodes, the average energy price of two nodes is found.

Since generation units are installed at some buses, for general formulation a nodal generation $P_{b,s,t}^G$ used in the objective function (3.21) is found as follows

$$P_{b,s,t}^G = \begin{cases} P_{g,s,t}^G, & \text{if } g = b \\ 0, & \text{if } g \neq b \end{cases}, \quad (4.2)$$

where g indicates a bus number where generation unit is installed.

Real power production constraint for thermal generation unit is respected with the following inequality constraint

$$-\bar{P}_{g,s}^G \leq P_{g,s,t}^G \leq 0, \forall g \in G, s \in S, t \in T, \quad (4.3)$$

where $\bar{P}_{g,s}^G$ is the maximum power output of a thermal generation unit.

Thermal limits of power lines are considered within a barrier function in the objective function (3.21).

4.1.2 Network, Generation, and Power Lines Data

The methodology provided in the previous chapter has been demonstrated on the IEEE ten generators 39-bus transmission network, which represents the existing network of New England, USA [126]. The network is depicted in Figure 4.1.

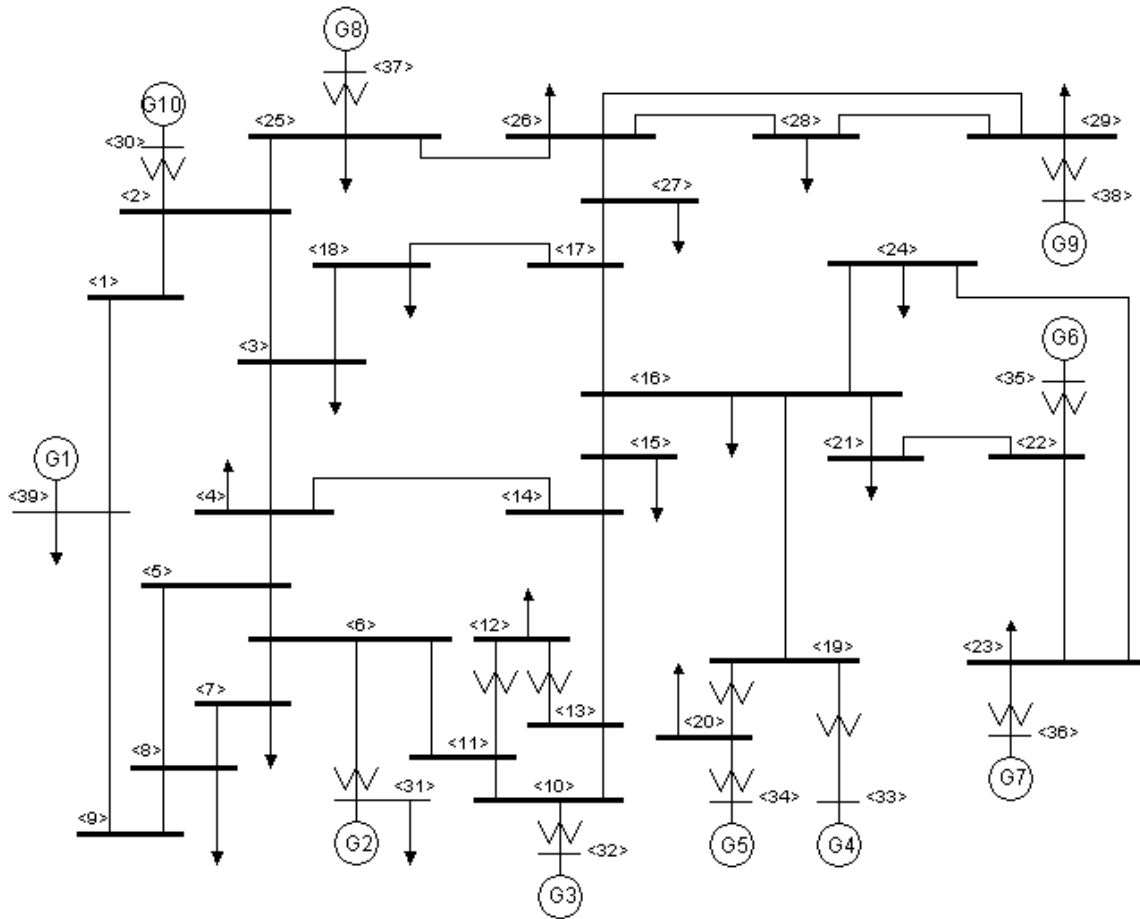


Figure 4.1: IEEE ten generators 39-bus network [126]

The network contains ten generation units, which parameters are given in Table C.1 of Appendix C, 46 branches, which data are presented in Table C.2 of Appendix C, and 19 aggregated power consumers, which data are provided in the next subsection.

4.1.3 Demand Data

Demand data were taken from the Customer-Led Network Revolution project [109]. Demand profiles used in the case study are illustrated in Figure 4.2, where the location of a particular demand is distinguished with the corresponding bus number in Figure 4.1.

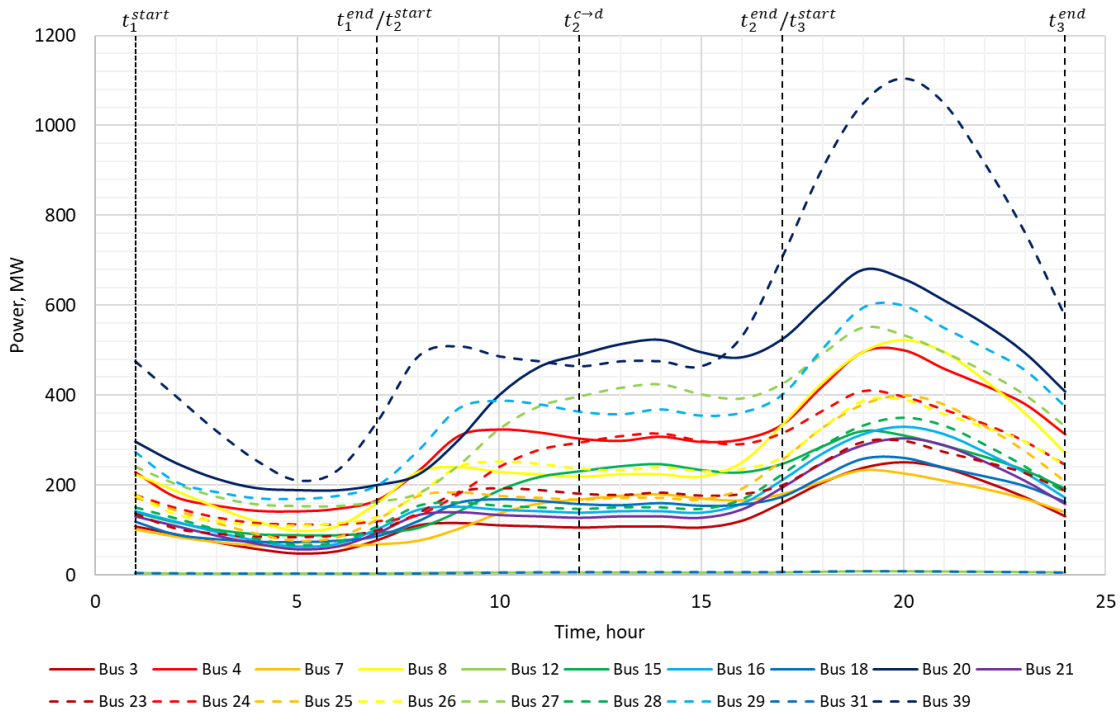


Figure 4.2: Demand profiles

To project the demand profiles for the future, an annual load growth of one percent is considered for 15 years ahead, which corresponds to the maximum calendar lifetime of the considered energy storage technologies.

As was proposed in Chapter 3, Section 3.1.2, demand scenarios might be used to formulate the DoD limit constraints (3.31), and the average cycle temperature constraints (3.32). From Figure 4.2, it can be noted that the demand profiles display two peaks and two valleys, which are considered to be the main indicators when the energy storage is charging or discharging when performing energy arbitrage. The expected state change moments are marked with vertical dashed lines in Figure 4.2. It has been assumed that energy storage would perform two half-cycles at the beginning [1h; 7h] and the end [17h; 24h] of the day, and one full cycle in the middle of the day [8h; 16h].

4.1.4 Energy Storage Characteristics

Four Li-ion based technologies are considered for the selection between or combination of LiFePO₄ (LFP), LiMn₂O₄ (LMO), LiNiMnCoO₂ (NMC), Li₄Ti₅O₁₂ (LTO). The proposed methodology accounts for charge and discharge efficiencies, self-discharge rate, EoL criterion, calendar lifetime, and the investment costs for the installed energy capacity. The corresponding energy storage characteristics are given in Table 4.1 [31], [127].

Table 4.1: Li-ion technologies' characteristics

j	Tech.	Disch. eff., %	Ch. eff., %	Self-dis., %/mon	EoL, %	Cal. Life years	Inv. Cost £/kWh
1	LFP	97.5	97.5	4	75	10	230
2	LMO	98.5	98.5	3	85	8	140
3	NMC	99	99	1	70	10	320
4	LTO	95	95	2	70	15	570

Capacity fade degradation characteristics for each technology are given in Table B.1 and Table B.2 of Appendix B.

4.2 Results Analysis

4.2.1 Optimal Solution

The methodology proposed in the previous chapter for the optimal siting, sizing, and technology selection has been applied to the case study provided above. Integer variables that represent an operational strategy $DoD_{b,j,c}^{Cyc}$ and $SoC_{b,j}^{Idl}$ are defined in the search space [0;1] with a discrete step size of 0.1, which corresponds to 10% increment. Operational lifetime variable $T_{b,j}^{LT}$ is defined in the search space [1;15] with a discrete step size of 1, which corresponds to one year. Energy capacity variable $\bar{E}_{b,j}$ is defined in the search space [0;500] with a discrete step

size of 10, which corresponds to 10 MWh of installed capacity. Thus, the total search space of integer variables for a single subproblem contains 7,650,000 combinations, which is equivalent to 23 binary variables.

The results of the optimization are presented in Table 4.2. The optimal solution of the problem corresponds to 350 MWh of Li-ion NMC installed on bus 17 and 360 MWh of the same technology installed on bus 27. The optimal operational strategy is identical for both energy storage systems and corresponds to an average daily state of charge $SoC_{17,3}^{Idl}$ and $SoC_{27,3}^{Idl}$ equal to 50%, and depth of discharge equal to 80% for the two considered half-cycles $DoD_{17,3,1}^{Cyc}$, $DoD_{17,3,3}^{Cyc}$ and $DoD_{27,3,1}^{Cyc}$, $DoD_{27,3,3}^{Cyc}$. The depth of discharge of the full cycle $DoD_{17,3,2}^{Cyc}$ and $DoD_{27,3,2}^{Cyc}$ are 0%. According to (2.14), the capacity fade for the shallow cycle equals to zero or, in other words, the same as if there were no cycle irrelevant to the cycle temperature, which, however, contributes to the average daily temperature for degradation from idling. This energy storage operation strategy ensures that an average cycle temperature for the two half-cycles does not exceed 22.9°C and 23.6°C respectively for both energy storage systems, and an average daily temperature does not exceed 22.5°C for both systems. The optimal operational lifetime for both energy storage systems is equal to eight years, during which the installed capacity fades by 30%.

Table 4.2: Optimal solution

Objective Function, £/day	Bus	Tech.	Cap., MWh	Operation Strategy								Oper. Lifetime, y
				Idling		Cycling						
				SoC^{Idl} %	τ^{Idl} °C	DoD_1^{Cyc} %	τ_1^{Cyc} °C	DoD_2^{Cyc} %	τ_2^{Cyc} °C	DoD_3^{Cyc} %	τ_3^{Cyc} °C	
3,449,182	17	NMC	350	50	22.5	80	22.9	0	21.2	80	23.6	8
	27	NMC	360	50	22.5	80	22.9	0	21.2	80	23.6	8

The objective function (average daily network operation cost) equals to 3,449,182 £/day, which comprise 3,304,041 £/day of generation cost, 67,334 £/day of thermal losses, and 77,808 £/day of per diem investment cost for energy storage.

4.2.2 Comparison with State-of-the-Art

At the moment, the most detailed degradation mechanism used within the problem of optimal siting, sizing, and technology selection of energy storage has been proposed by *Alsaidan et al.* in [90], where a nonlinear relationship between the energy storage DoD and lifecycle is taken into account. The proposed methodology extends the state-of-the-art approach by considering the complex degradation mechanism of Li-ion battery storage from idling and cycling that takes into account SoC, DoD, and storage temperature.

To be able to evaluate the effect of the proposed methodology, it is worth comparing the obtained results with the state-of-the-art approach performed for the same case study, as well as the cases when energy storage degradation is omitted [83], and power system operation without storage. In the comparative analysis below, the results obtained with the proposed methodology are referred to as Proposed SST case, the approach from [90] is referred to as State-of-the-Art SST case, the approach from [83] is referred to as No Degradation case, and the base case is referred to as No Storage case.

To simulate No Storage case, the proposed methodology has to be enhanced with the additional constraint (4.4), which effectively makes the proposed optimization problem equivalent to a multi-period DC OPF problem [128].

$$\bar{E}_{bj} = 0 \quad (4.4)$$

The optimal solution of the proposed methodology is opposed to No Storage case, No Degradation case, and State-of-the-Art SST case in Table 4.3, where Optimal Solution column corresponds to the solution of a particular optimization problem and Simulation column corresponds to accurate post-process degradation-aware simulation as in [38]. Based on the results of optimization problems, it can be assumed that the No Degradation case gives the most beneficial solution, then comes the state-of-the-art methodology, which provides a more beneficial solution than in the case of the Proposed SST case. However, when the accurate post-process degradation-aware simulation is performed, the solution provided by the proposed methodology is found to be the most beneficial. Particularly, the error in degradation estimation obtained for the No Degradation case comprises 59.8%, adding up an additional 56,071 £/day, which wipes out the whole benefit. For the State-of-the-Art case, the degradation error comprises 8.5%, which adds up an additional 6,661 £/day making an average daily operation cost of the network equal 3,451,846 £/day. In the case of the proposed methodology, a degradation estimation error comprises 1.1% in the optimization process, which adds up an additional 856 £/day to average network operation cost, which is equal to 3,450,039 £/day.

Table 4.3: Comparative study

#	Case	Optimal Solution				Simulation [38]	
		Bus	Technology	Capacity, MWh	Objective function, £/day	Operation Cost, £/day	Degradation error, £/day
1	No Storage [128]	-	-	-	3,457,323	3,457,323	0
2	No Degradation	17	LMO	915.45	3,422,765	3,478,836	56,071
		27	LMO	1025.42			
		28	LMO	13.31			
3	State-of-the-Art SST [90]	17	LFP	605.88	3,445,185	3,451,846	6,661
		27	LFP	637.82			
4	Proposed SST	17	NMC	350	3,449,182	3,450,039	856
		27	NMC	360			

A stacked chart of the daily network operation cost for all cases is illustrated in Figure 4.3. The difference between the Network Operational Cost of a particular case and the Network Operational Cost of No Storage case from Figure 4.3 gives a daily benefit of energy storage use. The expenditures are defined by per diem investment cost. And the revenue is found as a sum of benefits and expenditures. To get the annual values, one shall multiply them by 365.

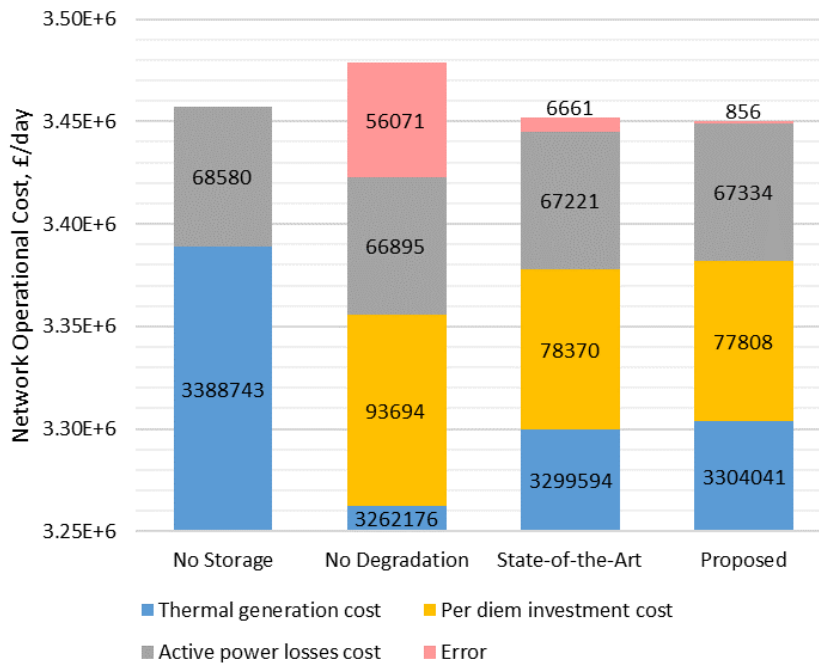


Figure 4.3: Objective function stacked chart

The maximum investment in energy storage is observed for the No Degradation case, where the optimal solution suggests installing 1954.18 MWh of LMO technology. This technology was selected by the optimizer because it has the lowest price for capacity. However, when the cost of degradation is included, the estimated daily benefit falls by 56,071 £/day. This shows the importance of taking degradation into account as the optimal investment and operation strategy derived neglecting degradation proves to be inefficient as it completely wipes out

benefits from the use of energy storage. Consequently, when estimating annual revenue, expenditure, and profitability, the results of the state-of-the-art methodology corresponds to annual revenue from energy storage operation equals to £30.6M, where £28.61M covers investment cost in energy storage and £1.99M is a benefit, which makes an investment return equal 7.0%. In the case of the proposed methodology, annual revenue from energy storage operation equals £31.06M, where £28.4M covers investment cost in energy storage, and £2.66M is a benefit, what makes an investment return ratio equal 9.4%.

4.2.3 Network and Energy Storage Operation

Figure 4.4 illustrates the optimal placement and size of energy storage systems that correspond to the optimal solution of the proposed methodology. During the high demand period from 18 until 22 hours, the network operation is accompanied by line congestions, which break the network into several price zones. Even though that energy storage is used to resolve network congestion problems, there are still four lines that carry the maximum power (red lines 10-32, 16-17, 16-19, and 17-27). This results in non-uniform energy price distribution within the network, which drives the need for energy storage installation at a certain bus. Comparing the results with No Storage case, in addition to the lines above, there were two more congested lines (green lines 13-14, and 25-37), and generator G8 operated at the maximum power output when energy storage was not used.

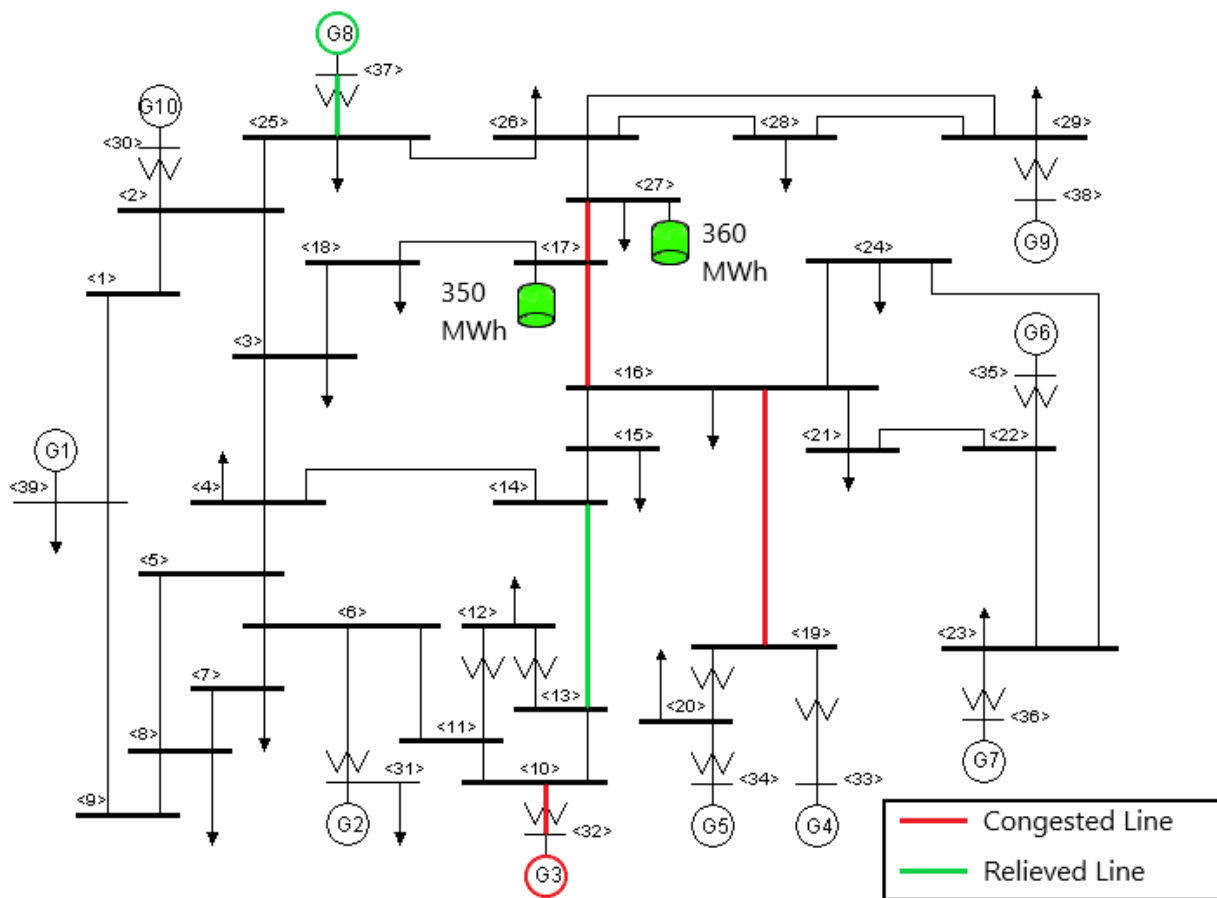


Figure 4.4: Network operation during high demand period

Figure 4.5 illustrates LMPs for the No Storage case (a) and the Proposed SST case (b) for all buses. When energy storage is not used, LMPs at bus 17 and bus 27 are above 200 £/MWh during the high peak demand, at the neighbor buses LMPs are not far below. When energy storage is used to perform transmission congestion management application, the maximum LMP at bus 17 drops to 175 £/MWh and 184 £/MWh at bus 27 – a market response to energy storage integration. LMPs at other buses are also affected by the energy storage systems on bus 17 and 27. The price difference between the valley price (from 4:00 to 6:00), when storage charges, and peak price, when storage discharges, gives the price difference of 150 £/MWh for the bus 17 and

158 £/MWh for the bus 27, decreasing which with more capacity of storage would not result into the decrease of total network operation costs.

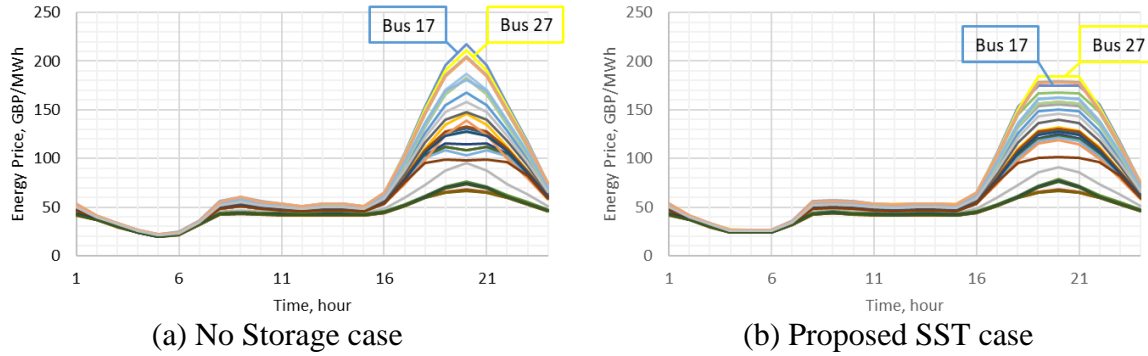


Figure 4.5: LMPs at 39-bus network

The energy storage state of charge profiles for each scenario are presented in Figure 4.6. Similarly to Figure 4.2, the state change instances for the energy storage are marked with black dotted vertical lines. As it can be seen from Figure 4.6, each of the considered cycles is limited within the proposed time frames, meaning that DoD limit constraints (3.31) and cycle temperature constraints (3.32) have been formulated appropriately for the particular case study. If they were not, the time frames have to be updated according to the results of the optimization problem.

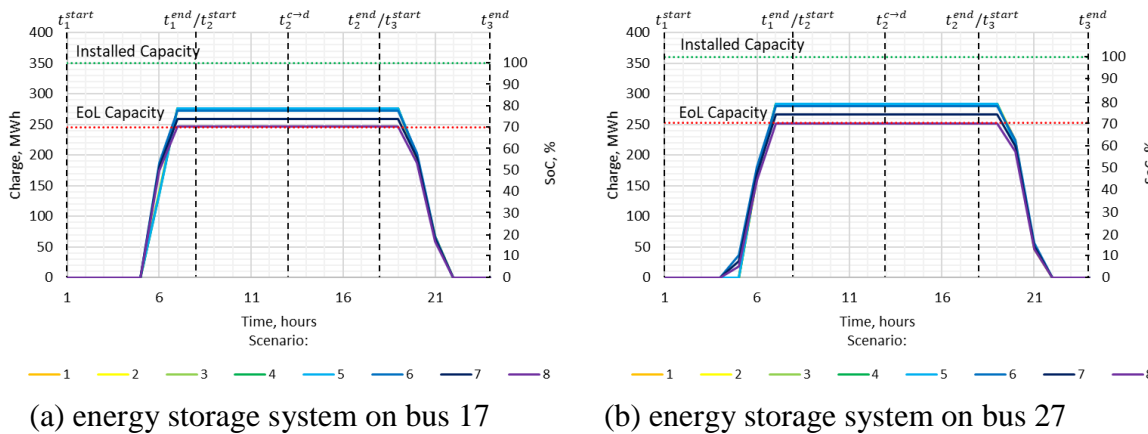


Figure 4.6: Charge of energy storage

From Figure 4.6, it can be noted that during the first five scenarios (years), energy storage systems operate with the maximum allowed depth of discharge of 80% until the remaining capacity allows it. After that time, the remaining capacity drops below 80% to 77.5% in the sixth year, 73.8% in the seventh year, and 70.1% in the eighth year, resulting in the corresponding depth of discharge drop during the last three years.

The temperature variation during the operation of energy storage systems is illustrated in Figure 4.7. It can be noted that with the decrease of the remaining capacity and depth of discharge value during the last three years of operation, the temperature variation decreased as well.

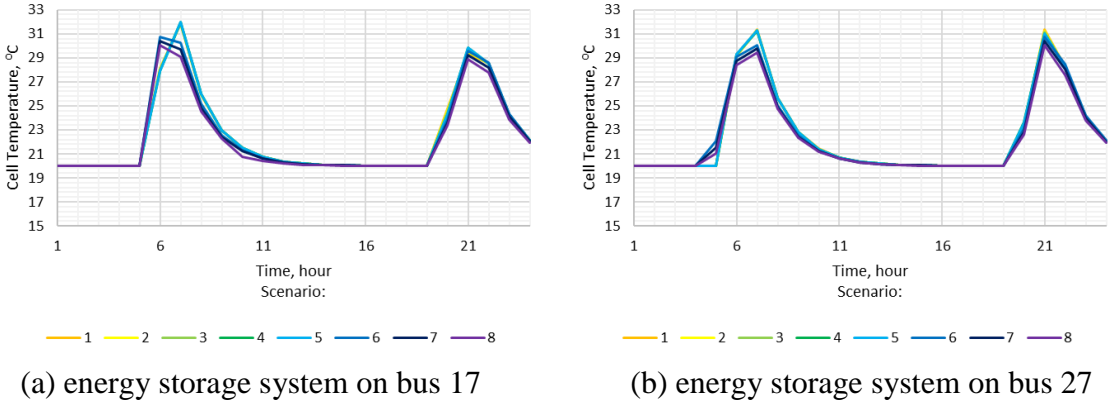


Figure 4.7: Storage temperature

Since the actual operation of energy storage systems is different from the operational strategy during the last three years, Figure 4.8 is presented to illustrate how the actual capacity fade (dotted lines) differs from the one considered within the optimization problem (solid lines). The difference between the linear capacity fade, considered within the optimization problem, and the actual one is within 1.1% error for both energy storage systems.

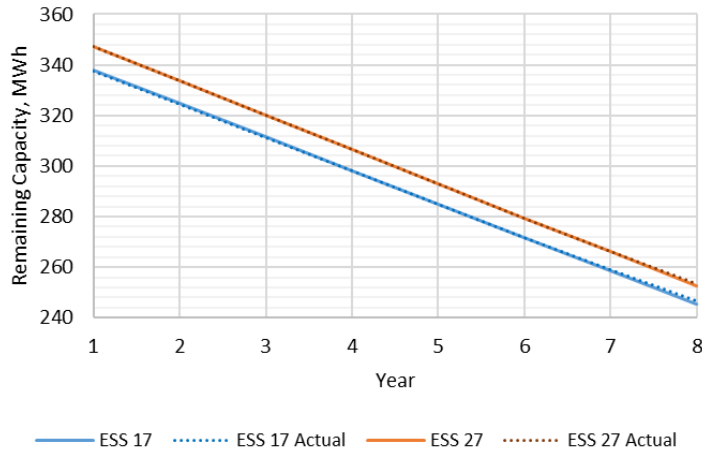


Figure 4.8: Energy storage capacity fade

4.3 Performance Value Analysis

In this section, an analysis of the energy storage value is performed to evaluate its effect on the profitability of a particular energy storage technology. The lower the price for the installed capacity, the more capacity might be installed in the network, resulting in more benefits.

To eliminate the effect from demand growth and stochasticity, the proposed in the previous chapter methodology has been solved deterministically for a single scenario, which corresponds to the 10th year of operation (original demand is increased by 10%). Since the optimal operational lifetime of energy storage systems might be different for different technologies, the optimization problem is solved for various operational lifetime limits by fixing operational lifetime variable $T_{b,j}^{LT}$ with integer values from 1 to 15.

4.3.1 Performance Value of Energy Storage Technologies

Figure 4.9 illustrates the results of the optimization problem for the original prices of energy storage technologies. According to Figure 4.9, Li-ion NMC technology is able to

decrease network operation cost more effectively if it is operated according to the operational strategy that corresponds to eight years of operational lifetime. Not far behind, Li-ion LTO technology that allows decreasing network operation cost effectively, when it is aimed at 15 years of operation. Li-ion LFP technology performs effectively for six years of operational lifetime, and Li-ion LMO technology is effective for three years of operation. In the following two subsections, the breakeven cost analysis is performed with respect to the most cost-effective energy storage solution (NMC); hence, its maximum performance is taken as 100%.

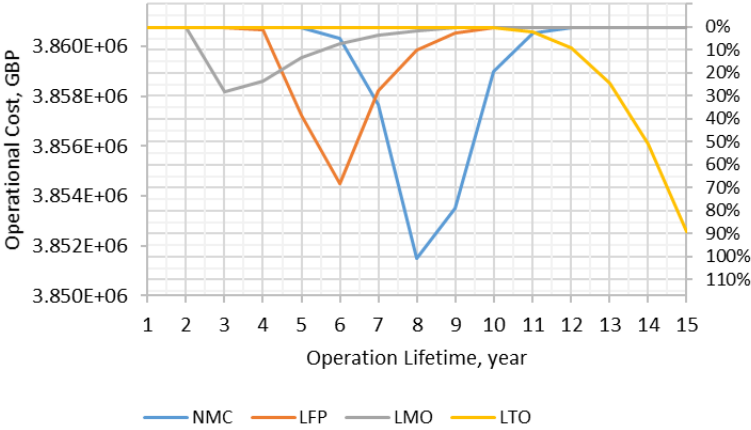


Figure 4.9: Performance value of energy storage technologies

4.3.2 Breakeven Cost of New Energy Storage

To evaluate the extent to which a particular energy storage technology is overpriced compared to other technologies for the particular application, a breakeven cost analysis is performed. Similarly to the performance evaluation, described in the previous subsection, the methodology has been solved deterministically for each energy storage technology and various operational lifetime values but with the reduced investment cost for energy capacity. The decrement of the reduction is 3%. Figure 4.10 illustrates the performance of each technology for

the original (solid lines) and reduced price (dashed lines) for the installed capacity. Such that, if the investment cost of LMO, LFP, and LTO is decreased by 12%, 6%, and 3% respectively, these technologies would be able to perform better than Li-ion NMC with the original price.

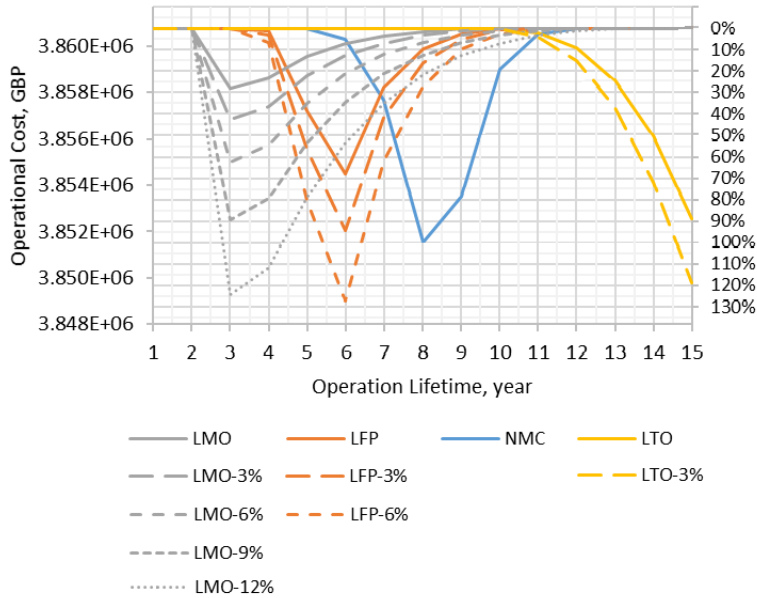


Figure 4.10: Breakeven cost of new energy storage technologies

4.3.3 Breakeven Cost of Second-Life Energy Storage

Similarly to the previous section, a storage value analysis is performed for second-life energy storage to determine a breakeven cost of the second-life solutions comparing with its off-the-shelf equivalent and the most cost-effective Li-ion NMC technology.

The operation of second-life energy storage is different from a new battery from at least two perspectives. First, the degradation processes are much more intensive in an old battery. As can be seen from Figure 2.24 of Chapter 2, the remaining capacity of second life energy storage is characterized by a rapid decrease after reaching the EoL point. Assuming that a capacity fade function follows the same functional relationship from SoC, DoD, and storage temperature but

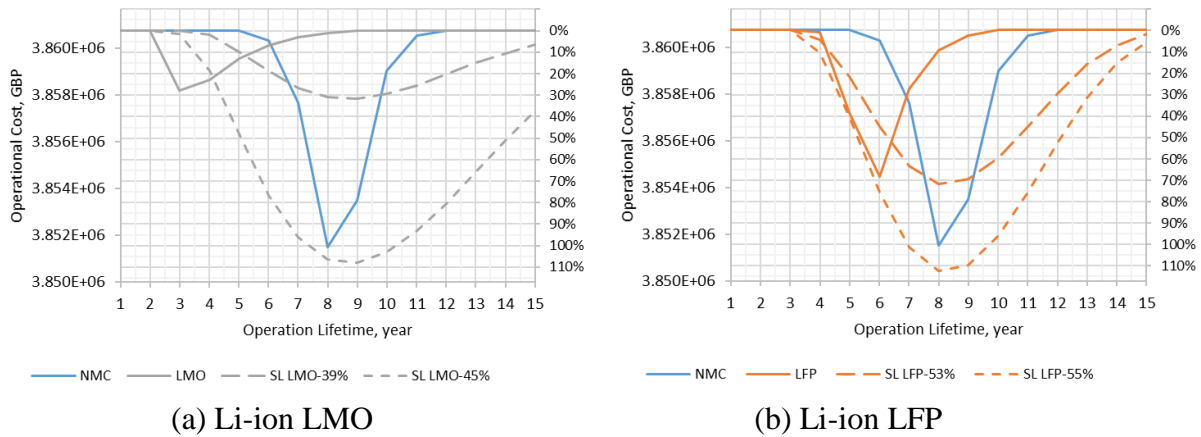
k_j^{SL} times more intensive than during the main degradation period, the charge constraint (3.28) of the original problem formulation would look as follows

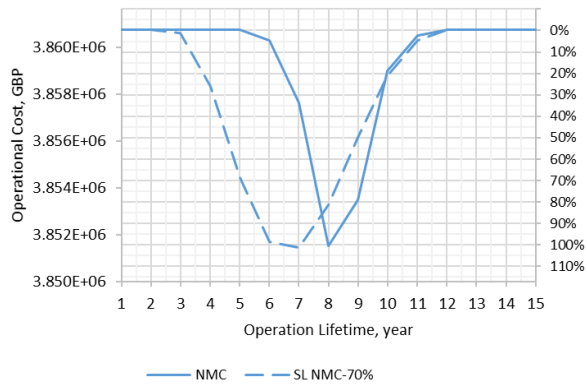
$$0 \leq E_{b,j,s,t} \leq \bar{E}_{b,j} (1 - k_j^{SL} 365 y_{b,j} \delta_{b,j}^{CF}). \quad (4.5)$$

Second, second-life energy storage starts its new life with the remaining capacity equal to the EoL threshold of a new battery, and it is able to fade until zero. To accommodate that, the constraint (3.29) of the original problem formulation is substituted with the following one

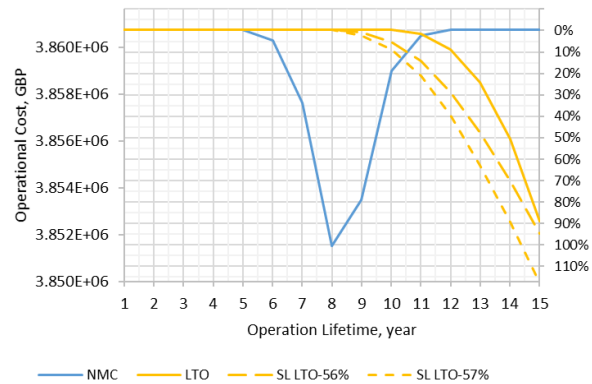
$$T_{b,j}^{LT} \geq \frac{EoL_j}{k_j^{SL} 365 \delta_{b,j}^{CF}} \quad (4.6)$$

Figure 4.11 illustrates the performance of each second-life energy storage technology comparing with its off-the-shelf equivalent and Li-ion NMC technology, which was found as the most cost-effective solution.





(c) Li-ion NMC



(d) Li-ion LTO

Figure 4.11: Performance value of second-life energy storage technologies

Table 4.4 aggregates the results obtained from the second-life energy storage performance evaluation, where the column BEC1 provides breakeven cost related to the considered technology, and column BEC2 provides breakeven cost related to the most cost-effective technology – NMC. Second-life LMO technology can bring a similar profit as the new battery if its price is 39% lower than the original. If the price is reduced by 45%, LMO technology is able to bring more profit than off-the-shelf NMC technology. In both cases, the optimal operational lifetime, during which the storage can perform the best, is increased from three years to nine years. For LFP second-life solution, it is able to perform the same as the new one when the price for it is 53% lower than the new storage. If the price is reduced by 55%, a second-life LFP technology is able to perform better than the new NMC battery. The optimal operational lifetime of the second-life LFP technology is increased from six to eight years compared to the off-the-shelf equivalent. Second-life NMC technology is able to bring the same benefit as the new one if its price is decreased by 70% with the optimal operational lifetime of 7 years. Second-life LTO battery is able to perform the same as the new one if its price is dropped

by 56%. When the price of second-life LTO technology is lower by 57%, it is able to perform better than the new NMC battery.

Table 4.4: Breakeven cost of second-life energy storage technologies

	LMO			LFP			NMC		LTO		
	Orig.	BEC1	BEC2	Orig.	BEC1	BEC2	Orig.	BEC1/2	Orig.	BEC1	BEC2
Discount, %	0	39	45	0	53	55	0	70	0	56	57
Price, £/kWh	140	85.4	77	230	108.1	103.5	320	96	570	250.8	245.1
Capacity, MWh	290	1560	4120	690	2000	2800	850	2500	800	1890	2200
Op.Life-time, y	3	9	9	6	8	8	8	7	15	15	15
Annual Profit, M£	0.94	1.06	3.62	2.29	2.41	3.77	3.37	3.4	2.99	3.18	3.95
Return, %	6.95	7.16	10.26	8.71	8.92	10.40	9.88	9.91	9.88	10.08	10.97

Here a comparison analysis is performed for the nameplate capacity, meaning that the investment cost for both off-the-shelf and second-life energy storage systems is for the original capacity of a new battery. To convert the investment cost value of a second-life battery from nameplate capacity to the actual capacity, one might divide the price values by EoL value of the corresponding technology.

4.4 Discussion

4.4.1 Siting, Sizing, and Technology Selection Decision Making

As it can be concluded from the comparative analysis of the Proposed SST case, State-of-the-Art case, No Degradation case and No Storage case, the optimal location for energy storage installation may be determined from LMPs, where the main contributing factors for non-uniform energy price distribution are power line thermal limits and active power losses, which

are considered within the proposed methodology. Particularly, the results suggest installing energy storage at those locations, where LMP variation is the highest in a daily scenario. To satisfy the thermal power limits of the line from bus 17 to bus 27 (line 17-27), the optimal solution suggests installing energy storage systems on both buses. Such that, energy storage at bus 17 feeds the loads on buses 18 and 3, while energy storage at bus 27 feeds the load on buses 26, 27, and 28. Even though there are alternative routes to feed these loads through the lines 3-4 and 1-39, transmission cost, which is induced by the active power losses, make the energy price at the bus 17 and bus 27 significantly higher than at the low price locations, such as bus 22 or bus 23, where the maximum LMPs reach 72.2 £/MWh.

The main driven factor for the sizing of energy storage, which performs energy arbitrage, is a price difference between the moments of time when energy storage charges (buys energy) and discharges (sells energy). When energy storage possesses a sufficient amount of capacity to influence LMPs (price maker), an accurate tool for power system modeling is required to track the influence of energy arbitrage on LMP. Particularly, the DC OPF framework has been used to model the network operation, which includes power generation and power flows within the network. For the No Storage case, a daily energy price difference on bus 17 is equal to 197.4 £/MWh, and 189.7 £/MWh on bus 27. The incorporation of energy storage reduced the price variation to 150.1 £/MWh on bus 17, where 350 MWh energy storage capacity is installed, and 158.2 £/MWh on bus 27, where 360 MWh energy storage capacity is installed.

Technology selection is driven by the internal parameters of a particular technology, such as self-discharge, round-trip efficiency, degradation, and price. The results of the Proposed SST case suggest installing Li-ion NMC technology, which is characterized by a relatively high price

for the installed capacity equal to 320 £/kWh, while LMO and LFP prices are 140 £/kWh and 230 £/kWh respectively. However, NMC battery possesses relatively mild degradation characteristics for idling and cycling, as well as the highest round-trip efficiency, which makes it a better choice for installation. In addition, the analysis showed that LTO technology, which has the highest price for the installed capacity of 570 £/kWh and the lowest degradation rate, is able to provide nearly the same return as NMC (see Table 4.4) but in a longer time period, what increases investment risks.

4.4.2 Method Applicability

Given the need to account for degradation (i.e., cycling requirements in Table D.1), DC OPF formulation and time discretization of one hour and assuming that it can easily be translated to 15-30 minutes, the application of the proposed methodology is suitable for at least nine applications from the list of energy storage applications provided in Table 2.1. Particularly, the methodology can be applied to Energy Time-Shift, Supply Capacity, Load Following, Transmission Support, Congestion Management, Transmission Network Upgrade Deferral and Equipment Life Extension, Retail Energy Time-Shift, and Demand Charge Management applications.

4.4.3 Cycle Counting Method

The formulation of cycle depth of discharge (3.11) and temperature (3.12) constraints require knowledge of the initial and final time moments of a cycle. Such a formulation has been influenced by the Rainflow-counting (RFC) mechanism initially used for estimating the fatigue life of materials [129] but then accommodated for estimating degradation of energy storage [38].

Particularly, it is used to identify charge-discharge cycles and their depth of discharge based on the battery state of charge profile. The main drawback of the RFC mechanism resides in its sequential structure (basically, it is a flowchart with logical structure) [130], which cannot be directly incorporated into a formal optimization problem, as the latter allows using only equalities and inequalities. And given the fact that the optimal siting, sizing, and technology selection problem is solved with respect to the optimal scheduling of assets (energy storage state of charge profile is a variable of optimization problem), it is essential to predict cycle timeframes somehow. Studying the results of various case studies showed that the plausible suggestions for the start and the end time moments for each cycle could be made based on the demand profile. The similar is applied to renewable generation data, as in the stochastic problem formulation, we consider it predefined with a certain probability of occurrence. However, if the considered timeframes do not coincide with the optimal solution, it is proposed to update them according to the results of the optimization problem and solve it again. Alternatively, auxiliary binary variables might be incorporated to introduced the logic of RFC within the optimization problem. This would require having one binary variable per each pair of charge/discharge power output variables ($P_{b,j,s,t}^{Ch}$ and $P_{b,j,s,t}^{Dis}$), leading to a substantial increase in the problem size. This way, the number of auxiliary variables is a product of time intervals T, scenarios S, energy storage technologies J and number of buses B, which is considerably larger than observed for the original MICP problem.

4.4.4 Computational Time

The proposed methodology, as well as the decomposed optimization subproblem, have been formulated in JuMP (Julia for Mathematical Optimization). The Ipopt solver has been used

to solve the convex optimization problems, and GLPKMIP solver has been applied for mixed-integer problems. The optimization problems have been solved on Intel® Core™ i5-2410M CPU @ 2.3GHz 4GB RAM laptop computer. The convergence tolerance ϵ , which defines stopping criteria in (3.37) and accuracy of optimization, was set to 0.1 £/MWh.

To test the scalability of the proposed problem formulation, it has been solved for various case-study networks and a number of demand scenarios. Particularly, the optimization problem has been solved for the IEEE benchmark systems, i.e., 9-bus, 14-bus, 24-bus, and 39-bus. The network data of which have been taken from the MATPOWER data files [131]. The number of considered demand scenarios varied from one to ten. The results of the ten scenario cases are provided in Appendix E.

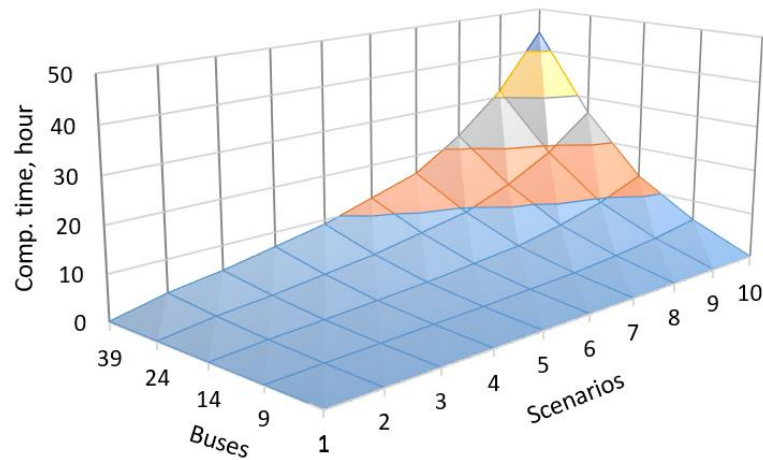


Figure 4.12: Computational time vs. number of buses and number of scenarios

Figure 4.12 illustrates how computational time is affected by the number of scenarios considered, as well as the number of candidate nodes within a network. The increased number of scenarios would only affect the convex part of the optimization problem, the complexity of which is polynomial-time dependent on the number of variables, hence, moderate growth along

with the number of scenarios axis. The same is applied to the number of considered buses as it is proportional to the subproblems number for ADMM to solve, which converges similarly to gradient methods [132].

4.4.5 Convergence of ADMM

The convergence of ADMM is still an open question. Even though in [132], *Boyd et al.* identified conditions for ADMM to converge, it only relates to ADMM for two-block (two subproblems) structures. Actually, it has been shown by *Chen et al.* [133] that even a three-block linear problem may diverge under some conditions. However, in practice, ADMM converges to modest accuracy even for large-scale problems [132], [134].

As for the proposed problem formulation, it satisfies the conditions identified in [132] but contains a multi-block structure, which does not allow proving its convergence for a general case. However, in the extensive numerical tests performed for studying breakeven cost in Section 4.3 and scalability of the method in the previous subsection, the problem formulation has been solved many times for the different variations of the considered case study, as well as for various IEEE benchmark systems, i.e., 9-bus, 14-bus, 24-bus, and 39-bus. In all cases, ADMM showed good performance and convergence properties. Figure 4.13 shows a primal residual of the auxiliary fixed dual variables of ADMM (i.e., the value of penalty) during the optimization process.

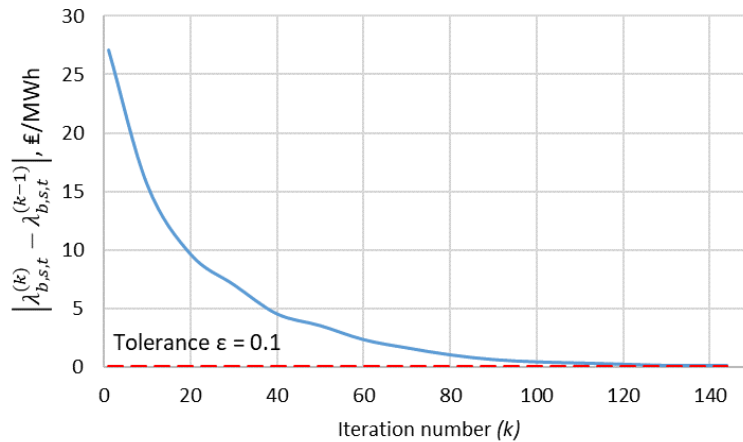


Figure 4.13: Primal residual during the optimization

4.5 Conclusions

The proposed methodology has been demonstrated on IEEE ten generators 39-bus benchmark system for transmission congestion management application of energy storage with the objective of minimum network operation cost. Demand data have been taken from the Customer-Led Network Revolution project and projected for a 15-year time horizon with an assumption of annual load growth of 1%.

The optimal solution suggests installing energy storage at two neighbor buses, where daily LMP variation for energy is the highest. Energy market response to a sufficient amount of energy storage capacity has been modeled with DC OPF framework, which showed that the integration of energy storage reduced daily LMP variation by 47 €/MWh. Even with the reduced LMP variation, the benefit from energy storage covers the investment cost and gives the investment return ratio of 9.4% for the particular case study.

Finally, the proposed methodology has been exploited to perform a sensitivity analysis of price for storage technologies. Particularly, energy storage performance value has been

obtained, which allowed comparing by how much a particular technology is overpriced comparing to the most cost-effective solution. In addition to that, second-life storage performance has been evaluated to define its equivalent value compared to the off-the-shelf solutions.

Chapter 5. Conclusion

5.1 Summary

Ubiquitous electrification of industry and households, and the increased share of less controllable distributed energy sources, including intermittent renewable energy sources, push the existing power systems to their operational limits. Conventional methods to reinforce the power systems, such as building new lines and thermal generation units, cannot adequately address the upcoming challenges.

Controllable energy storage is one of the key elements to address new challenges in power systems. Particularly, at least 18 applications exist at present, where energy storage can bring benefit to a utility company, transmission and distribution network operators, and an end-customer. However, the high upfront investment cost for energy storage technologies requires performing a detailed techno-economic analysis to find the best combination of site, size, and technology of energy storage to be installed to bring the most benefit and justify the investment. Such an analysis is known as optimal siting, sizing, and technology selection.

The present thesis has addressed the problem of optimal siting, sizing, and technology selection of energy storage systems for power system applications by applying the formal optimization methods, i.e., convex programming and mixed-integer programming. A formal optimization allows finding the globally optimal solution, which uniqueness is mathematically proven. However, the numerical methods used to resolve a formal optimization problem impose certain limitations on its formulation to ensure tractability, uniqueness of a solution, and its accuracy. This includes using only equalities and inequalities to model energy storage and its

environments, which have to be either linear or convex, and accurately represent their physical equivalence. For the particular problem, these requirements are found contradictory as accurate modeling of energy storage, particularly storage degradation processes, can be hardly done with convex equalities and inequalities.

To find the optimal site, size, and technology of energy storage system and account for a complex degradation function of Li-ion based energy storage that is neither linear nor convex, the mixed-integer problem reformulation has been proposed, where the problem meets the convexity requirements for the fixed integer variables. Thus, to find the globally optimal solution of the problem, the convex optimization problem has to be solved for every combination of integer variables (whole enumeration), which yields an intractable number even for a small problem. Even though the existing mixed-integer solvers apply partial enumeration techniques to mixed-integer problems (e.g., Branch-and-Bound algorithm), they cannot resolve the tractability issue when the search space of integer variables is significantly big. For example, the proposed mixed-integer problem formulation applied to the considered 39-bus network and four energy storage technologies yields $>10^{936}$ combinations of integer variables, which is equivalent to 3,110 binary variables. To resolve the problem of intractability, the proposed mixed-integer convex programming problem has been decomposed by the ALR technique per each bus and energy storage technology, which are then solved (potentially in parallel) according to ADMM procedure. The search space of each subproblem has been decreased to 7,650,000 combinations (equivalent to 23 binary variables), which does not depend on network size and can be effectively solved with the Branch-and-Bound algorithm within seconds.

The proposed methodology has been demonstrated on IEEE ten generators 39-bus benchmark system for transmission congestion management application of energy storage. For the particular case study, energy storage yields benefit from an energy arbitrage (buy low – sell high) and reduction of active power losses within a network. The optimal solution suggests installing energy storage at certain buses, where daily LMP variation for energy is the highest. Energy market response to a sufficient amount of energy storage capacity, which has been modeled with DC OPF framework, showed that the integration of energy storage reduced daily LMP variation by 47 £/MWh, what reduces the benefit from price arbitrage. Even with the reduced LMP variation, the benefit from energy storage covers the investment cost and gives the investment return ratio of 9.4% for the particular case study.

Finally, the proposed methodology allows performing analyses of various energy storage characteristics. Particularly, energy storage price analysis has been performed to define the performance value of the considered storage technologies, and by how much it is overpriced compared to the most cost-efficient solution. In addition to that, second-life storage performance has been evaluated to define its equivalent value compared to the off-the-shelf solutions.

5.2 Fulfillment of Research Objectives

1) Describe how an energy storage investment decision and benefits can be translated into a formal optimization problem and what challenges does it possess to find the optimal solution.

The benefit from an energy storage deployment is highly dependent on a specific application, operational strategy of storage, location(s) of where it is installed, its size (i.e., power and energy ratings), and technology applied to store energy. An informative decision making on energy storage design for power system applications requires knowledge about:

- The main principles of a particular service – product required (active, reactive power), technical requirements (response time, duration), frequency of calls, reward policy, historical data, future expectations.
- The prospective energy storage technologies, their characteristics, and processes that occur during its service lifetime, which include degradation, active power losses, state of charge evolution, and etc.
- The environment (a particular power network), where prospective locations for energy storage installation are identified, as well as other network-related characteristics, such as power lines' parameters and limits.
- Other assets that may affect the environment, as well as the operation of energy storage. This may include conventional generation, renewable generation, and demand.

The proposed formal optimization problem consolidates the necessary knowledge and resolves a trade-off between long-term investment decisions and daily scheduling problems, which yield a benefit from energy storage operation. The stochastic optimization problem accounts for a number of network scenarios that are expected in the future with a certain probability to determine the expected daily operation benefit. In opposite to that, per diem investment cost for energy storage is found based on the installed capacity and unit price of a particular technology divided by the operational lifetime, which in turn is defined from storage degradation and driven by daily operation of storage. Thus, the proposed problem formulation performs an operation and degradation-aware siting, sizing, and technology selection, where benefits and costs are expressed in terms of money. The particular challenge of degradation-aware sizing resides in the interdependency of an energy storage operation and available capacity

that causes nonconvexity of the original problem, meaning that the globally optimal solution cannot be found with off-the-shelf optimization solvers.

2) Propose a problem formulation for optimal siting, sizing, and technology selection of energy storage systems for power system applications that take into account the most relevant characteristics.

In the literature, researches apply models of energy storage, as well as models of an environment, into the optimization problem to perform an accurate techno-economic analysis of energy storage integration. Particularly, energy storage models include charge-discharge efficiencies, self-discharge, calendar lifetime, operational lifetime, energy to power ratio, degradation, and the end of life criterion. To model an environment, which includes buses, power lines, and transformers, power flow modeling is applied. The proposed methodology accounts for all of the above, where the particular contribution resides in operation and degradation-aware sizing, where degradation is considered as an incremental decrease of an available capacity and possesses nonlinear and nonconvex functional dependency from the actual operation of an energy storage, which is expressed in state of charge, storage temperature, and depth of discharge. The proposed mixed-integer convex programming problem formulation allows finding the globally optimal solution of the initially nonconvex problem that accounts for complex degradation characteristics.

3) Develop a methodology that can be effectively applied to resolve the design problem of energy storage for big-scale network and number of energy storage technologies considered;

The search space of a combinatorial problem, such as the MICP problem, increases in a power law dependence with the number of integer variables, which in the case of the proposed

mixed-integer problem formulation increases with network size and a number of storage technologies. Hence, the main drawback of the proposed mixed-integer problem reformulation resides in the scalability issue, where the problem may easily become intractable with the increased network size and number of storage technologies. To overcome the problem of tractability and scalability, the proposed MICP problem has been decomposed per each bus and energy storage technology, where power balance constraints of the original problem have been relaxed and added to the objective function according to ALR principle, and power flow limit constraints have been relaxed with barrier functions. As a result of problem decomposition, the search space of each subproblem has been decreased to a tractable number, which does not depend on network size and a number of considered storage technologies. The distinctive characteristic of the proposed problem decomposition technique resides in the fact that the resulting optimization subproblems are independent of each other, hence, can be solved in parallel what further increases computational efficiency.

4) Examine the main driven factors for energy storage siting, sizing, and technology selection.

For energy storage, which performs energy arbitrage, the optimal site and size are driven by LMPs, where the main contributing factors for non-uniform energy price distribution are power line thermal limits and active power losses. When energy storage possesses a sufficient amount of capacity to influence LMPs (price maker), a tool for power system modeling is required to track the influence of energy arbitrage on LMPs. Particularly, the DC OPF framework has been used to model the network operation, which includes power generation and power flows within the network. Technology selection, in its turn, is driven by the internal

parameters of a particular technology, such as self-discharge, round-trip efficiency, degradation, and price, where the most cost-effective combination is advantageous.

5.3 Conclusions

The particular contributions of the proposed methodology for the optimal siting, sizing, and technology selection problem resides in a tractable problem formulation, and accurate modeling of energy storage degradation to perform informative techno-economic analysis of energy storage integration. In addition to that, an analysis performed within the proposed framework allows evaluating the performance value of a particular energy storage characteristic. This hallmark is of particular importance when evaluating second-life energy storage solutions, which value cannot be defined with manufacturing costs but needs to be determined with the actual performance.

Bibliography

- [1] L. Kristov, “Power System Evolution From the Bottom Up,” 2018.
- [2] “Directive 2009/28/EC of the European Parliament and of the Council of 23 April 2009 on the promotion of the use of energy from renewable sources and amending and subsequently repealing Directives 2001/77/EC and 2003/30/EC,” *Off. J. Eur. Union*, pp. 16–62, 2009.
- [3] “Digest of UK Energy Statistics (DUKES): Renewable sources of energy,” 2018.
- [4] A. Adrees, J. V. Milanović, and P. Mancarella, “Effect of Inertia Heterogeneity on Frequency Dynamics of Low-Inertia Power Systems,” *IET Gener. Transm. Distrib.*, 2019.
- [5] “Energy Storage,” *Revolv*. [Online]. Available: <https://www.revolv.com/page/Energy-storage>. [Accessed: 17-Apr-2019].
- [6] S. Schwunk, “Battery systems for storing renewable energy,” Germany: Fraunhofer--Institut für Solare Energie, 2011.
- [7] X. Luo, J. Wang, M. Dooner, and J. Clarke, “Overview of current development in electrical energy storage technologies and the application potential in power system operation,” *Appl. Energy*, vol. 137, pp. 511–536, 2015.
- [8] B. J. Lowe and R. Scully, “To Energy Conservation,” New York: EBASCO Services Incorporated, 1991.
- [9] W. Yuan, “Second-generation high-temperature superconducting coils and their applications for energy storage (Doctoral thesis),” University of Cambridge, 2010.
- [10] E. Elshazly, N. Emam, and N. Eltayeb, “Attributes affecting energy of Superconducting

Magnetic Energy Storage systems,” *Int. J. Sci. Eng. Res.*, vol. 6, no. 3, pp. 356–361, 2015.

- [11] M. Farhadi and O. Mohammed, “Energy Storage Technologies for High-Power Applications,” *IEEE Trans. Ind. Appl.*, vol. 52, no. 3, pp. 1953–1962, 2015.
- [12] “The Energy Storage Association,” 2018. [Online]. Available: <http://energystorage.org>. [Accessed: 18-May-2019].
- [13] Abbas A. Akhil *et al.*, “DOE/EPRI Electricity Storage Handbook,” Sandia National Laboratories, 2015.
- [14] “DOE Global Energy Storage Database,” 2017. [Online]. Available: <https://www.energystorageexchange.org/>. [Accessed: 18-May-2019].
- [15] V. A. Boicea, “Energy storage technologies: The past and the present,” *Proc. IEEE*, vol. 102, no. 11, pp. 1777–1794, 2014.
- [16] “Ares - The power of gravity.” [Online]. Available: <https://www.aresnorthamerica.com>. [Accessed: 18-May-2019].
- [17] G. Bottenfield, K. Hatipoglu, W. Virginia, and W. Virginia, “Advanced Rail Energy and Storage Analysis of Potential Implementations for the State of West Virginia,” *2018 North Am. Power Symp.*, pp. 1–4, 2018.
- [18] J. Taylor and A. Haines, “Analysis of compressed air energy storage,” in *PCIC Europe 2010*, 2010, pp. 1–5.
- [19] D. J. Swider, “Compressed Air Energy Storage in an Electricity,” *IEEE Trans. Energy Convers.*, vol. 22, no. 1, pp. 95–102, 2007.
- [20] F. N. Werfel *et al.*, “A Compact HTS 5 kWh / 250 kW Flywheel Energy Storage

- System,” *IEEE Trans. Appl. Supercond.*, vol. 17, no. 2, pp. 2138–2141, 2007.
- [21] D. Peralta, C. Cañizares, and K. Bhattacharya, “Practical Modeling of Flywheel Energy Storage for Primary Frequency Control in Power Grids,” in *2018 IEEE Power & Energy Society General Meeting (PESGM)*, 2018, pp. 1–5.
- [22] “Britain builds the world’s first grid-level thermal storage energy storage system,” *CSPPLAZA*, 2019. [Online]. Available: <http://www.cspplaza.com/article-14093-1.html>. [Accessed: 12-Apr-2019].
- [23] P. Wang *et al.*, “Optimal scheduling of multi-carrier energy networks considering liquid air energy storage,” in *2018 2nd IEEE Conference on Energy Internet and Energy System Integration (EI2)*, 2018, pp. 1–4.
- [24] G. Brett and M. Barnett, “Utility-scale energy storage: Liquid air a pioneering solution to the problem of energy storage,” in *IET Conference Proceedings*, 2013, pp. 1–18.
- [25] M. Kolhe and O. Atlam, “Empirical Electrical Modeling for a Proton Exchange Membrane Electrolyzer,” in *2011 International Conference on Applied Superconductivity and Electromagnetic Devices*, 2011, pp. 131–134.
- [26] S. V. M. Guaitolini, I. Yahyaoui, J. F. Fardin, L. F. Encarnação, and F. Tadeo, “A review of fuel cell and energy cogeneration technologies,” in *2018 9th International Renewable Energy Congress (IREC)*, 2018, pp. 1–6.
- [27] S. Dey, R. Dash, and S. C. Swain, “Fuzzy based Optimal Load Management in Standalone Hybrid Solar PV / Wind / Fuel Cell Generation System,” in *2015 Communication, Control and Intelligent Systems (CCIS)*, 2015, pp. 486–490.
- [28] Y. Li *et al.*, “Day-ahead Schedule of a Multi-energy System with Power-to-Gas

- Technology,” in *2017 IEEE Power & Energy Society General Meeting*, 2017, pp. 1–5.
- [29] P. Krivik and P. Baca, “Electrochemical Energy Storage,” in *Energy Storage-Technologies and Applications*, 2013, pp. 79–100.
- [30] “Lead Storage Battery,” *Lumen: Introduction to Chemistry*. [Online]. Available: <https://courses.lumenlearning.com/introchem/chapter/lead-storage-battery/>. [Accessed: 31-May-2019].
- [31] X. Hu, C. Zou, C. Zhang, and Y. Li, “Technological Developments in Batteries: A Survey of Principal Roles, Types, and Management Needs,” *IEEE Power Energy Mag.*, vol. 15, no. 5, pp. 20–31, 2017.
- [32] P. Huang, J. Kuo, and C. Huang, “A new application of the UltraBattery to hybrid fuel cell vehicles,” *Int. J. Energy Res.*, vol. 40, no. 2, pp. 146–159, 2016.
- [33] J. Pegueroles-Queralt, F. D. Bianchi, and O. Gomis-Bellmunt, “A Power Smoothing System Based on Supercapacitors for Renewable Distributed Generation,” *IEEE Trans. Ind. Electron.*, vol. 62, no. 1, pp. 343–350, 2014.
- [34] International Electrotechnical Commission, “White Paper: Electrical Energy Storage,” Geneva, Switzerland, 2011.
- [35] “Lithium Ion (li-ion) Batteries.” [Online]. Available: <http://energystorage.org/energy-storage/technologies/lithium-ion-li-ion-batteries>. [Accessed: 17-Apr-2019].
- [36] Y. Zhang *et al.*, “Grid-Level Application of Electrical Energy Storage,” *IEEE Power Energy Mag.*, vol. 15, no. 5, pp. 51–58, Oct. 2017.
- [37] J. Eyer and G. Corey, “Energy Storage for the Electricity Grid : Benefits and Market Potential Assessment Guide,” 2010.

- [38] D. I. Stroe, M. Swierczynski, A. I. Stroe, R. Laerke, P. C. Kjaer, and R. Teodorescu, “Degradation Behavior of Lithium-Ion Batteries Based on Lifetime Models and Field Measured Frequency Regulation Mission Profile,” *IEEE Trans. Ind. Appl.*, vol. 52, no. 6, pp. 5009–5018, 2016.
- [39] Y. Du, R. Jain, and S. M. Lukic, “A novel approach towards energy storage system sizing considering battery degradation,” in *IEEE Energy Conversion Congress and Exposition, Proceedings*, 2016, pp. 1–8.
- [40] B. Xu, A. Oudalov, A. Ulbig, G. Andersson, and D. S. Kirschen, “Modeling of Lithium-Ion Battery Degradation for Cell Life Assessment,” *IEEE Trans. Smart Grid*, vol. 9, no. 2, pp. 1131–1140, 2018.
- [41] IEA, “Technology Roadmap: Energy Storage,” 2014.
- [42] “Electric Supply Benefits,” *Energy Storage Association*. [Online]. Available: <http://energystorage.org/energy-storage/energy-storage-benefits/benefit-categories/electric-supply-benefits>. [Accessed: 17-Apr-2019].
- [43] T. Sayfutdinov *et al.*, “Degradation and Operation-Aware Framework for the Optimal Siting , Sizing and Technology Selection of Battery Storage,” *IEEE Trans. Sustain. Energy*, no. Early Access, pp. 1–11, 2019.
- [44] “FERC: Guide To Market Oversight - Glossary.” [Online]. Available: <http://www.ferc.gov/market-oversight/guide/glossary.asp>. [Accessed: 30-May-2019].
- [45] “Grid Operations Benefits,” *Energy Storage Association*. [Online]. Available: <http://energystorage.org/energy-storage/energy-storage-benefits/benefit-categories/grid-operations-benefits>. [Accessed: 17-Apr-2019].

- [46] M. Kintner-Meyer, “Regulatory policy and markets for energy storage in North America,” *Proc. IEEE*, vol. 102, no. 7, pp. 1065–1072, 2014.
- [47] E. Serban, M. Ordonez, and C. Pondiche, “Voltage and Frequency Grid Support Strategies Beyond Standards,” *IEEE Trans. Power Electron.*, vol. 32, no. 1, pp. 298–309, 2016.
- [48] H. H. Abdeltawab and Y. A. I. Mohamed, “Mobile Energy Storage Scheduling and Operation in Active Distribution Systems,” *IEEE Trans. Ind. Electron.*, vol. 64, no. 9, pp. 6828–6840, 2017.
- [49] S. Quaia and F. Tosato, “Interruption costs caused by supply voltage dips and outages in small industrial plants : a case study and survey results,” in *The IEEE Region 8 EUROCON 2003*, 2003, pp. 258–262.
- [50] T. Sayfutdinov, P. Lyons, and M. Feeney, “Laboratory evaluation of a deterministic optimal power flow algorithm using Power Hardware in the Loop,” in *CIREN Workshop 2016*, 2016, pp. 1–4.
- [51] F. Qiu, J. Wang, C. Chen, and J. Tong, “Optimal Black Start Resource Allocation,” *IEEE Trans. Power Syst.*, vol. 31, no. 3, pp. 2493–2494, 2015.
- [52] G. Wang, M. Ciobotaru, and V. G. Agelidis, “Power Management for Improved Dispatch of Utility-Scale PV Plants,” *Power Syst. IEEE Trans.*, vol. 31, no. 3, pp. 2297–2306, 2016.
- [53] “Grid Infrastructure Benefits,” *Energy Storage Association*. [Online]. Available: <http://energystorage.org/energy-storage/energy-storage-benefits/benefit-categories/grid-infrastructure-benefits>. [Accessed: 17-Apr-2019].

- [54] L. S. Vargas, G. Bustos-Turu, and F. Larraín, “Wind Power Curtailment and Energy Storage in Transmission Congestion Management Considering Power Plants Ramp Rates,” *IEEE Trans. Power Syst.*, vol. 30, no. 5, pp. 2498–2506, 2014.
- [55] D. M. Greenwood, N. S. Wade, P. C. Taylor, P. Papadopoulos, and N. Heyward, “A Probabilistic Method Combining Electrical Energy Storage and Real-Time Thermal Ratings to Defer Network Reinforcement,” *IEEE Trans. Sustain. Energy*, vol. 8, no. 1, pp. 374–384, 2017.
- [56] T. Sayfutdinov, C. Patsios, J. W. Bialek, D. M. Greenwood, and P. C. Taylor, “Incorporating variable lifetime and self-discharge into optimal sizing and technology selection of energy storage systems,” *IET Smart Grid*, vol. 1, no. 1, pp. 11–18, 2018.
- [57] M. Humayun, A. Safdarian, M. Z. Degefa, and M. Lehtonen, “Demand response for operational life extension and efficient capacity utilization of power transformers during contingencies,” *IEEE Trans. Power Syst.*, vol. 30, no. 4, pp. 2160–2169, 2014.
- [58] “Customer Sited Benefits,” *Energy Storage Association*. [Online]. Available: <http://energystorage.org/energy-storage/energy-storage-benefits/benefit-categories/customer-sited-benefits>. [Accessed: 17-Apr-2019].
- [59] G. Strbac *et al.*, “Opportunities for Energy Storage: Assessing Whole-System Economic Benefits of Energy Storage in Future Electricity Systems,” *IEEE Power Energy Mag.*, vol. 15, no. 5, pp. 32–41, 2017.
- [60] M. Zidar, P. S. Georgilakis, N. D. Hatziargyriou, T. Capuder, and D. Škrlec, “Review of energy storage allocation in power distribution networks: applications, methods and future research,” *IET Gener. Transm. Distrib.*, vol. 10, no. 3, pp. 645–652, 2016.

- [61] J. Eyer, J. Iannucci, and P. C. Butler, “Estimating Electricity Storage Power Rating and Discharge Duration for Utility Transmission and Distribution Deferral. A Study for the DOE Energy Storage Program,” Albuquerque, New Mexico, 2005.
- [62] X. Y. Wang, D. M. Vilathgamuwa, and S. S. Choi, “Determination of Battery Storage Capacity in Energy Buffer for Wind Farm,” *IEEE Trans. Energy Convers.*, vol. 23, no. 3, pp. 868–878, 2008.
- [63] J. Mitra, “Reliability-Based Sizing of Backup Storage,” *IEEE Trans. Power Syst.*, vol. 25, no. 2, pp. 1198–1199, 2010.
- [64] B. Hartmann and A. Dán, “Methodologies for Storage Size Determination for the Integration of Wind Power,” *IEEE Trans. Sustain. Energy*, vol. 5, no. 1, pp. 182–189, 2013.
- [65] T. K. A. Brekken, A. Yokochi, A. Von Jouanne, Z. Z. Yen, H. M. Hapke, and D. A. Halamay, “Optimal Energy Storage Sizing and Control for Wind Power Applications,” *IEEE Trans. Sustain. Energy*, vol. 2, no. 1, pp. 69–77, 2010.
- [66] B. S. Borowy and Z. M. Salameh, “Methodology for Optimally Sizing the Combination of a Battery Bank and PV Array in a Wind/PV Hybrid System,” *IEEE Trans. Energy Convers.*, vol. 11, no. 2, pp. 367–375, 1996.
- [67] V. Mallawaarachchi, “Introduction to Genetic Algorithms — Including Example Code,” *Towards Data Science*, 2017. [Online]. Available: <https://towardsdatascience.com/introduction-to-genetic-algorithms-including-example-code-e396e98d8bf3>. [Accessed: 17-Apr-2019].
- [68] M. Mitchell, *An Introduction to Genetic Algorithms*. MIT press, 1998.

- [69] “Testing and Analysis of Algorithmic Trading Strategies in MATLAB (Part 4) – Genetic Algorithms,” *Matlab Trading*, 2016. [Online]. Available: <http://www.matlabtrading.com/2016/12/testing-and-analysis-of-algorithmic-trading-strategies-in-matlab-part4-genetic-algorithms.html>. [Accessed: 18-May-2019].
- [70] K. Khalid Mehmood, S. U. Khan, S.-J. Lee, Z. M. Haider, M. K. Rafique, and C.-H. Kim, “Optimal sizing and allocation of battery energy storage systems with wind and solar power DGs in a distribution network for voltage regulation considering the lifespan of batteries,” *IET Renew. Power Gener.*, vol. 11, no. 10, pp. 1305–1315, 2017.
- [71] Y. Luo, L. Shi, and G. Tu, “Optimal sizing and control strategy of isolated grid with wind power and energy storage system,” *Energy Convers. Manag.*, vol. 80, pp. 407–415, 2014.
- [72] G. Carpinelli, F. Mottola, D. Proto, and A. Russo, “Optimal Allocation of Dispersed Generators , Capacitors and Distributed Energy Storage Systems in Distribution Networks,” in *2010 Modern Electric Power Systems*, 2010, pp. 1–6.
- [73] C. Chen, S. Duan, T. Cai, B. Liu, and G. Hu, “Optimal Allocation and Economic Analysis of Energy Storage System in Microgrids,” *IEEE Trans. Power Electron.*, vol. 26, no. 10, pp. 2762–2773, 2011.
- [74] M. Ghofrani *et al.*, “A Framework for Optimal Placement of Energy Storage Units Within a Power System With High Wind Penetration,” *IEEE Trans. Sustain. Energy*, vol. 4, no. 2, pp. 434–442, 2013.
- [75] Y. Zheng, Z. Y. Dong, F. J. Luo, K. Meng, J. Qiu, and K. P. Wong, “Optimal Allocation of Energy Storage System for Risk Mitigation of DISCOs With High Renewable

Penetrations,” *IEEE Trans. Power Syst.*, vol. 29, no. 1, pp. 212–220, 2013.

- [76] M. Sedghi, M. Aliakbar-Golkar, and M. Haghifam, “Electrical Power and Energy Systems Distribution network expansion considering distributed generation and storage units using modified PSO algorithm,” *Int. J. Electr. Power Energy Syst.*, vol. 52, pp. 221–230, 2013.
- [77] S. Kahrobaee, S. Asgarpoor, and W. Qiao, “Optimum Sizing of Distributed Generation and Storage Capacity in Smart Households,” *IEEE Trans. Smart Grid*, vol. 4, no. 4, pp. 1791–1801, 2013.
- [78] J. J. Jamian, M. W. Mustafa, H. Mokhlis, and M. A. Baharudin, “Electrical Power and Energy Systems Simulation study on optimal placement and sizing of Battery Switching Station units using Artificial Bee Colony algorithm,” *Int. J. Electr. Power Energy Syst.*, vol. 55, pp. 592–601, 2014.
- [79] B. Bahmani-Firouzi and R. Azizipanah-Abarghooee, “Electrical Power and Energy Systems Optimal sizing of battery energy storage for micro-grid operation management using a new improved bat algorithm,” *Int. J. Electr. Power Energy Syst.*, vol. 56, pp. 42–54, 2014.
- [80] D. Pudjianto, M. Aunedi, P. Djapic, and G. Strbac, “Whole-Systems Assessment of the Value of Energy Storage in Low-Carbon Electricity Systems,” *IEEE Trans. Smart Grid*, vol. 5, no. 2, pp. 1098–1109, 2014.
- [81] P. D. Brown, J. A. Peças Lopes, and M. A. Matos, “Optimization of pumped storage capacity in an isolated power system with large renewable penetration,” *IEEE Trans. Power Syst.*, vol. 23, no. 2, pp. 523–531, 2008.

- [82] R. S. Garcia and D. Weisser, "A wind – diesel system with hydrogen storage : Joint optimisation of design and dispatch," *Renew. Energy*, vol. 31, no. 14, pp. 2296–2320, 2006.
- [83] S. Wogrin and D. F. Gayme, "Optimizing Storage Siting, Sizing, and Technology Portfolios in Transmission-Constrained Networks," *IEEE Trans. Power Syst.*, vol. 30, no. 6, pp. 3304–3313, 2015.
- [84] M. Nick, R. Cherkaoui, and M. Paolone, "Electrical Power and Energy Systems Optimal siting and sizing of distributed energy storage systems via alternating direction method of multipliers," *Int. J. Electr. Power Energy Syst.*, vol. 72, pp. 33–39, 2015.
- [85] P. Fortenbacher, A. Ulbig, and G. Andersson, "Optimal Placement and Sizing of Distributed Battery Storage in Low Voltage Grids Using Receding Horizon Control Strategies," *IEEE Trans. Power Syst.*, vol. 33, no. 3, pp. 2383–2394, 2018.
- [86] Y. Dvorkin, R. Fernandez-Blanco, D. S. Kirschen, H. Pandzic, J. P. Watson, and C. A. Silva-Monroy, "Ensuring Profitability of Energy Storage," *IEEE Trans. Power Syst.*, vol. 32, no. 1, pp. 611–623, 2017.
- [87] H. Pandzic, Y. Wang, T. Qiu, Y. Dvorkin, and D. S. Kirschen, "Near-Optimal Method for Siting and Sizing of Distributed Storage in a Transmission Network," *IEEE Trans. Power Syst.*, vol. 30, no. 5, pp. 2288–2300, 2015.
- [88] X. Qiu, T. A. Nguyen, and M. L. Crow, "Heterogeneous Energy Storage Optimization for Microgrids," *IEEE Trans. Smart Grid*, vol. 7, no. 3, pp. 1453–1461, 2016.
- [89] I. Miranda, N. Silva, and H. Leite, "A Holistic Approach to the Integration of Battery Energy Storage Systems in Island Electric Grids with High Wind Penetration," *IEEE*

Trans. Sustain. Energy, vol. 7, no. 2, pp. 775–785, 2016.

- [90] I. Alsaidan, A. Khodaei, and W. Gao, “A Comprehensive Battery Energy Storage Optimal Sizing Model for Microgrid Applications,” *IEEE Trans. Power Syst.*, vol. 33, no. 4, pp. 3968–3980, 2018.
- [91] F. Oldewurtel *et al.*, “A Framework for and Assessment of Demand Response and Energy Storage in Power Systems,” in *2013 IREP Symposium Bulk Power System Dynamics and Control-IX Optimization, Security and Control of the Emerging Power Grid*, 2013, pp. 1–24.
- [92] F. Caponio, A. Abba, P. Baruzzi, G. Ripamonti, and A. Geraci, “Modular and Bi-Directional Energy Storage System Compliant with Accumulators of Different Chemistry,” in *11th International Conference on Electrical Power Quality and Utilisation*, 2011, pp. 1–6.
- [93] A. H. Zimmerman, “Self-Discharge Losses in Lithium-Ion Cells,” *IEEE Aerosp. Electron. Syst. Mag.*, vol. 19, no. 2, pp. 19–24, 2004.
- [94] M. Swierczynski, D.-I. Stroe, A. Stan, R. Teodorescu, and S. K. Kær, “Investigation on the Self-discharge of the LiFePO₄ / C Nanophosphate Battery Chemistry at Different Conditions,” in *2014 IEEE Conference and Expo Transportation Electrification Asia-Pacific (ITEC Asia-Pacific)*, 2014, pp. 1–6.
- [95] Y. Zhang, X. Cheng, Y. Fang, and Y. Yin, “On SOC estimation of lithium-ion battery packs based EKF,” in *Proceedings of the 32nd Chinese Control Conference*, 2013, pp. 7668–7673.
- [96] A. Waheed and K. Buss, “Modeling and validation of a three-dimensional

thermoelectric model of a 50 Ah lithium-iron-phosphate battery cell at three different ambient temperatures in the New European Driving Cycle (NEDC),” in *AmE 2016-Automotive meets Electronics; 7th GMM-Symposium*, 2016, pp. 74–79.

- [97] B. Bole, C. S. Kulkarni, and M. Daigle, “Adaptation of an Electrochemistry-based Li-Ion Battery Model to Account for Deterioration Observed Under Randomized Use,” in *Annual Conference of the Prognostic and Health Management Society*, 2014, pp. 502–510.
- [98] R. Spotnitz, “Simulation of capacity fade in lithium-ion batteries,” *J. Power Sources*, vol. 113, no. 1, pp. 72–80, 2003.
- [99] S. Cleveland, S. J. Devlin, and E. Grosse, “Regression by local fitting: methods, properties, and computational algorithms,” *J. Econom.*, vol. 37, no. 1, pp. 87–114, 1988.
- [100] C. Mi, B. Li, D. Buck, and N. Ota, “Advanced electro-thermal modeling of lithium-ion battery system for hybrid electric vehicle applications,” in *2007 IEEE Vehicle Power and Propulsion Conference*, 2007, pp. 107–111.
- [101] F. He, A. A. Ams, Y. Roosien, W. Tao, B. Geist, and K. Singh, “Reduced-order Thermal Modeling of Liquid-cooled Lithium-ion Battery Pack for EVs and HEVs,” in *2017 IEEE Transportation Electrification Conference and Expo (ITEC)*, 2017, pp. 507–511.
- [102] J. J. Grainger and W. D. Stevenson, *Power System Analysis*. 2003.
- [103] S. Frank and S. Rebennack, “An introduction to optimal power flow: Theory, formulation, and examples,” *IIE Trans.*, vol. 48, no. 12, pp. 1172–1197, 2016.
- [104] J. Carpentier, “Contribution to the economic dispatch problem,” *Bull. la Soc. Fr. des*

Electr., vol. 3, no. 8, pp. 431–447, 1962.

- [105] H. Dommel and W. Tinney, “Optimal Power Flow Solutions,” *Trans. Power Appar. Syst.*, vol. 10, pp. 1866–1876, 1968.
- [106] B. C. Lesieutre, D. K. Molzahn, A. R. Borden, and C. L. DeMarco, “Examining the Limits of the Application of Semidefinite Programming to Power Flow Problems,” in *2011 49th annual Allerton conference on communication, control, and computing (Allerton)*, 2011, pp. 1492–1499.
- [107] D. T. Phan, “Lagrangian Duality and Branch-and-Bound Algorithms for Optimal Power Flow,” *Oper. Res.*, vol. 60, no. 2, pp. 275–285, 2012.
- [108] M. Farivar and S. H. Low, “Branch flow model: Relaxations and convexification—Part I,” *IEEE Trans. Power Syst.*, vol. 28, no. 3, pp. 2554–2564, 2013.
- [109] “Customer-Led Network Revolution,” 2016. [Online]. Available: <http://www.networkrevolution.co.uk/resources/project-data/>. [Accessed: 20-Dec-2018].
- [110] Q. Ahsan and M. Uddin, “A Probabilistic Approach of Electrical Energy Forecasting,” in *2005 IEEE Instrumentation and Measurement Technology Conference Proceedings*, 2005, pp. 1070–1074.
- [111] California ISO, “What the duck curve tells us about managing a green grid,” 2016.
- [112] B. Pitt, “Applications of Data Mining Techniques to Electric Load Profiling,” University of Manchester, 2000.
- [113] R. Fernandez-Blanco, Y. Dvorkin, B. Xu, Y. Wang, and D. S. Kirschen, “Optimal Energy Storage Siting and Sizing: A WECC Case Study,” *IEEE Trans. Sustain. Energy*, vol. 8, no. 2, pp. 733–743, 2017.

- [114] “National Renewable Energy Laboratory: Wind Data.” [Online]. Available: <https://www.nrel.gov/gis/data-wind.html>. [Accessed: 24-Mar-2019].
- [115] S. Venkataraman, C. Ziesler, P. Johnson, and S. Van Kempen, “Integrated Wind, Solar, and Energy Storage: Designing Plants with a Better Generation Profile and Lower Overall Cost,” *IEEE Power Energy Mag.*, vol. 16, no. 3, pp. 74–83, 2018.
- [116] A. Soroudi, *Power system optimization modeling in GAMS*. Switzerland: Springer, 2017.
- [117] Z. Ugray, L. Lasdon, J. Plummer, F. Glover, J. Kelly, and R. Martí, “Scatter Search and Local NLP Solvers : A Multistart Framework for Global Optimization Scatter Search and Local NLP Solvers : A Multistart Framework for Global Optimization,” *INFORMS J. Comput.*, vol. 19, no. 3, pp. 328–340, 2007.
- [118] T. Qiu, B. Xu, Y. Wang, Y. Dvorkin, and D. S. Kirschen, “Stochastic Multistage Coplanning of Transmission Expansion and Energy Storage,” *IEEE Trans. Power Syst.*, vol. 32, no. 1, pp. 643–651, 2017.
- [119] “Hyak Next Generation Supercomputer,” *IT Connect*, 2015. [Online]. Available: <https://itconnect.uw.edu/research/hpc/hyak-next-generation-supercomputer/>. [Accessed: 07-Apr-2019].
- [120] M. Barati and A. Kargarian, “A global algorithm for AC optimal power flow based on successive linear conic optimization,” in *2017 IEEE Power & Energy Society General Meeting*, 2017, pp. 1–5.
- [121] M. R. Hestenes, “Multiplier and Gradient Methods,” *J. Optim. Theory Appl.*, vol. 4, no. 5, pp. 303–320, 1969.

- [122] P. Fortenbacher and M. Zellner, “Optimal Sizing and Placement of Distributed Storage in Low Voltage Networks,” in *2016 Power Systems Computation Conference (PSCC)*, 2016, pp. 1–7.
- [123] K. Strunz, N. Hatziargyriou, and C. Andrieu, “Benchmark systems for network integration of renewable and distributed energy resources,” *Cigre Task Force*, vol. 6, no. 4, p. 78, 2009.
- [124] A. J. Conejo, E. Castillo, and R. M. R. García-bertrand, *Decomposition techniques in mathematical programming: engineering and science applications*. Springer Science & Business Media, 2006.
- [125] G. R. Parker and R. L. Rardin, *Discrete Optimization*. Elsevier, 2014.
- [126] R. Ramos and I. Hiskens, “Benchmark Systems for Small-Signal Stability Analysis and Control,” *IEEE Power Energy Soc. Tech. Rep*, 2015.
- [127] R. Fu, T. Remo, R. Margolis, R. Fu, T. Remo, and R. Margolis, “2018 U . S . Utility-Scale Photovoltaics- Plus-Energy Storage System Costs Benchmark,” 2018.
- [128] A. Gopalakrishnan, A. U. Raghunathan, D. Nikovski, and L. T. Biegler, “Global Optimization of Multi-period Optimal Power Flow,” in *2013 American Control Conference*, 2013, pp. 1157–1164.
- [129] M. Matsuishi and T. Endo, “Fatigue of metals subjected to varying stress,” *Japan Soc. Mech. Eng.*, vol. 68, no. 2, pp. 37–40, 1968.
- [130] I. Rychlik, “A new definition of the rainflow cycle counting method,” *Int. J. Fatigue*, vol. 9, no. 2, pp. 119–121, 1987.
- [131] R. D. Zimmerman, C. E. Murillo-sánchez, and R. J. Thomas, “MATPOWER : Steady-

State Operations, Systems Research and Education,” *IEEE Trans. Power Syst.*, vol. 26, no. 1, pp. 12–19, 2011.

- [132] S. Boyd, N. Parikh, E. Chu, B. Peleato, and J. Eckstein, “Distributed Optimization and Statistical Learning via the Alternating Direction Method of Multipliers,” *Found. Trends® Mach. Learn.*, vol. 3, no. 1, pp. 1–122, 2011.
- [133] C. Chen, B. He, Y. Ye, and X. Yuan, “The direct extension of ADMM for multi-block convex minimization problems is not necessarily convergent,” *Math. Program.*, vol. 155, no. 1–2, pp. 57–79, 2016.
- [134] Y. Nie, M. Farrokhifar, and D. Pozo, “Electricity and Gas Network Expansion Planning : an ADMM-based Decomposition Approach,” in *2019 IEEE Milan PowerTech*, 2019, pp. 1–6.
- [135] S. F. Schuster *et al.*, “Nonlinear aging characteristics of lithium-ion cells under different operational conditions,” *J. Energy Storage*, vol. 1, pp. 44–53, 2015.
- [136] E. Namor, D. Torregrossa, F. Sossan, R. Cherkaoui, and M. Paolone, “Assessment of Battery Ageing and Implementation of an Ageing Aware Control Strategy for a Load Leveling Application of a Lithium Titanate Battery Energy Storage System,” in *2016 IEEE 17th Workshop on Control and Modeling for Power Electronics (COMPEL)*, 2016, pp. 1–6.

Appendix A: Technical Data of Energy Storage Technologies

Table A.1: Technical characteristics of energy storage technologies [6]

Technology	Nom. Volt., V	Capacity per cell, Ah	Response Time	Energy Dens., Wh/l	Power Dens., W/l	Discharge Time	Efficiency, %	Calendar Lifetime, y	Cycle Lifetime, cyc
Pumped Hydro	-	-	min	0.2-2	0.1-0.2	hours	70-80	> 50	> 15,000
Compressed Air	-	-	min	2-6	0.2-0.6	ours	40-75	> 25	> 10,000
Flywheel	-	0.7-1.7 MW	< sec	20-80	5,000	seconds	80-90	15-20	2*10 ⁴ -10 ⁷
Lead-acid	2	1-4,000	< sec	50-80	90-700	hours	75-90	3-15	250-1,500
NiCd	1.2	0.05-1,300	< sec	15-110	75-700	hours	60-80	5-20	500-3,000
NiMH	1.2	0.05-110	< sec	80-200	500-3,000	hours	65-75	5-10	600-1,200
Li-Ion	3.7	0.05-100	< sec	200-400	1,300-10,000	hours	85-98	5-15	500-10 ⁴
Zinc Air	1	1-100	< sec	130-200	50-100	hours	50-70	> 1	> 1,000
Sodium Sulfur	2.1	4-30	< sec	150-300	120-160	hours	70-85	10-15	2,500-4,500
NaNiCl	2.6	38	< sec	150-200	250-270	hours	80-90	10-15	~1,000
Vanadium Redox flow	1.6	-	sec	20-70	0.5-2	hours	60-75	5-20	> 10,000
Hybrid Flow Battery	1.8	-	sec	65	1-25	hours	65-75	5-10	1,000-3,650
Hydrogen	-	-	sec-min	600	0.2-20	hours-weeks	35-45	10-30	10 ³ -10 ⁴
Synthetic natural gas	-	-	min	1,800	0.2-2	hours-weeks	30-38	10-30	10 ³ -10 ⁴
Double-layer capacitors	2.5	0.1-1,500 F	< sec	10-20	> 40,000	seconds	85-98	4-12	10 ⁴ -10 ⁵
Superconducting magnetic	-	-	<sec	6	2,600	seconds	75-80	-	-

Appendix B. Degradation Data of Li-ion Technologies

The technology selection in the present case study is performed between four Li-ion energy storage technologies: LiFePO₄ (LFP), LiMn₂O₄ (LMO), LiNiMnCoO₂ (NMC), Li₄Ti₅O₁₂ (LTO). The capacity fade rate characteristics of each type of Li-ion technology, considered within the study, for the C-rate less or equal to one are depicted in Figure B.1. These characteristics have been taken from [38], [40], [135], [136], and reproduced from the initial nonuniform data by means of multiplication of two quadratic functions as in (B.1) and (B.2) using the least-squares fitting method [99]. Functions' parameters used within the optimal problem formulation are presented in Table B.1 for degradation from idling and Table B.2 for degradation from cycling.

Table B.1: Idling degradation data

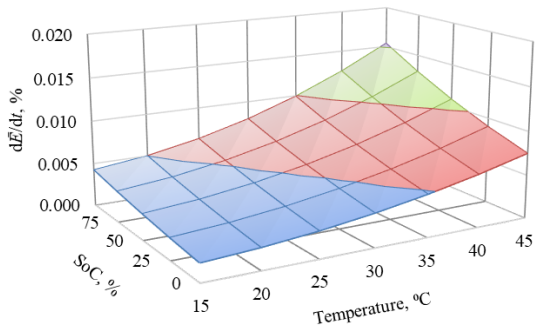
#	Technology	A_{SoC}^{Idl}	B_{SoC}^{Idl}	C_{SoC}^{Idl}	A_{τ}^{Idl}	B_{τ}^{Idl}	C_{τ}^{Idl}
1	LFP	6.02E-06	1.35E-05	1.85E-05	2.31E-03	-4.01E-02	1.21E+00
2	LMO	6.81E-05	4.02E-05	1.63E-05	1.89E-03	-3.30E-02	9.20E-01
3	NMC	8.07E-06	3.41E-06	2.83E-05	2.02E-03	-2.98E-02	1.05E+00
4	LTO	3.03E-06	2.81E-05	5.02E-06	1.04E-03	-2.02E-02	1.01E+00

Table B.2: Cycling degradation data

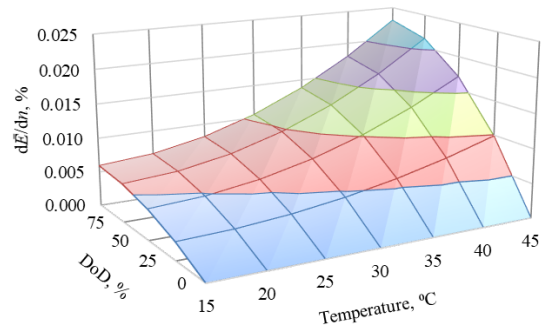
#	Technology	A_{DoD}^{Cyc}	B_{DoD}^{Cyc}	A_{τ}^{Cyc}	B_{τ}^{Cyc}	C_{τ}^{Cyc}
1	LFP	-4.72E-05	9.62E-05	3.62E-03	-1.05E-01	1.93E+00
2	LMO	-1.21E-04	4.01E-04	2.38E-03	-8.90E-02	1.45E+00
3	NMC	-4.05E-05	1.01E-04	3.10E-03	-9.04E-02	1.79E+00
4	LTO	-1.57E-05	4.40E-05	2.08E-03	7.02E-02	1.40E+00

$$\delta^{CF_{Idl}} = \left(A_{SoC}^{Idl} SoC^{D^2} + B_{SoC}^{Idl} SoC^D + C_{SoC}^{Idl} \right) \left(A_{\tau}^{Idl} \tau^{D^2} + B_{\tau}^{Idl} \tau^D + C_{\tau}^{Idl} \right), \quad (B.1)$$

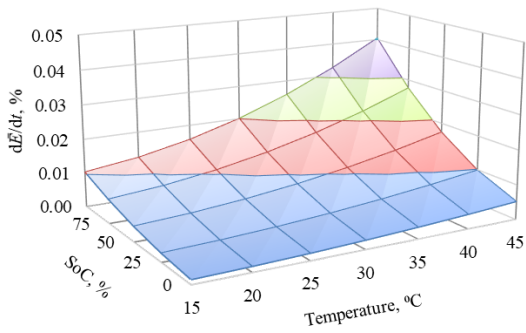
$$\delta^{CF_{Cyc}} = \left(A_{DoD}^{Cyc} DoD^{C^2} + B_{DoD}^{Cyc} DoD^C \right) \left(A_{\tau}^{Cyc} \tau^{C^2} + B_{\tau}^{Cyc} \tau^C + C_{\tau}^{Cyc} \right), \quad (B.2)$$



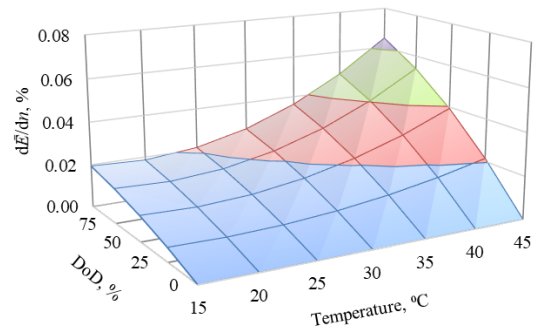
(a) LFP degradation from idling



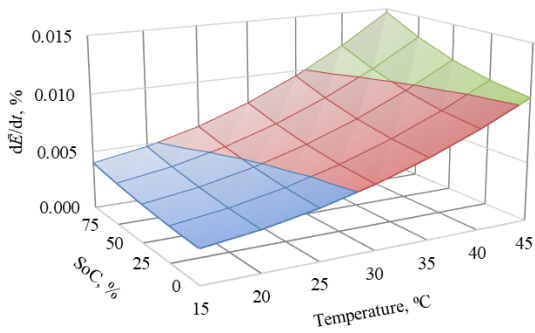
(b) LFP degradation from cycling



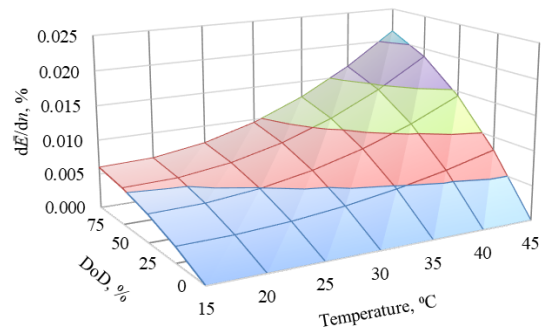
(c) LMO degradation from idling



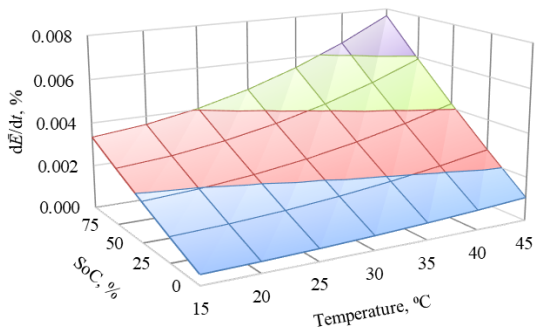
(d) LMO degradation from cycling



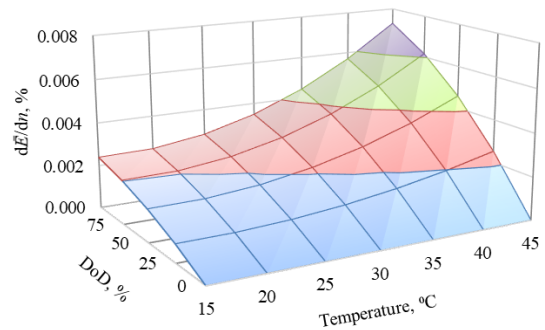
(e) NMC degradation from idling



(f) NMC degradation from cycling



(g) LTO degradation from idling



(h) LTO degradation from cycling

Figure B.1: Capacity fade rate characteristics of Li-ion energy storage

Appendix C. IEEE 10 Generators 39-Bus Network Data

The proposed methodology has been demonstrated on IEEE ten generators 39-bus transmission network, which represents the existing network of New England, USA [126]. The network contains ten generation units, which parameters are given in Table C.1, 46 branches, which data are presented in Table C.2, and 19 aggregated power consumers, which data is provided in Section 4.1.3.

$$C^{Gen} = A^G P^{G^2} - B^G P^G \quad (C.1)$$

Table C.1: Generators' data

#	Bus	Pmax, MW	A^G , £/MW ²	B^G , £/MW
1	30	1,900	0.15	0.3
2	31	1,800	0.05	0.3
3	32	900	0.05	0.3
4	33	900	0.05	0.3
5	34	900	0.05	0.3
6	35	900	0.05	0.3
7	36	900	0.05	0.3
8	37	900	0.1	0.3
9	38	1,200	0.11	0.3
10	39	900	0.11	0.3

Table C.2: Branches' data

#	From Bus	To Bus	r , pu	x , pu
1	1	2	3.50E-03	4.11E-02
2	1	39	1.00E-03	2.50E-02
3	2	3	1.30E-03	1.51E-02
4	2	25	7.00E-03	8.60E-03
5	2	30	1.00E-04	1.81E-02
6	3	4	1.30E-03	2.13E-02
7	3	18	1.10E-03	1.33E-02
8	4	5	8.00E-04	1.28E-02
9	4	14	8.00E-04	1.29E-02
10	5	6	2.00E-04	2.60E-03
11	5	8	8.00E-04	1.12E-02
12	6	7	6.00E-04	9.20E-03
13	6	11	7.00E-04	8.20E-03

#	From Bus	To Bus	r , pu	x , pu
14	6	31	1.00E-04	2.50E-02
15	7	8	4.00E-04	4.60E-03
16	8	9	2.30E-03	3.63E-02
17	9	39	1.00E-03	2.50E-02
18	10	11	4.00E-04	4.30E-03
19	10	13	4.00E-04	4.30E-03
20	10	32	1.00E-04	2.00E-02
21	12	11	1.60E-03	4.35E-02
22	12	13	1.60E-03	4.35E-02
23	13	14	9.00E-04	1.01E-02
24	14	15	1.80E-03	2.17E-02
25	15	16	9.00E-04	9.40E-03
26	16	17	7.00E-04	8.90E-03
27	16	19	1.60E-03	1.95E-02
28	16	21	8.00E-04	1.35E-02
29	16	24	3.00E-04	5.90E-03
30	17	18	7.00E-04	8.20E-03
31	17	27	1.30E-03	1.73E-02
32	19	20	7.00E-04	1.38E-02
33	19	33	7.00E-04	1.42E-02
34	20	34	9.00E-04	1.80E-02
35	21	22	8.00E-04	1.40E-02
36	22	23	6.00E-04	9.60E-03
37	22	35	1.00E-04	1.43E-02
38	23	24	2.20E-03	3.50E-02
39	23	36	5.00E-04	2.72E-02
40	25	26	3.20E-03	3.23E-02
41	25	37	6.00E-04	2.32E-02
42	26	27	1.40E-03	1.47E-02
43	26	28	4.30E-03	4.74E-02
44	26	29	5.70E-03	6.25E-02
45	28	29	1.40E-03	1.51E-02
46	29	38	8.00E-04	1.56E-02

Appendix D. Energy Storage Applications' Requirements

Summary of energy storage applications' requirements from [12], [13] is provided in

Table D.1

Table D.1: Energy storage applications' requirements

#	Application	Storage Size Range	Discharge Time	Cycles per Year
1	Electric Energy Time-Shift (Arbitrage)	1 – 500 MW	30 min – 8 hours	250+
2	Electric Supply Capacity	1 – 500 MW	2 – 6 hours	5 – 100
3	Regulation	10 – 40 MW	15 min – 1 hour	250 – 10,000
4	Spinning, Non-Spinning and Supplemental Reserves	10 – 100 MW	15 min – 1 hour	20 – 50
5	Voltage Support	1 – 10 MVAR	N/Ap	N/Ap
6	Black Start	5 – 50 MW	15 min – 1 hour	10 – 20
7	Load Following	1 – 100 MW	15 min – 1 hour	365
8	Frequency Response	~20 MW	15 min – 30 min	10,000
9	Ramping Support for Renewables	1 – 100 MW	15 min – 1 hour	1,000
10	Transmission Support	10 – 100 MW	2 – 8 hours	~50
11	Transmission Congestion Management	1 – 100 MW	1 – 4 hours	50 – 100
12	T&D Upgrade Deferral	0.5 – 10 MW (D) 10 – 100 MW (T)	2 – 8 hours	50 – 100
13	T&D Equipment Life Extension	50 kW – 1 MW (D) 1 – 10 MW (T)	1 – 4 hours (D) 2 – 8 hours (T)	50 – 100
14	Substation On-site Power	N/Av	N/Av	N/Av
15	Power Quality	0.1 – 10 MW	10 sec – 15 min	10 – 200
16	Power Reliability	C/S	C/S	C/S
17	Retail Electric Energy Time-Shift	1 kW – 1 MW	1 – 6 hours	50 - 250
18	Demand Charge Management	50 kW – 10 MW	1 – 4 hours	50 – 500

Key: N/Ap – Not Applicable; N/Av – Not Available; C/S – Case-Specific

Appendix E. Results of Optimal Siting, Sizing, and Technology Selection for IEEE

Benchmark Systems

The results of optimal siting, sizing, and technology selection for various IEEE benchmark systems, i.e., 9-bus, 14-bus, 24-bus, and 39-bus, are provided in Table E.1.

Table E.1: Results of optimal siting, sizing, and technology selection

#	Network	Comp. Time, sec	Solution				
			Objective Function, £/day	Bus	Tech.	Cap., MWh	Operational. Life-time, y
1	9-bus	19,750	391,269	5	NMC	320	8
2	14-bus	47,412	573,434	3	NMC	150	8
				7	NMC	60	8
				10	NMC	20	8
				12	NMC	10	8
				13	NMC	30	8
				14	NMC	40	8
3	24-bus	94,778	1,742,109	3	NMC	140	8
				6	NMC	130	8
				9	NMC	130	8
				10	NMC	150	8
				14	NMC	130	8
4	39-bus	159,782	3,449,182	17	NMC	350	8
				27	NMC	360	8